NOTICE

The quality of this microform is heavily dependent upon the quality of the original thesis submitted for microfilming. Every effort has been made to ensure the highest quality of reproduction possible.

If pages are missing, contact the university which granted the degree.

Some pages may have indistinct print especially if the original pages were typed with a poor typewriter ribbon or if the university sent us an inferior photocopy.

Reproduction in full or in part of this microform is governed by the Canadian Copyright Act, R.S.C. 1970, c. C-30, and subsequent amendments.

AVIS

La qualité de cette microforme dépend grandement de la qualité de la thèse soumise au microfilmage. Nous avons tout fait pour assurer une qualité supérieure de reproduction.

S'il manque des pages, veuillez communiquer avec l'université qui a conféré le grade.

La qualité d'impression de certaines pages peut laisser à désirer, surtout si les pages originales ont été dactylographiées à l'aide d'un ruban usé ou si l'université nous a fait parvenir une photocopie de qualité inférieure.

La reproduction, même partielle, de cette microforme est soumise à la Loi canadienne sur le droit d'auteur, SRC 1970, c C-30, et ses amendements subséquents

ISBN 0-315-56098-3

Canada

Tryptophan Fluorescence of Hemeproteins

M. Leonor Ferreira-Rajabi

A Thesis

in

The Department

of

Chemistry & Biochemistry

Presented in Partial Fulfillment of the Requirements

for the Degree of Master of Science at

Concordia University

Montréal, Québec, Canada

April 1990

ABSTRACT

Tryptophan Fluorescence of Hemeproteins

M. Leonor Ferreira-Rajabi

The intrinsic tryptophan fluorescence of two heme containing proteins was monitored as a probe of their global conformations in response to chemical and physical perturbations. Cytochrome oxidase has been shown to exist in different conformational states, some of which have been proposed to play a key role in the linkage of electron transport and proton translocation. Copeland et al. (987) have recently shown that the emission maximum of the tryptophan fluorescence of cytochrome oxidase is shifted 20 nm to the red upon reduction of the enzyme. They have proposed that this is indicative of a gross conformational change in the enzyme due specifically to the reduction of Cu_A and represents the conformational change required in a redox-linked proton pump (Copeland et al., 1987, 1988). The fluorescence emission maximum of bovine heart cytochrome oxidase is constant, ca. 328 nm, regardless of the redox state of the enzyme. A red-shift of approximately 20 nm in the fluorescence emission maximum of cytochrome oxidase as reported by Copeland et al. (1987) and attributed to the reduction of Cu_A is an artifact due to the optical filtering effect of the reductant, dithionite. Tryptophan fluorescence from cytochrome oxidase incorporated into phospholipid vesicles is seen in the low nanomolar range. Fluorescence emission of

membrane-incorporated cytochrome oxidase is similar to that observed for solubilized cytochrome oxidase. Preliminary results show that a pH gradient of 3 pH units across cytochrome oxidase vesicles has no significant effect on the tryptophan fluorescence of the oxidase.

Yeast cytochrome c peroxidase contains 7 tryptophans, 1 heme and has a molecular weight of ca. 35kD (Yonetani, 1976). The native enzyme and its ruthenated complex, Ru-His(60)-CcP, have tryptophan fluorescence emission maxima of 326 nm and 323 nm, respectively. The quantum yield of native CcP is 5% compared to N-ATA. The ruthenated CcP complex has a quantum yield of 86% relative to the native protein. The fluorescence of a solvent accessible tryptophan, Trp-57, is quenched in the ruthenated derivative. The fluorescence of CcP and its derivative is dependent on the excitation wavelength. Excitation at 295 nm results in the resolution of an independent fluorescence peak at 340 nm upon quenching of external tryptophans. This peak arises from a contribution by tyrosinate in the overall fluorescence of CcP. The Stern-Volmer quenching constants for fluorescence quenching of CcP by acrylamide, iodide and cesium are 3.0 M^{-1}, 1.5 M^{-1} and 0.66 M^{-1}, respectively. Urea denaturation of CcP was monitored using tryptophan fluorescence. The dependence of the fluorescence intensity and fluorescence emission maximum on the urea concentration demonstrates that the denaturation process involves two states only, the native and denatured state. No evidence is seen for the existance of intermediates in the denaturation process.

ACKNOWLEDGEMENTS

I would like take this opportunity to thank fellow graduate students, too numerous to mention, who have generously given their time and shared their expertise with me. I am especially indebted to Paul Taslimi, Joe Albanese, Joe Lepore and last but not least Ted Fox for kindly allowing me to use protein he worked so hard to obtain as well as for making me somewhat computer literate.

I also thank Dr.L.D.Colebrook and Dr.A.M.English for serving on my committee and for their interest in my work. I am most of all indebted to my supervisor, Dr.B.C.Hill who shared his time generously through the process of this work. I thank-you for the great care you took in proofreading this text. I am honoured to have done my graduate work under your excellent supervision. I wish you all the best in future endeavours and may our paths cross again someday.

I dedicate this thesis

to

my husband, Heshmat

and

my son, Alexander

TABLE OF CONTENTS:

LIST OF DIAGRAMS, FIGURES, SCHEMES & TABLES

PAGE

PAGE

PAGE

PAGE

PAGE

SCHEMES:

TABLES:

LIST OF ABBREVIATIONS

CcP - Cytochrome c Peroxidase

Ru-CcP - Pentaammineruthenium(III) His(60)-cytochrome c peroxidase

RCR- Respiratory Control Ratio

TMPD - N,N,N',N'-tetramethyl-p-phenylenediamine

CCCP - carbonylcyanide m-chlorophenyl hydrazone

aa_3 - cytochrome oxidase

N-ATA - N-acetyltryptophanamide

EDTA - ethylenediaminetetraacetate

deazaflavin - 3,10-dimethyl-5-deazaisoalloxazine

DCCD - N,N'-dicyclohexylcarbodiimide

EPR - electron paramagnetic resonance

Pi - phosphate buffer

1.INTRODUCTION

The use of tryptophan fluorescence as a method of monitoring protein conformation has, in the past, been mostly applied to soluble proteins. More recently, studies involving tryptophan fluorescence have been broadened to include purified membrane proteins but the research has been limited. Tryptophan fluorescence has been used to detect conformational changes in cytochrome c reductase (Valpuesta et al., 1987) occurring upon reduction of the enzyme. In the sarcoplasmic reticulum calcium ATPase (Dupont, 1976), interactions between Ca^{2+} ions and the sarcoplasmic reticulum are accompanied by modification of the intrinsic tryptophan fluorescence. I have investigated the utility of this technique as a method of monitoring conformational changes in bovine heart cytochrome oxidase (ferrocytochrome c: O_2 oxidoreductase; EC 1.9.3.1). The oxidase is an integral membrane protein found in the inner mitochondrial membrane. The oxidase consists of 13 distinct subunits with a total of 1793 amino acids of which 54 are tryptophan residues (Buse et al.,1985).

The tryptophan fluorescence of cytochrome oxidase was first reported by Hill et al. (1986). Cytochrome oxidase has a tryptophan fluorescence emission maximum at 328 nm, which is independent of excitation wavelength and its quantum yield is established at ca. 35% compared to N-ATA. A relationship between shifts in the tryptophan fluorescence emission maximum of cytochrome oxidase and the enzyme's redox state have been reported (Copeland et al., 1987). A red-shift in the tryptophan fluorescence maximum from 328 to 348 nm is observed and assigned to a large

conformational change occuring upon reduction of the enzyme. This "conformational change" is attributed to an 'open-closed' transition of cytochrome oxidase thought to be undergone during the process of redox turnover (Brzezinski & Malmstrom, 1987). Copeland et al. (1988) have correlated the redox-linked tryptophan fluorescence shift to the reduction of the Cu_A center. In the course of the work presented in this thesis similar experiments have been done with conflicting results. The red-shift on which these proposals are based has been shown to be artifactual (Ferreira-Rajabi & Hill, 1989) and due to the optical properties of the reductant.

The indole nucleus of tryptophan is sensitive to the polarity of its immediate environment. Tryptophan at physiological pH is uncharged but because it contains an amine it can easily H-bond to other polar groups in its vicinity. The ease with which the indole nucleus can redistribute and accommodate added electron density makes it a versatile amino acid since depending on its location in the protein matrix it will adapt accordingly. For instance, if it is found on or near the surface of the protein it will H-bond with either water or other polar amino acids in its immediate surrounding. In the interior of the protein it may H-bond with the peptide backbone. Each of these situations is reflected in the fluorescence pattern of the indole side chain making tryptophan a good indicator of changes occurring in the protein matrix. Due to the sensitivity of the technique, tryptophan fluorescence may prove to be a powerful tool in establishing to what extent the redox or ligation state, of the metal centers of hemeproteins, is directly related to the overall

conformational state of the enzyme. The interpretation of intrinsic tryptophan fluorescence data is hindered in multi-tryptophan proteins due to the heterogeneity of the fluorescence emission exhibited, but the sensitivity of the tryptophan residue to its environment may be exploited in looking for protein conformational changes.

The aim of this thesis is to investigate the intrinsic tryptophan fluorescence of cytochrome oxidase that occurs as a result of different redox or ligation states of its redox-active centers. The steady-state tryptophan fluorescence of cytochrome oxidase in various redox forms was investigated. The redox forms studied were the fully oxidized, resting $\underline{aa}_3$, mixed-valence CO-bound $\underline{aa}_3$, fully dithionite-reduced $\underline{aa}_3$, fully dithionite-reduced CO-bound $\underline{aa}_3$ and fully deazaflavin-reduced CO-bound $\underline{aa}_3$.

Yeast cytochrome $\underline{c}$ peroxidase (ferrocytochrome $\underline{c}$: hydrogen peroxide oxidoreductase; E.C.1.11.1.5) contains 7 tryptophan residues and its crystal structure has been established (Poulos et al., 1980; Finzel et al., 1984). For these reasons C$\underline{c}$P is an interesting case to investigate using intrinsic tryptophan fluorescence. C$\underline{c}$P is a mitochondrial hemeprotein that catalyzes the reduction of hydrogen peroxide using reduced cytochrome $\underline{c}$ as its electron donor (Yonetani, 1976). The enzyme catalyzed reaction is as follows:

$$2\ \underline{c}\text{-}Fe^{2+} + H_2O_2 + 2\ H^+ \text{------>} 2\ \underline{c}\text{-}Fe^{3+} + 2\ H_2O$$

$\underline{c}$-Fe^{2+} represents reduced cytochrome $\underline{c}$ and $\underline{c}$-Fe^{3+} oxidized cytochrome $\underline{c}$. The amino acid sequence of C$\underline{c}$P is known (Takio et

al., 1980) to consist of 294 residues (Finzel et al., 1984). The enzyme has a single non-covalently bound heme and is a water-soluble monomeric protein. Cytochrome c peroxidase may represent a good model system for determining the utility of tryptophan fluorescence in the study of conformational states in heme-containing enzymes. Two surface histidine residues have also been covalently linked to pentaammineruthenium(III) (T.Fox & A.M.English, unpublished results) and investigations of the tryptophan fluorescence of one of these derivatives is reported.

2. LITERATURE REVIEW

2.1 GENERAL CHARACTERISTICS OF CYTOCHROME OXIDASE

Cytochrome oxidase (E.C.1.9.3.1; ferrocytochrome c: O_2 oxidoreductase) is an integral component of the inner mitochondrial membrane in eukaryotes. It is an oxygen-activating enzyme involved in cellular respiration. In prokaryotes, it is part of the cell membrane. The basic function of this enzyme is the catalysis of electron transfer from reduced cytochrome c to molecular oxygen. This process allows cells to use O_2 to oxidize foodstuffs. Cytochrome oxidase is a hemeprotein consisting of four metal centers, all of which are redox active. Of the four centers two are heme groups, known as cytochrome a and cytochrome a_3. The other two are copper atoms, known as Cu_A and Cu_B. Cytochrome a and Cu_A function to receive electrons from cytochrome c, whereas cytochrome a_3 and Cu_B function to bind and activate dioxygen. The two hemes, although named differently, are chemically identical, the structure of which is shown in diagram 2.1 (Wikström et al., 1981). The different nomenclatures were assigned by Keilin and Hartree (1939) "on the basis of their spectral and ligand-binding properties". Since the heme of cytochromes a and a_3 are found in different environments they are distinguishable. Cytochrome a_3 is usually found in a high spin state and is reactive to ligands. O_2 and CO bind to the ferrous state of cytochrome a_3 whereas HCN, NH_3 and H_2S bind to the ferric state of cytochrome a_3. These ligands all bind to the cytochrome a_3 iron at the sixth axial position. By contrast, cytochrome a is unreactive to ligands and is in a low

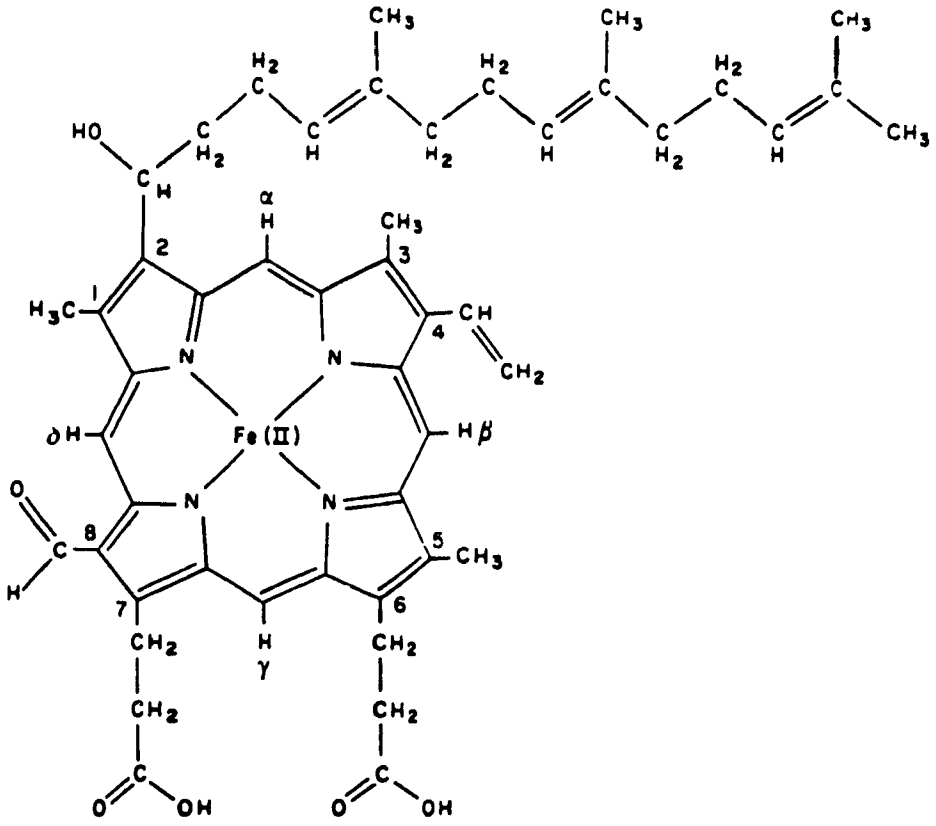

Diagram 2.1: STRUCTURE OF CYTOCHROME OXIDASE HEME A.

spin state. Likewise, the copper ions are also found in different environments and can be distinguished (Beinert et al., 1962). For example, Cu_A is EPR detectable in the oxidized enzyme while Cu_B is EPR silent. This property of Cu_B originally led to the suggestion that Cu_B was physically close to the Fe atom of cytochrome a_3 and this has been supported in numerous studies, e.g. Thomson et al. (1982). Cytochrome a_3 and Cu_B are thought to form a binuclear ligand binding site.

The most commonly used method of monitoring oxidoreduction in the cytochrome oxidase redox centers is optical spectrophotometry. The resting, fully oxidized enzyme ($a^{3+}a_3{}^{3+}Cu_A{}^{2+}Cu_B{}^{2+}$), has a Soret band at 420 nm as well as an α-band at 605 nm, both due to the π-π^* transition of the porphyrin ring and a broad band at ca. 820 nm. The latter band is due to $Cu_A{}^{2+}$ (Diagram 2.2). The fully reduced enzyme ($a^{2+}a_3{}^{2+}Cu_A{}^{+}Cu_B{}^{+}$), has spectral peaks at 605 nm and 445 nm. Ferrous cytochrome a contributes 85% to the 605 nm band while ferrous cytochromes a and a_3 contribute equally to the peak at 445 nm (Nicholls, 1972). The band at 820 nm disappears when Cu_A becomes cuprous. The fully oxidized enzyme requires four electrons in order to become fully reduced. Cytochrome oxidase can also be poised in a mixed-valence or half-reduced state with carbon monooxide bound to ferrous cytochrome a_3 and cytochrome a oxidized. In this mixed-valence (X) adduct Cu_A is oxidized and Cu_B is reduced.

The molecular weight of cytochrome oxidase is estimated at ca. 200kD The protein is 70 A in diameter and 95 A in length,

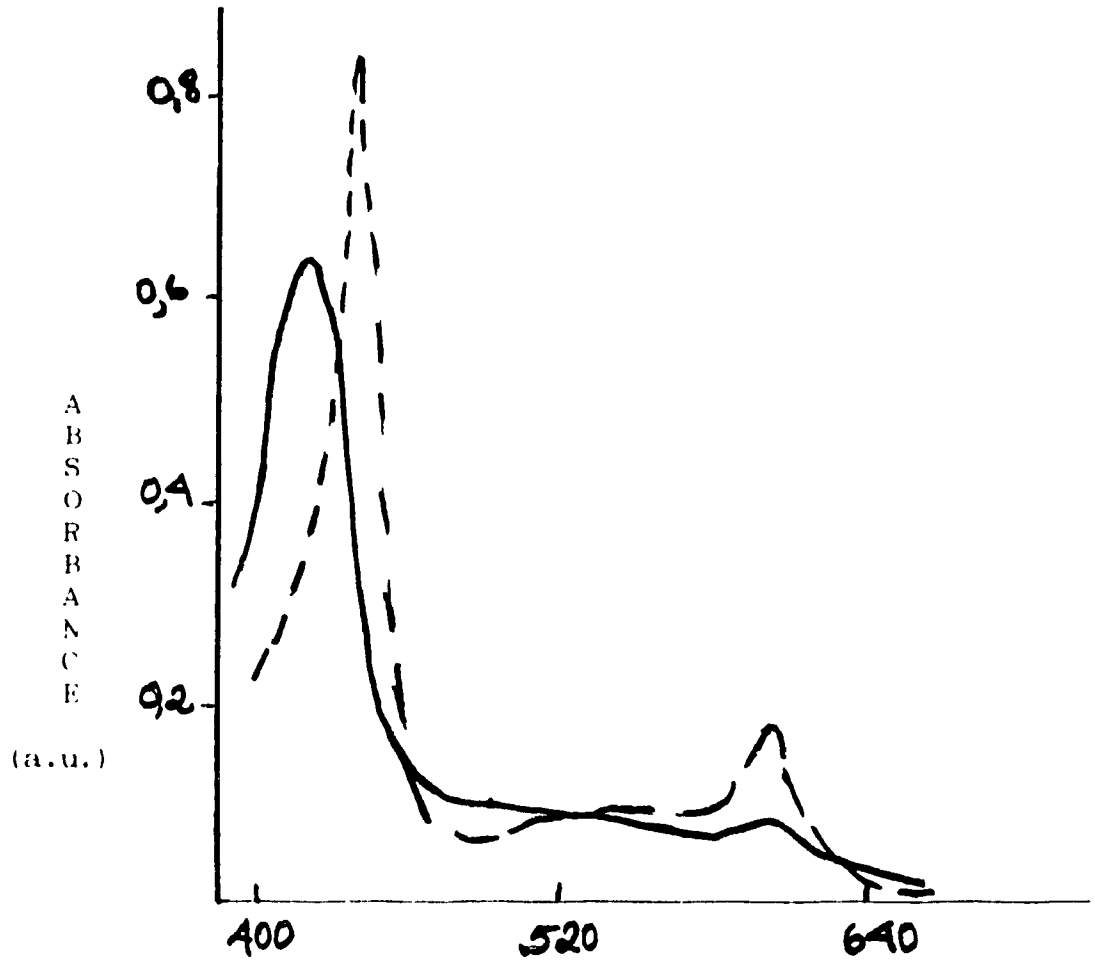

Diagram 2.2: OPTICAL SPECTRA OF CYTOCHROME OXIDASE - in the fully oxidized, resting state (____) and fully reduced state (-----).

and spans the inner mitochondrial membrane. It consists of 13 chemically distinct subunits, present in a 1:1 stoichiometry. Subunits I and II provide likely binding sites for the 4 redox active metal centers while subunit III is involved in the proton pumping phenomenon attributed to the oxidase. Cytochrome a and Cu_A are situated towards the cytoplasmic side of the membrane close to the cytochrome c binding site. Cytochrome a_3 and Cu_B are buried in the membrane closer to the matrix side and constitute the dioxygen binding site. The basic reaction catalyzed by the oxidase is the following:

$$4 \text{ cytochrome } c\text{-}Fe^{2+} + 4H^{+} + O_2 \xrightarrow{aa_3} 4 \text{ cytochrome } c\text{-}Fe^{3+} + 2H_2O$$

where cytochrome c-Fe^{2+} is reduced cytochrome c and cytochrome c-Fe^{3+} is oxidized cytochrome c.

Nicholls and Chance (1974) have proposed a sequential reaction mechanism for the reduction of aa_3 by cytochrome c (Scheme 2.1). In this scheme electrons entering through the cytochrome c binding site are shuttled from cytochrome a through the copper centers into cytochrome a_3 followed by reduction of dioxygen. The first two redox centers, cytochrome a and Cu_A are involved in catalyzing the entry of electrons into the oxidase while the latter centers are responsible for the reduction of dioxygen to water. The reduction of O_2 to water generates a large amount of energy, ΔE=550-350 mV (Papa, 1988), which is converted into a transmembranous $\Delta\mu_{H^+}$, a high-energy intermediate in oxidative-

phosphorylation. This is equivalent to the net translocation of protons from the matrix to the cytosolic side of the membrane. This phenomenon is described as the proton pumping activity of $\underline{aa}_3$.

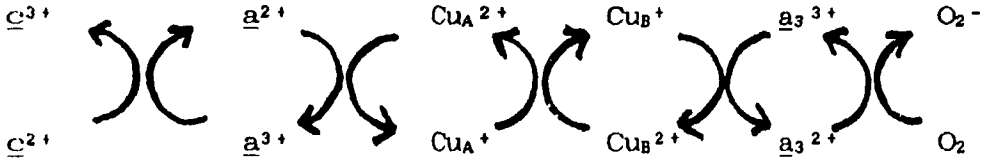

Scheme 2.1: SEQUENTIAL REACTION MECHANISM FOR THE REDUCTION OF CYTOCHROME OXIDASE.

The method by which cytochrome oxidase "pumps" protons remains a serious topic of debate, although, several proposals have been put forth. Papa's hypothetical model for proton translocation postulates that "co-operative, thermodynamic linkage between the redox state of the metals and protolytic groups in the enzyme can result in proton pumping, provided the protonation-deprotonation steps are asymmetrically and vectorially arranged" (Papa, 1988). Along this line, Malmström elaborates that electrons entering the oxidase via cytochrome a equilibrate with Cu_A. Reduction of both these centers induces a conformational change which provides access to a protolytic group, on the matrix side, to be subsequently protonated. Transfer of electrons to the $\underline{a}_3$-Cu_B site would result in the exposure of an acidic group on the cytosolic side followed by its deprotonation (Malmström, 1987). Therefore, upon electron transfer through cytochrome oxidase proton translocation is

catalyzed such that 2 protons per electron are picked up from the matrix side and one proton per electron is released into the cytosol (Wikström & Saari, 1977) (note that the second proton is utilized in the formation of H_2O)(see Diagram 2.3). The electrochemical proton gradient, $\Delta\mu_{H^+}$, generated in this reaction is subsequently utilized in the generation of ATP. Therefore, cytochrome oxidase is one of the coupling centers between respiration and oxidative-phosphorylation. The proton pumping phenomenon is supported experimentally by its observation in vesicular cytochrome oxidase. Addition of ferrocytochrome c to fully oxidized cytochrome oxidase proteoliposomes induces a decrease in the external pH. The decrease in pH is attributed to a net increase of protons in the external medium as a result of their ejection through the vesicular membrane upon cytochrome oxidase turnover.

During a normal cycle of its catalytic function cytochrome oxidase passes through different redox forms. There are two types of the oxidized form known as the resting and pulsed state and a reduced form. The resting form of the enzyme is that normally encountered prior to onset of catalytic function and is characterized spectrophotometrically by a Soret band at 417 nm. The pulsed form of the enzyme is generated upon aeration of reduced cytochrome oxidase and is characterized by a red-shifted Soret arising at 428 nm. The pulsed form accepts 4 electrons as does the resting form and has been shown to have identical EPR and MCD spectra to those observed for the resting form (Muijsers et al.,

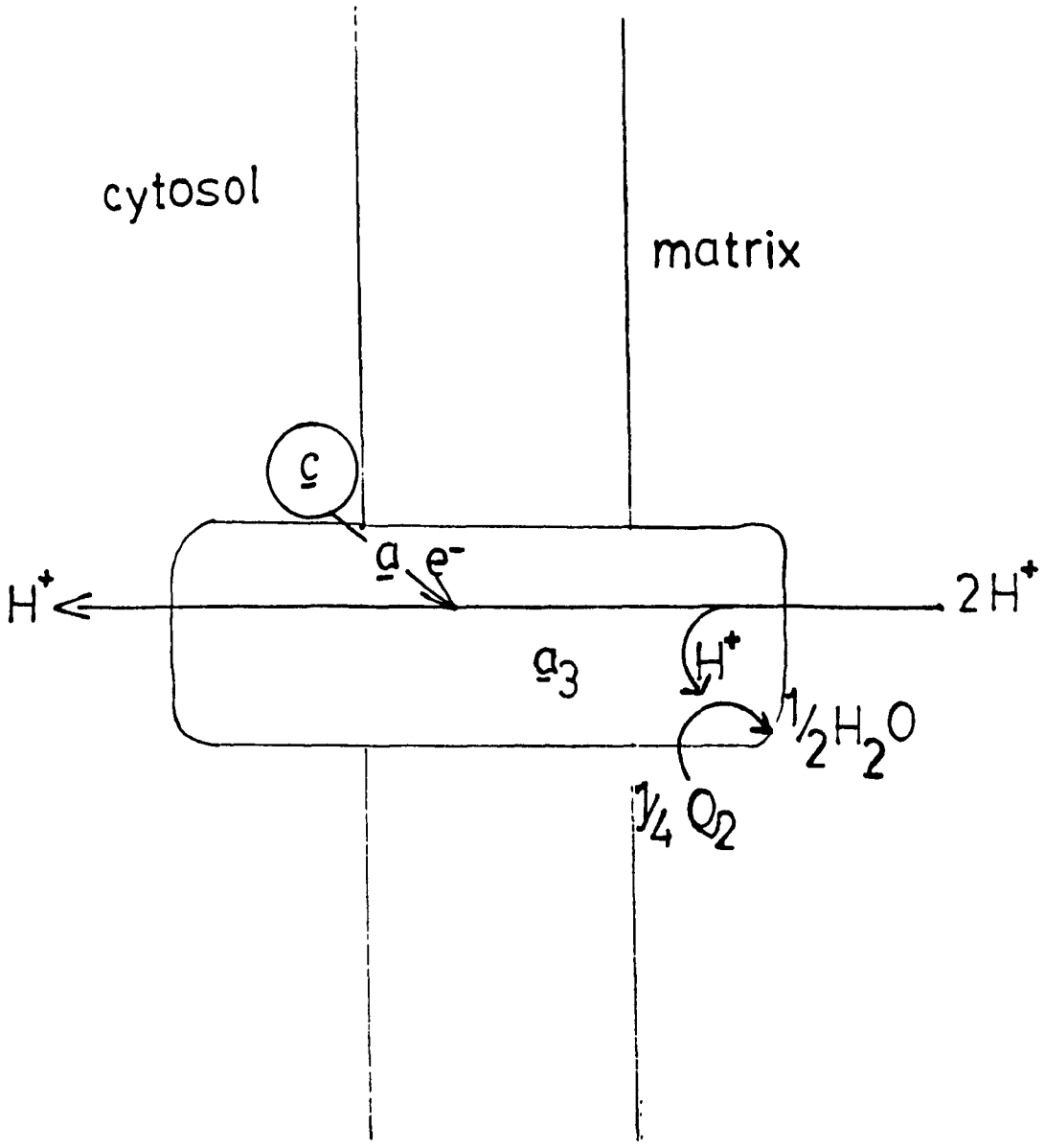

Diagram 2.3: SCHEMATIC REPRESENTATION OF THE REDOX-LINKED PROTON PUMP OF CYTOCHROME OXIDASE.

1971; Babcock et al., 1976). The CD spectrum of the oxidized forms have been observed to be different (Myer, 1972; Muijsers et al., 1971). It is believed that the pulsed form is a conformational variant of the resting enzyme.

2.2 CARBON MONOOXIDE BINDING PROPERTIES OF CYTOCHROME OXIDASE

As stated previously, each of the four metal centers of cytochrome oxidase is capable of undergoing oxidoreduction. To achieve complete reduction four electrons are required. The redox behaviour of cytochrome oxidase may be simplified if some of its metal centers are "locked" into specified redox states. This can be achieved with the use of ligands which bind at cytochrome a_3. CO is one such ligand which stabilizes both the heme of cytochrome a_3 and Cu_B in their reduced states (Wilson & Nelson, 1982).

Upon incubation of resting, fully oxidized cytochrome oxidase in a CO atmosphere under anaerobic conditions, the mixed-valence state of the enzyme is obtained. This state is defined as the "form of the enzyme in which the cytochrome a_3-Cu_B site has been reduced and bound CO, whereas cytochrome a and Cu_A remained oxidized" (Greenwood et al., 1974). Since the addition of external chemical reductants is unneccessary to achieve the partially reduced state of the enzyme, this type of reduction has been termed 'autoreduction', perhaps inappropriately. The source of electrons is most likely CO. This is substantiated by data which show that cytochrome aa_3 is able to oxidize CO to CO_2 in the presence of O_2 (Nicholls & Chanady, 1981), thereby suggesting that CO can donate electrons to the electron transfer sites of the enzyme. Bickar et

al. (1984) have also shown that not only is CO able to function as a reducing to $\underline{aa}_3$, it is also able to function in this manner with other dioxygen-binding proteins. The mechanism proposed by Bickar et al. (1984) on reduction of $\underline{aa}_3$ by CO is shown in equation 2.1. The reaction scheme presented was supported by the fact that the rate of 'autoreduction' was decreased dramatically upon lowering of the pH (Brzezinski & Malmström, 1985).

$$\begin{array}{l} \underline{a}_3\text{-}Fe^{3+} \\ \quad | \\ Cu_B{}^{2+} \end{array} + CO + 2\ OH^- \longrightarrow \begin{array}{l} \underline{a}_3\text{-}Fe^{2+} \\ \quad | \\ Cu_B{}^{+} \end{array} + CO_2 + H_2O \qquad \text{Eq.2.1}$$

The CO reduction of $\underline{aa}_3$ can be monitored spectrophotometrically in the Soret and α-band regions of the $\underline{aa}_3$ spectrum. Diagram 2.4 demonstrates the Soret and α-band regions of the $\underline{aa}_3$ spectrum upon CO reduction. The peak at 430 nm has been assigned to the formation of the $\underline{a}_3{}^{2+}$-CO species, while a shoulder at 420 nm is indicative of the oxidized state of cytochrome $\underline{a}$ (resolution inadequate in diagram 2.4). The latter point is supported by a lack of a 605 nm peak which would be associated with a reduced form of cytochrome $\underline{a}$. Therefore, incubation of fully oxidized, resting $\underline{aa}_3$ in a CO atmosphere induces the reduction of cytochrome $\underline{a}_3$ without reduction of cytochrome $\underline{a}$. Since only 2 electrons are required to fully reduce the mixed-valence oxidase one of the coppers is also reduced by CO. Greenwood et al. (1974) have shown that no spectral changes are observed in the 830 nm region of the oxidase optical spectrum upon formation of the CO-

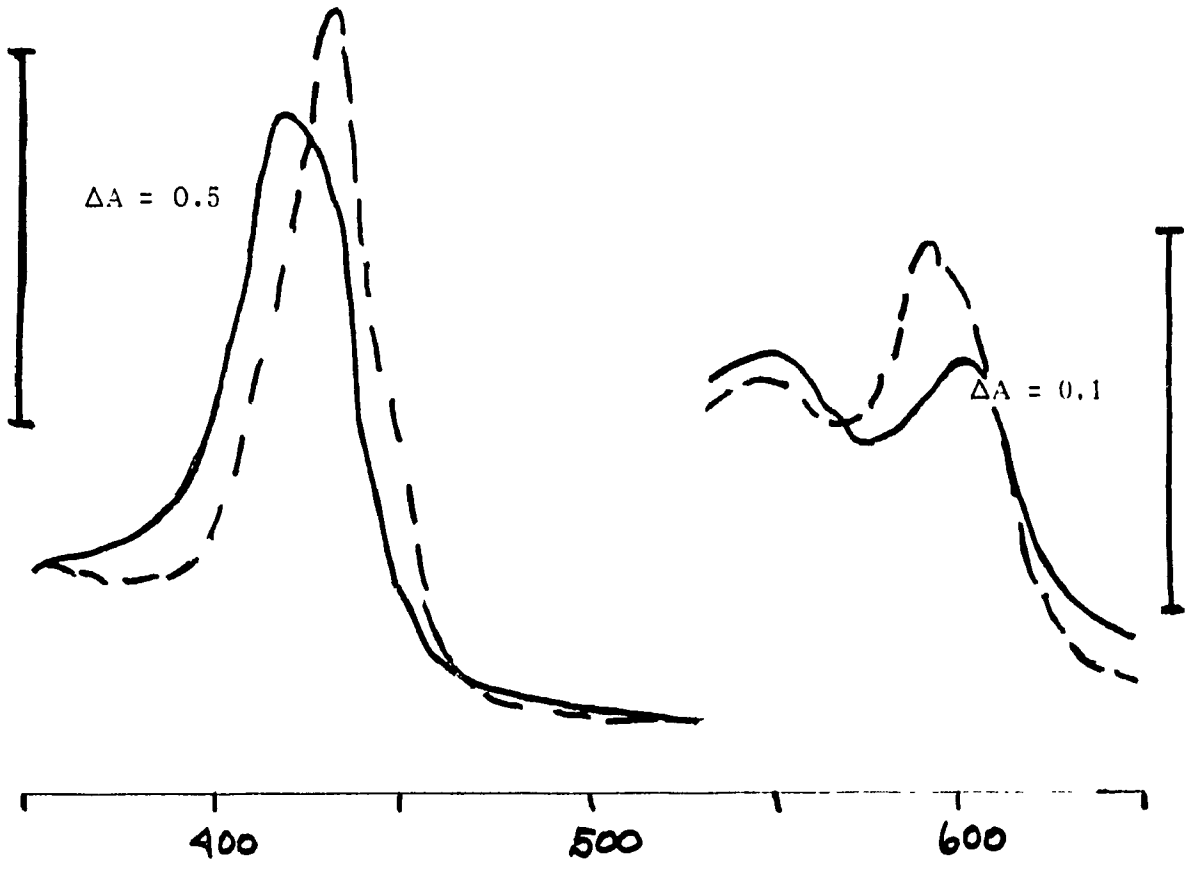

Diagram 2.4: SPECTRAL CHARACTERISTICS OF RESTING, FULLY OXIDIZED (____) AND MIXED-VALENCE CO-BOUND aa_3 (-----).

bound species, indicating that Cu_A is not reduced in the mixed-valence state of the enzyme. The second electron of the mixed-valence species must therefore reside on Cu_B. Prior to reduction of the $\underline{a}_3$-Cu_B binuclear site there is co-ordination of CO at this site. Brzezinski and Malmström (1985) demonstrated that the reaction of CO with the oxidase was biphasic. The slow, but major phase was independent of the CO concentration. They concluded that the "reduction process involves primary binding of CO to the oxidase, followed by a slow electron transfer in the complex" (Brzezinski & Malmström, 1985). This would entail an affinity for CO although cytochrome $\underline{a}_3$ is oxidized. The interaction between CO and oxidized cytochrome $\underline{a}_3$ has been established from EPR studies (Shaw et al., 1978a). They observed changes in the high-spin EPR signal of $\underline{a}_3^{3+}$, regarding its size and line shape upon interaction with CO. This proposal is contradictory to previous studies by several groups who demonstrated that both cytochrome $\underline{a}_3$ and Cu_B must be in the reduced form to bind CO (Boelens & Wever, 1980; Wever et al., 1977; Wilson & Miyata, 1977; Babcock et al., 1978). Although the actual sequence of events in the CO-oxidase reaction may still not be completely resolved, agreement is universal on the redox state of the mixed-valence species. The four metal centers of cytochrome oxidase upon interaction with CO, thereby generating the mixed-valence enzyme, are in the following redox states; cytochrome $\underline{a}$, ferric, cytochrome $\underline{a}_3$, ferrous, Cu_A, cupric, Cu_B, cuprous.

In general the pathways which the hemes of cytochrome

oxidase can take in going from fully oxidized to fully reduced are represented in diagram 2.5 (Caughey et al., 1976). Binding of CO

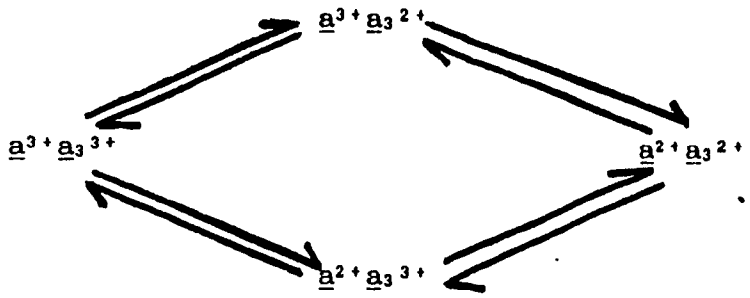

Diagram 2.5: POSSIBLE PATHWAYS IN THE REDUCTION PROCESS OF RESTING FULLY OXIDIZED CYTOCHROME OXIDASE.

to the oxidase forces the upper pathway in the reduction sequence by stabilizing the a_3 heme in the ferrous form. For this reason the carbonmonooxy derivative of the oxidase is often used in physical studies of the enzyme since it simplifies the system. For example, the dynamic interactions between CO and ferrous cytochrome a_3 and cuprous Cu_B have been studied by Fiamingo et al. (1982) using Fourier transform infrared spectroscopy. Their work showed that upon photolysis of mixed-valence CO-bound aa_3 the resultant aa_3 species consisted of a Cu_B-CO complex which relaxed to form an a_3-Fe-CO complex. Furthermore, from the CO vibrational bandwidths of the two complexes it was concluded that the environment of the ferrous complex was very non-polar and highly ordered whereas that of the cuprous complex exhibited a broader bandwidth, indicative of a wider assortment of interactions between

the complex and the dipoles of the local environment. It was concluded from the sharpness of the ferrous complex signal that Cu_B did not perturb this site, thus proposing that Cu_B is situated at a distance greater than the required interactive Van der Waal's radii of the $\underline{a}_3$-heme-CO complex.

2.3 REDUCTION OF CYTOCHROME OXIDASE BY SODIUM DITHIONITE

Dithionite reduction of biologically relevant redox proteins was first investigated by Lambeth & Palmer (1973). This chemical reductant has become the most commonly used reductant of redox proteins. In studies involving the redox-active protein cytochrome oxidase dithionite is the common alternate to the natural substrate reductant cytochrome $\underline{c}$. The reaction between dithionite and cytochrome oxidase has been extensively investigated. Studies of the reduction reaction of dithionite with cytochrome oxidase have been instrumental in differentiation of the heme contribution in the Soret and α-band regions of the oxidase heme spectra. It has been shown (Halaka et al., 1981; Jones et al., 1983) that upon rapid mixing of sodium dithionite with the resting, fully oxidized form of the oxidase redox changes are observed for at least two distinct chromophores. Two phases in the α-band region are observed. The major contribution arises from the reduction of cytochrome $\underline{a}$ and is linked to the fast phase. The minor contribution, associated with the slow phase, is due to the reduction of cytochrome $\underline{a}_3$. The reduction reaction of dithionite and cytochrome oxidase can be represented schematically as shown in Scheme 2.3. k_{obs} is the observed pseudo-first order rate constant

for rapid reduction of cytochrome a at a given total concentration of reductant. The nature of the reactive reducing species is irrelevant in this scheme. Internal electron transfer from cytochrome a to a_3 follows the initial reduction of cytochrome a and is characterized by the rate constant, k_1. Therefore, reduction of cytochrome oxidase is achieved by donation of

$$\text{reductant} + a^{3+}a_3^{3+} \xrightarrow{k_{obs}} a^{2+}a_3^{3+} \qquad (1)$$

$$a^{2+}a_3^{3+} \xrightarrow{k_1} a^{3+}a_3^{2+} \qquad (2)$$

$$\text{reductant} + a^{3+}a_3^{2+} \longrightarrow a^{2+}a_3^{2+} \qquad (3)$$

Scheme 2.3: SIMULATION OF THE REDUCTION OF CYTOCHROME OXIDASE BY SODIUM DITHIONITE.

electrons from dithionite to cytochrome a followed by subsequent electron transfer to cytochrome a_3. The redox sites cytochrome a and Cu_A are in rapid redox equilibrium, $1/\tau=100\ s^{-1}$ (Greenwood et al., 1976), such that electrons donated directly to cytochrome a would be rapidly transferred to Cu_A. Redox studies of cytochrome oxidase with N-methylphenaziniummethylsulphate (Halaka et al., 1981), hexaaquochromium (II) (Greenwood et al., 1977) and hexaammineruthenium(II) (Scott & Gray, 1980) have all shown that the initial site of electron entry is cytochrome a followed by intramolecular reduction of cytochrome a_3. Jones et al. (1983)

have shown that at concentrations of dithionite less than 50 μM it appears that cytochrome $\underline{a}_3$ is reduced first. This artifact arises since at these low concentrations the internal electron transfer from cytochrome $\underline{a}$ to cytochrome $\underline{a}_3$ is more rapid than the original electron transfer from the reductant to cytochrome $\underline{a}$.

The solution chemistry of the reaction between sodium dithionite and metalloproteins, in general, under strict anaerobic conditions, as postulated by Jones et al. (1983) is shown in Scheme 2.4 . Dissociation of dithionite to the anion radical gives rise to

$$S_2O_4^{2-} \underset{k_a}{\overset{k_D}{\rightleftharpoons}} 2\ SO_2^{\bullet -} \qquad (1)$$

$$S_2O_4^{2-} + P_{ox} \xrightarrow{k(S_2O_4^{2-})} P_{red} \qquad (2)$$

$$SO_2^{\bullet -} + P_{ox} \xrightarrow{k(SO_2^{\bullet -})} P_{red} \qquad (3)$$

Scheme 2.4: SOLUTION CHEMISTRY OF THE REACTION OF DITHIONITE WITH METALLOPROTEINS.

the possibility of two reducing species since, in principle, both $S_2O_4^{2-}$ and $SO_2^{\bullet -}$ are reducing agents. The rate constants stated in reaction 1 of Scheme 2.4 have been determined to be :- $k_D = 1.7\ s^{-1}$ and $k_a = 2 \times 10^9\ M^{-1}s^{-1}$ (Lambeth & Palmer, 1973). Although the existence of the dithionite anion $S_2O_4^{2-}$ is favoured the anion radical, $SO_2^{\bullet -}$ is a much more reactive species. In general, both species act as reducing agents as supported by the fact that the rate of reduction of the metalloprotein is not strictly linear with

respect to the dithionite concentration (Jones et al., 1983). Determination of the rate constants for the reduction of metalloproteins by either $S_2O_4^{2-}$ or $SO_2^{\bullet-}$ has shown that the rate constant for radical reduction is approximately 10^4 times greater than reduction by di-anion. The rate constants for the reduction of cytochrome $\underline{aa_3}$ were determined by Jones et al. (1983) to be $k(SO_2^{\bullet-})=8.4 \times 10^4\ M^{-1}s^{-1}$ and $k(S_2O_4^{2-})=18.8\ M^{-1}s^{-1}$. By comparison, reduction of cytochrome $\underline{c}$ by the same reducing species yielded rate constants of a fairly larger magnitude, $4.59 \times 10^7\ M^{-1}s^{-1}$ and $1.5 \times 10^4\ M^{-1}s^{-1}$ (Lambeth & Palmer, 1973). The decrease in the reduction rates of cytochrome oxidase compared to those for cytochrome $\underline{c}$ suggests that the reduction site of the oxidase is kinetically inaccessible by comparison. This is consistent with the postulated sites of entry. In the oxidase, cytochrome a is not on the surface but buried. By contrast, the heme of cytochrome c is more surface accessible. Electrostatic interactions between the metalloproteins and the reducing agent also play a major role. In the case of cytochrome $\underline{c}$, the surrounding amino acid environment of the heme crevice is largely positively charged in nature, the probable function being in directing negatively charged redox reactants to the redox center. By contrast, the amino acids in the vicinity of cytochrome $\underline{a}$ of cytochrome oxidase can be postulated to be largely negative in nature due to the strong electrostatic interaction between cytochrome $\underline{c}$ and cytochrome oxidase. If this is true, then reductants such as $S_2O_4^{2-}$ and $SO_2^{\bullet-}$ would be repulsed by this site. This notion is supported by the differences seen in

the reduction rate constants. Based on the possible electrostatic role existing between reductant and the oxidase, the anion radical is expected to be the least affected by the possible electrostatic repulsion between the two reactants. In addition the anion radical is a smaller species. The combination of a decreased size and charge supports the higher reactivity of $SO_2^{\bullet -}$ with the oxidase.

2.4 PHOTOREDUCTIVE PROPERTIES OF DEAZAFLAVIN

The photoreductive properties of deazaflavins and their potential use as reductants of hemeproteins were first reported by Massey and Hemmerich (1977). The deazaflavins were presented as alternatives to the more commonly used chemical reductants, such as, ascorbate, dithionite, reduced dyes and hydrogen/Pt or Pd systems. These chemical reductants of oxidation-reduction proteins all have certain drawbacks associated with them. Due to its relatively high redox potential, ascorbate is a poor reductant and often of limited utility. The use of dithionite requires either strict anaerobic conditions, or reactive and spectrophotometric tolerance of excess reagent. Reduced dyes add an extra chromophore to the experimental system rendering spectrophotometric analysis more complicated. Direct electrochemical reduction requires special experimental set-ups since the catalyst must be filtered out prior to spectrophotometric analysis. By contrast, photoreduction by deazaflavins offers several advantages. Catalytic amounts of deazaflavin are used thereby generally not interfering with the absorption spectra of the protein under investigation. Careful control of light

intensity and illumination period can be used to quantitatively generate different redox states in a multi-redox center protein. The use of stable oxidants such as ferricyanide can be used to titrate the photochemically reduced protein in order to ascertain the number of reducing equivalents fed into the protein. Furthermore, the reactive species, the deazaflavin radical, has a very low potential and a high reactivity making it capable of reducing any number of hemeproteins, even those which are generally unreactive to dithionite, such as catalase.

The deazaflavin system requires three basic ingredients, deazaflavin, EDTA and light. The catalytic effect of deazaflavin is derived from photochemical generation of the deazaflavin radical. In these photochemical reactions the ultimate source of reducing equivalents is ethylenediaminetetraacetate (EDTA). Although the deazaflavins encompass several photocatalytic flavins emphasis will be placed on 3,10-dimethyl-5-deazaisoalloxazine, the photocatalyst used in this study.

The choice of using deazaflavin as a reductant of cytochrome oxidase was based primarily on the possibility of utilizing such low quantities of the catalyst that the absorption spectrum of the hemeprotein would remain virtually unchanged. A scheme explaining how deazaflavins function in photoreduction of hemeproteins has been proposed by Massey and Hemmerich (1978) (Scheme 2.5). The active reductant is the flavin radical which is generated upon further illumination of the EDTA-light product, $(dzH)_2$.

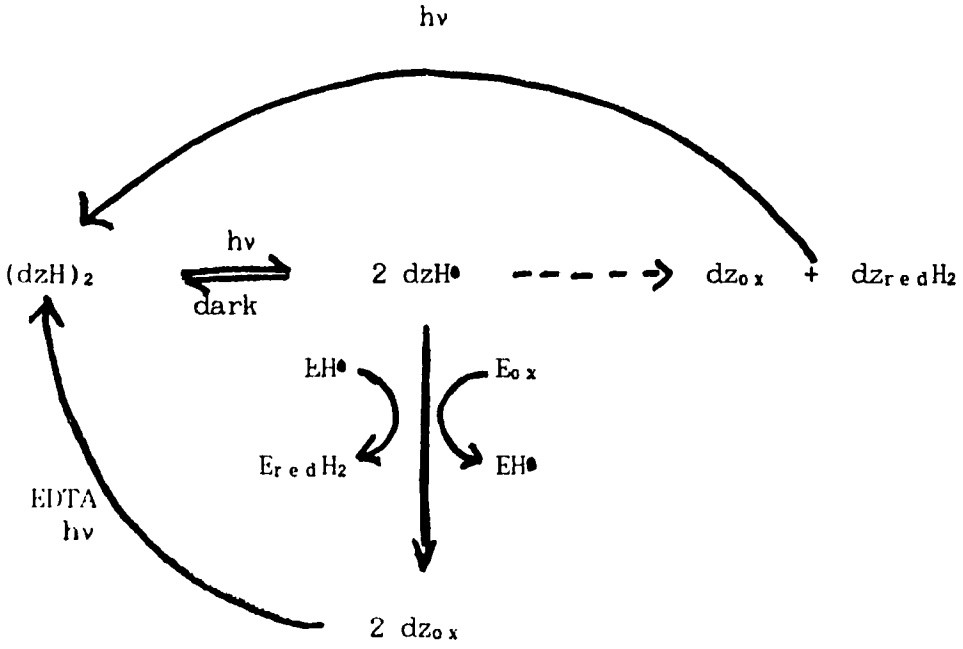

Scheme 2.5: SCHEME PROPOSED BY MASSEY AND HEMMERICH FOR THE CATALYTIC ROLE OF DEAZAFLAVINS IN PHOTOCHEMICAL REDUCTIONS.

The redox potential of the $dz_{ox}/dzH^{\bullet}$ couple has been measured polarographically to be approximately -0.65V at pH=7.0 (Blankenhorn,1976), therefore, the flavin radical constitutes a very powerful one-electron reductant.

As previously mentioned, several hemeproteins have been shown to be easily reduced by catalytic amounts of deazaflavin in the presence of EDTA upon irradiation (Peterson et al., 1977; Massey & Hemmrich, 1977). More recently, Nicholls and Chanady (1981) demonstrated that 3,10-dimethyl-5-deazaisoalloxazine was capable of fully reducing cytochrome oxidase in the presence of

light. The use of deazaflavin as reductant in studies of cytochrome oxidase eliminates the often occurring side reactions involved in the use of dithionite. Therefore, deazaflavin appears to be an appropriate alternative to the more conventional chemical reductant.

2.5 CONFORMATIONAL CHANGES IN CYTOCHROME OXIDASE

The notion that protein molecules are static entities has long been discarded. Whether in solution or in crystal-form it is universally accepted that protein molecules have a dynamic nature allowing for conformational motions. Of all the possible motions experienced by such a molecule it is highly probable that some will be of functional significance. The individual residues of a protein will occupy a certain region of conformational space due to fluctuations which occur around the average structure of the molecule (Campbell et al.,1985). Due to these fluctuations the conformational state observed will consist of average conformations which are experimentally indistinguishable. Different conformational states arise from distinguishable differences in the average conformations. These major changes are the most likely associated with the function of the molecule.

In cytochrome oxidase the relationship between conformation and redox activity or ligand binding has in the past two decades been given considerable attention. In the early seventies Yamamoto & Okunuki (1970) demonstrated that ferrous cytochrome $\underline{aa}_3$ was more susceptible to proteolysis than its ferric form. Their work was the first indication that a conformational

change occurred upon reduction of the oxidase. Since then numerous groups have gathered evidence which suggests that the oxidase undergoes a conformational change upon reduction (Urry et al., 1972; Cabral & Love, 1972; Van Buuren et al., 1972; Kornblatt et al., 1975). Furthermore, it has been shown by several groups that oxidized cytochrome oxidase can in fact exist in different conformations (Muijsers et al.,1971; Antonini et al.,1977; Rosen et al.,1977; Shaw et al.,1978b; Petersen & Cox,1980). The two most easily discerned conformations are the resting and pulsed oxidase. The former is present in the oxidase as isolated while the latter is transiently obtained upon re-oxidation of reduced oxidase by O_2. These two species may be distinguished by the position of their Soret maxima (Okuniki et al.,1958). The pulsed and resting enzyme states have the same oxidation level and thus the spectroscopic differences observed between them are postulated to arise from conformational differences. Besides their Soret differences these conformers can be distinguished by their respective reactivities with O_2. Upon mixture with reductant and O_2, the resting conformation has been shown to react slowly with O_2 while the pulsed conformation reacts rapidly (Antonini et al.,1977; Rosen et al.,1977). The resting enzyme is believed to consist of more than one conformation such that the Soret maximum observed is an average contribution of all the existing conformers. This is based on the wide range of Soret maximum values obtained, 417-424 nm, from freshly isolated oxidase (Lemberg,1969). Although the pulsed enzyme does not present such a variation in its Soret maximum, it

has nonetheless been shown to also consist of different conformers. Shaw et al. (1978b) demonstrated that at least two distinct conformers exist 'within' the pulsed population. These appear to form sequentially upon re-oxidation of the enzyme with O_2. These species are distinguishable by their respective EPR signals. It should be noted that the resting enzyme obtained after a cycle of reduction and re-oxidation by O_2 does not always exhibit the same Soret maximum as did the starting uncycled resting oxidase (Muijsers et al.,1971). More recently Brudvig et al. (1981) found evidence that the freshly isolated enzyme consists of at least three conformers together forming what is generally referred to as the resting enzyme. These conformers, which are not in rapid equilibrium, accounted for approximately 100% of the total enzyme and can be distinguished on the basis of their EPR properties. The percentage of each is shown to vary among preparations accounting for the variation in the Soret maximum of the resting enzyme in different preparations. The three conformers are denoted as resting, g12 and pulsed. The transient conformer g5 produced upon re-oxidation of reduced $\underline{aa}_3$ was observed to relax into the pulsed conformation, identified by a Soret at 428 nm and the lack of EPR signal at g=5, 1.78 and 1.69. A percentage of the pulsed enzyme relaxes further to produce a g12 conformer, characterized by an EPR signal at g'=12. The resting conformer was not observed upon re-oxidation of reduced $\underline{aa}_3$ such that its existence was restricted to the freshly isolated enzyme. The occurrence of more than one conformer in the isolated enzyme creates certain complications in

the interpretation of physical data of the oxidase since it is not certain if the various conformers exhibit identical properties, e.g. in the affinity of each towards cytochrome c.

The search for conformational changes in cytochrome oxidase derives its enthusiasm from the possibility that such changes may be the link between electron transport and proton translocation. In this quest Kornblatt & Williams (1975) have shown that the 418-424 nm form of the enzyme was prevalent in oxidase undergoing low turnover, whereas the 428 nm form appeared as electron flow through the enzyme was increased. These two forms of the enzyme have also been shown to be linked directly through a protonation-deprotonation reaction (Kornblatt, 1977; Kornblatt, 1980). The 418 nm form being the high spin, protonated conformation while the 428 nm form is the low spin deprotonated conformer. As mentioned previously, the ability of the aa_3 to function as an electron transport-driven proton pump resides in its capability of undergoing protonation-deprotonation reactions as a direct result of the redox state of the enzyme. The establishment of the occurrence of conformational changes in the enzyme during its turnover provides a possible mechanism by which the pK's of groups involved in the protonation-deprotonation process may be modulated. The redox-linked conformational transition occurring between resting and pulsed aa_3 has been shown to be too slow to participate in the proton pump (Brunori et al.,1979). Besides the afore mentioned conformers, 'open' and 'closed' conformations have also been attributed to the oxidized enzyme. The 'closed'

conformer is characterized by its slow binding of CN^-. Conversion of the 'closed' conformer to the 'open' conformer can be achieved upon partial reduction of the oxidized enzyme conformer. The 'open' conformer rapidly reacts with cyanide. The interconversion between the 'closed' and 'open' conformations has been monitored to be rapid enough to occur during turnover (Jones et al.,1984). Scholes & Malmström (1986) demonstrate that the 'open' conformation of $\underline{aa}_3$ is generated upon a two-electron transfer to the resting enzyme. These authors also observe that internal electron transfer to the $\underline{a}_3$-Cu_B site does not occur in oxidase having only one reduced center, which suggests that this transfer may require the enzyme to be in the 'open' conformation. In the event that 'closed ----> open' transitions provide the alternating access of acid-base groups, then this transition could be the coupling step between electron transfer and proton translocation in cytochrome oxidase. The requirement of a two-electron addition to generate the 'open' conformer attributes this conformational change to the reduction of cytochrome $\underline{a}$ and Cu_A. The involvement of these sites in the conformational change is supported by recent work. Ellis et al. (1986) calculated the thermodynamic parameters associated with reduction of the oxidase. From their work the standard entropy of reduction, ΔS^o was calculated to be large and negative suggesting that a significant conformational change occurred upon reduction of cytochrome $\underline{a}$. Based on the shift in the Cu_A EPR resonance line shape observed upon reduction of the cytochrome $\underline{a}$ heme, it has been proposed that reduction of cytochrome $\underline{a}$ induces a structural change

at the Cu_A site (Brudvig et al.,1984). This has subsequently led to the proposal that Cu_A may be directly involved in the energy transduction property of the oxidase (Wang et al.,1986). Michel & Bosshard (1989) have recently shown that the biphasic behaviour of cytochrome oxidase towards the cytochrome c concentration is due to the conformational transition phenomenon of the oxidase. The conformational transition mechanism of cytochrome oxidase is proposed as a method of regulating and coupling electron transfer and proton translocation (Malmström,1985; Brzezinski & Malmström,1986). This mechanism envisages the oxidase oscillating between two conformers, one with a high affinity for cytochrome c and the other with a low affinity. The transition between the conformers would be strongly related to the electron transfer process of the system. The two conformers would provide the appropriate intermediates required for the vectorial translocation of protons.

Based on the known existence of different conformations of the oxidase this study aims to determine whether the intrinsic steady-state tryptophan fluorescence of the oxidase can be used as a novel method of differentiating these conformers. The specific conformers that will be studied are the resting (as isolated), mixed-valence CO-bound, fully reduced (with or without CO-bound) and pulsed.

2.6 GENERAL CHARACTERISTICS OF FLUORESCENCE

Fluorescence is basically the emission of a photon from a singlet excited state. By contrast, emission of a photon from a

triplet excited state is termed phosphorescence. The difference between these two states lies in the spin orientation of the high energy level electron relative to that found in the lower energy level. In the singlet excited state both electrons are considered paired because they have opposite spin orientations. Unpaired electrons are those whose spin orientations are identical, such as those found in a triplet excited state. In order for an unpaired electron to return to the ground state from a triplet state a change in spin orientation must occur prior to emission. Fluorescence, can therefore be alternatively termed as the emission observed upon return of a paired electron to the ground state. Since these transitions are allowed emission rates are relatively fast and fluorescence lifetimes average 10 nanoseconds. The fluorescence lifetime is simply the lifetime of the excited state of the fluorescing species. Due to forbidden transitions from an excited triplet state to a singlet ground state, emission rates are relatively slow since they depend on deactivation processes differing from those seen in fluorescence emission. Phosphorescence lifetimes range from milliseconds to seconds.

Fluorescence is best described using the Jablonski diagram (Diagram 2.6). S_0, S_1 and S_2 represent the ground, first and second electronic states, respectively. Each electronic state can subsequently be subdivided into vibrational levels denoted simply as 0, 1, 2 etc. A fluorophore in any of the electronic states may reside within any of these vibrational levels, although, the overwhelming majority tend to reside primarily in the lowest

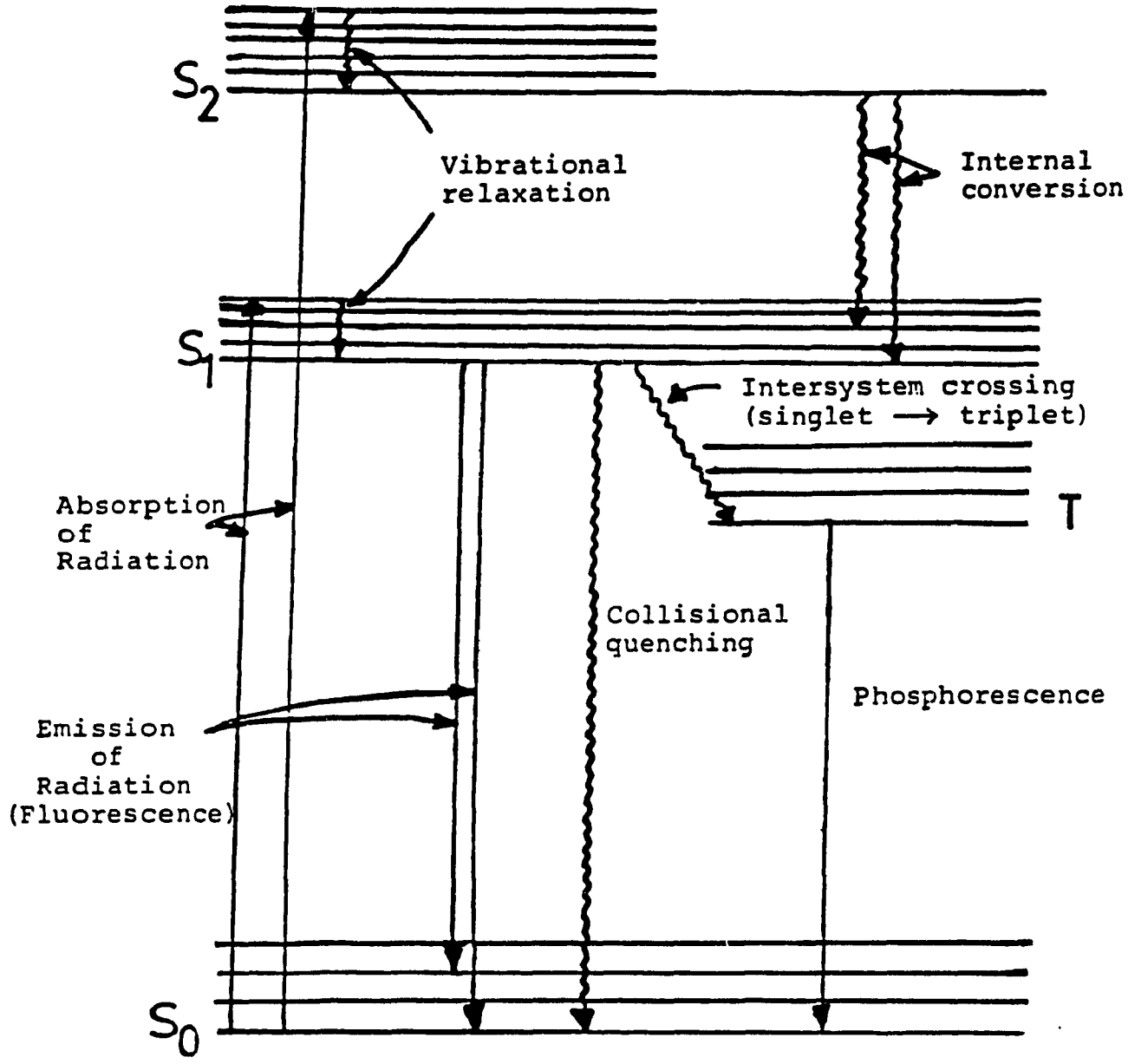

Diagram 2.6: JABLONSKI DIAGRAM - summarizing processes which occur upon absorption of radiation.

energy vibrational level, 0. Distribution of the electronic population amongst vibrational levels is accomplished simply with thermal energy. Thermal energy is insufficient to distribute the electrons amongst the different electronic levels to any significant extent due to the large energy differences between these levels.

The Franck-Condon principle states that no displacement of nuclei can be observed on the time scale for absorption of light, which is typically 10^{-15} seconds. For this reason, upon absorption of light the transitions effectuated between the different electronic levels are termed vertical and considered to be instantaneous. Excitation of an electron residing in the ground state, S_0, upon absorption of light causes it to occupy a higher vibrational level in S_1. Internal conversion, which occurs ususlly in 10^{-12} seconds, is simply the relaxation to the lowest vibrational level of an electron in the excited state. Internal conversion is complete prior to emission due to the short time required to thermally equilibrate the electronic population in S_1. Fluorescence emission is observed upon return of the thermally equilibrated S_1 electron to the ground state, S_0. Inter-system crossing arises when electrons in S_1 are converted to the triplet state, T_1. Transition from T_1 to S_0 is forbidden, therefore the lifetime of this transition is much longer than that seen for an S_1 to S_0 transition. Emission from T_1, phosphorescence, is shifted to longer wavelengths as compared to fluorescence due to the large loss in energy as a result of non-radiative deactivation processes.

The common denominator in the chemical structure of any fluorophore is typically the presence of delocalized electrons derived from conjugated double bonds. Generally, fluorescence spectral data are expressed in the form of a plot of fluorescence intensity, in arbitrary units, as a function of wavelength, in nanometers. These emission spectra are basically a reflection of the vibrational levels of S_0. By contrast, the vibrational levels of the electronically excited states, S_1 and S_2, are reflected in absorption spectra. Generally, fluorescence emission is observed at longer wavelengths compared to absorption. These shifts to lower energy are termed Stokes' Shifts and are commonly due to 1) rapid internal conversion and 2) transitions from S_1 to higher vibrational levels of S_0. Together these occurrences amount to a net loss of vibrational energy in the system. Excited state reactions and interactions with the solvent also contribute to Stokes' Shifts. The former is mostly due to collisional encounters of the excited states with other molecules, causing relaxation of the excited state. The latter can be distinguished by solvent dependent emission spectra. It should be noted that excitation on the extreme red-edge of the absorption band often yields emission spectra which are shifted to longer wavelengths. This is due to the selection of fluorophores which are interacting strongly with the solvent. Generally, emission spectra are independent of excitation wavelength.

In terms of studying molecular dynamics, fluorescence spectroscopy is preferred over absorption spectroscopy. The latter

method is insensitive due to its determination from the ground state of the molecules which absorb light. Absorption spectra will, therefore, only be affected by the solvent shell directly surrounding the given chromophore. Alternatively, the length of the lifetime of the excited state allows for any process occurring within that time frame to contribute to the fluorescence spectrum. Solvent interactions, therefore, play a key role in the interpretation of fluorescence spectra. These interactions are in the form of solvent relaxation. Upon absorption of light, the excited fluorophore generally has an increased dipole moment in comparison to the ground state. In the case where the solvent also has a dipole moment (e.g. aqueous media), the solvent will orient itself about the excited state dipole such that it decreases the energy of the excited state. This orientation of dipole moments resulting in lowered energy is termed as solvent relaxation and in fluid solvents occurs in 10^{-12} seconds (Lakowicz, 1983). An increase in the solvent relaxation process causes increased Stokes' Shifts. If no energy loss processes occurred, then the fluorescence emission maximum would coincide with the absorption maximum.

For a given fluorophore differences in emission spectra can be accounted for by differing solvent relaxation processes. The greater the Stokes' Shift, the more energy is dissipated by solvent relaxation. In the case of tryptophans buried in the protein matrix, solvent accessibility is insignificant, therefore, solvent relaxation is not a major contibuting factor. For this

reason the Stokes' Shift is not as pronounced for buried tryptophans as compared to surface tryptophans.

Proteins may contain three possible amino acid fluorophores. These fluorophores are simply the amino acids, phenylalanine, tyrosine and tryptophan, all of which absorb in the ultra-violet region of the absorption spectrum (Diagram 2.7). The dominant fluorescing species of these aromatic amino acids is tryptophan. The emission spectra of the aromatic amino acids is shown in diagram 2.8. Tyrosine and tryptophan emission may be distinguished by their relative emission maxima and by their respective sensitivities to polar environments. Tyrosine emission is insensitive to polarity but the indole nucleus of tryptophan is extremely sensitive to polarity. Tryptophan emission may range from 320 nm to 350 nm, depending on whether the environment of the indole nucleus is hydrophobic or hydrophilic, respectively. For single tryptophan containing proteins, the emission spectrum is reflective of the environment of that single fluorophore. In multitryptophan proteins, emission spectra are a compilation of the individual tryptophans and therefore reflect the total average nature of the fluorescing species. Variations in the emission maxima are due to the variable average location of tryptophans in the protein. The emission maximum is, therefore, an indicator of the average localization of the tryptophans. Denaturation of proteins may be visualized as a red-shift in the tryptophan emission maximum to 350 nm. The shift to longer wavelengths of the emission maximum indicates that in the native protein the three-

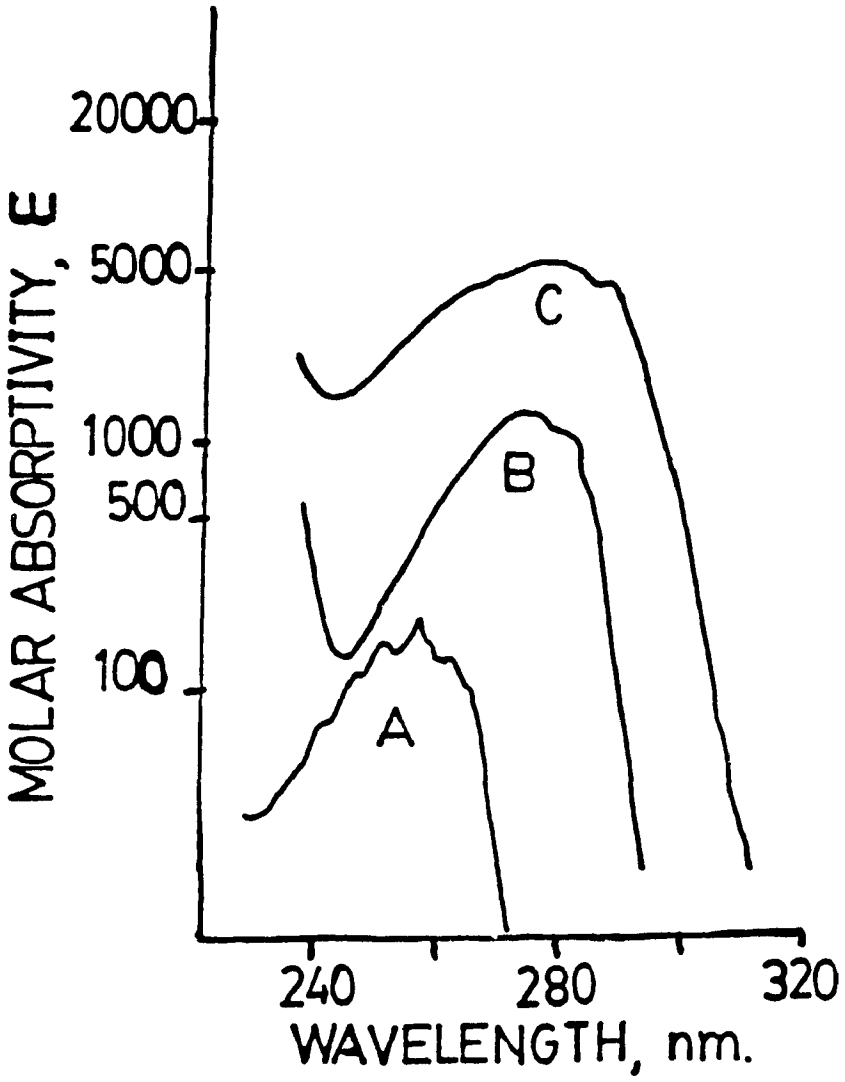

Diagram 2.7: ABSORPTION SPECTRA OF THE AROMATIC AMINO ACIDS - phenylalanine (A), tyrosine (B) and tryptophan (C). The excitation wavelengths are 250 nm and 280 nm for phenylalanine and tyrosine/tryptophan, respectively. Adapted from Lakowicz (1983).

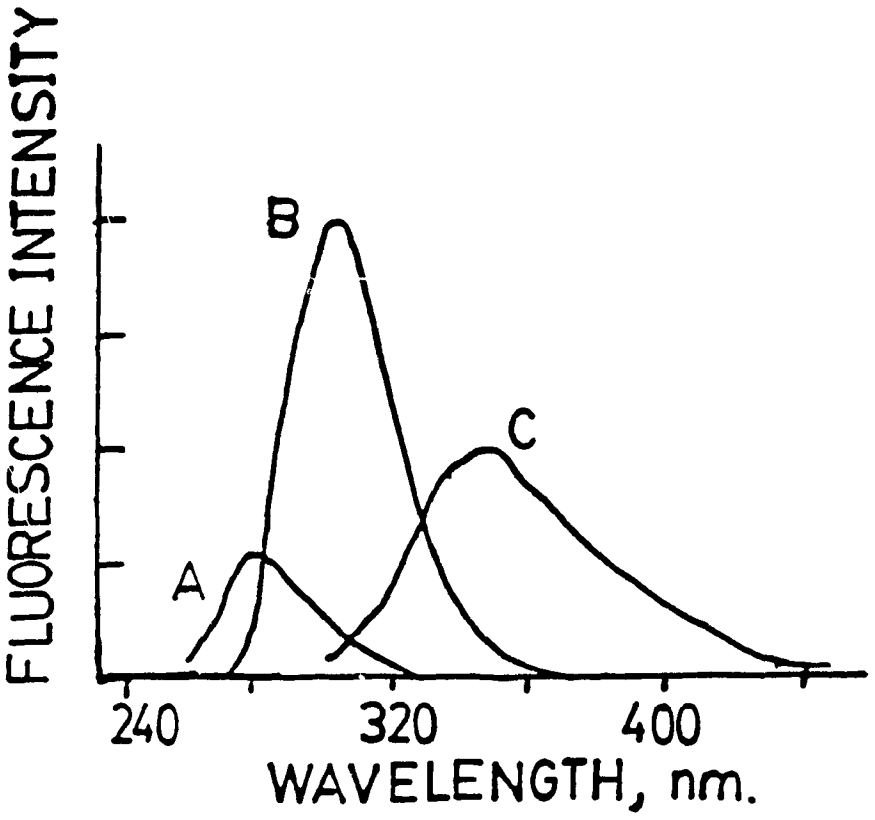

Diagram 2.8: FLUORESCENCE EMISSION SPECTRUM OF THE AROMATIC AMINO ACIDS - phenylalanine (A), tyrosine (B) and tryptophan (C). Adapted from Lakowicz (1983).

dimensional structure of the protein matrix shields the fluorophore from the external aqueous phase. The extent of shielding depends on the depth to which the tryptophan residues are buried. Emission maxima as low as 308 nm have been reported for azurin (Eftink & Ghiron, 1976). This extremely blue-shifted maximum has been speculated to be due to the excessively hydrophobic nature of the tryptophan environment, to the extent that no hydrogen bonding involving tryptophan occurs.

The occurrence of shifts in the emission maximum can be used to monitor the action of various processes on a specific protein exhibiting tryptophan fluorescence. Such processes may include association of the protein with a ligand or substrate, association of a protein complex and association of a protein with lipids. The association of mellitin with itself and with lipids has been shown to cause a blue-shift in the emission spectra of mellitin (Talbot et al., 1979; Faucon et al., 1979) indicating that upon associatin the fluorescing tryptophan residues have become more shielded from a hydrophilic environment. Such blue-shifted spectra in proteins arise from the inability of the solvent molecules to organize their dipole moments around the fluorophore in order to decrease the energy of the excited species. A decreased loss of energy occurs in buried tryptophans as compared to surface tryptophans.

Not only is the three-dimensional structure of importance in tryptophan fluorescence but also in tyrosine fluorescence. In the case of tyrosine, the three-dimensional

structure causes the tyrosine fluorescence to be negligible. Upon denaturation tyrosine fluorescence is enhanced. The absence of significant tyrosine fluorescence in most proteins is due to either energy transfer from tyrosine to tryptophan or quenching of tyrosine fluorescence by spatially close amino acids such as glutamate or aspartate. The Förster distance for tyrosine-tryptophan energy transfer is 10-18 Å (Lakowicz, 1983). Therefore, tyrosine emission will be efficiently quenched within this radius by tryptophans. Charged carboxyl groups or neutral amino groups will readily quench tyrosine fluorescence due to ready acceptance of the hydroxyl proton by these proton acceptors. Although, tyrosine fluorescence may be quenched by the presence of nearby proton acceptors, hydrogen bonding of the hydroxyl group enhances the possibility that upon excitation of tyrosine, ionization occurs. The excited state ionization product, tyrosinate, has been shown to be fluorescent, albeit not strongly (Shimizu & Imakuvo, 1977; Behmaarai et al., 1979; Szabo et al.,1978). Tyrosinate emission is observed at 345 nm and its spectral properties are comparable to those of tryptophan. The extent of this contribution in protein fluorescence is unkown but its possible occurrence must be considered in spectral analysis of protein fluorescence.

3. METHODS AND MATERIALS

3.1 TRYPTOPHAN FLUORESCENCE OF CYTOCHROME OXIDASE

3.1.1 PROTEIN SAMPLES AND DATA MANIPULATION

Cytochrome oxidase was isolated from beef heart submitochondrial particles, prepared by the method of Yonetani (1966), following the procedure of Kuboyama et al (1972). The 280 nm to 420 nm ratio was ca. 2.5 for all cytochrome oxidase samples used. Details on the experimental set-up for cytochrome oxidase studies are specified in individual segments of the accompanying text.

Spectrophotometric data were acquired on a Shimadzu UV-160 UV-VIS recording spectrophotometer. Fluorescence data were acquired from either a Perkin-Elmer fluorescence spectrophotometer, Model MBF-44B or a Shimadzu RF-5000 spectrofluorophotometer. Fluorescence spectra were corrected for inner filter effects using equation 3.1 (Lakowicz, 1983).

$$F_{cor} = F_{obs} \times \text{antilog}\,[(A_{ex} + A_{em})/2] \qquad \text{Eq.3.1}$$

where F_{cor} is the corrected fluorescence intensity, F_{obs} is the observed fluorescence intensity, A_{ex} and A_{em} are the absorbance values at the excitation and emission wavelengths, respectively. Emission spectra were digitized and corrected at 2 nm intervals within the emission range monitored. Absorption spectra were obtained prior and subsequent to fluorescence data acquisition to ensure that the sample was stable. A maximum deviation of 2% was sometimes observed during the time required to acquire fluorescence

data.

The fluorescence emission maximum of cytochrome oxidase differed by 2 nm when data were acquired using both fluorimeters. This discrepancy may be attributed to the differences in the optics of both instruments.

3.1.2 PREPARATION OF MIXED-VALENCE CO-BOUND CYTOCHROME OXIDASE

Mixed-valence CO-bound cytochrome oxidase was prepared using the following procedure: 250 µl of 121 µM aa_3 was diluted to a concentration of 7.58 µM in 20 mM Tris-Cl, 1 mM EDTA, 0.1 M NaCl, 1 mg/ml lauryl maltoside, pH7.8. The sample was sealed in a 1.5 ml fluorescence quartz cuvette. The sealed sample was put under vacuum and flushed with N_2 gas several times. Finally, the sample was flushed with CO for 3 minutes. CO binding to aa_3 was monitored spectrophotometrically in the visible region at regular time intervals. The optical spectra collected during the formation of mixed valence CO-bound $\underline{aa}_3$ are shown in figure 3.1. Time zero is taken as immediately after CO addition to the enzyme solution. Difference spectra between the reacting enzyme at different times and the oxidized enzyme are shown in figure 3.2. At the concentration of enzyme used no further changes were observed after 3 hours. Figure 3.1 clearly shows the shifts in the Soret and α-band regions of the oxidase spectrum. The Soret band is red-shifted from 418 nm, typical of the fully oxidized, resting form ($\underline{a}^{3+}Cu_A^{2+}\underline{a}_3^{3+}Cu_B^{2+}$), to 428 nm, the form of the enzyme denoted as the mixed-valence CO-bound $\underline{aa}_3$ ($\underline{a}^{3+}Cu_A^{2+}\underline{a}_3^{2+}Cu_B^{1+}$-CO). The α-band

Fig.3.1: ABSORPTION SPECTRA OF CO BINDING TO CYTOCHROME OXIDASE:- Spectra have been staggered by 1 cm to facilitate viewing. All spectra are on the same y-scale. (A) fully oxidized, resting aa_3 prior to the addition of CO, (B) t=0 min, immediately after CO addition, (C) t=30 min, (D) t=90 min, (E) t=120 min, (F) t=150 min and (G) t=3 h. Sample is 7.58 μM aa_3 in 20 mM Tris-Cl, 1 mM EDTA, 0.1 M NaCl, 1 mg/ml lauryl maltoside, pH7.8, ambient temperature.

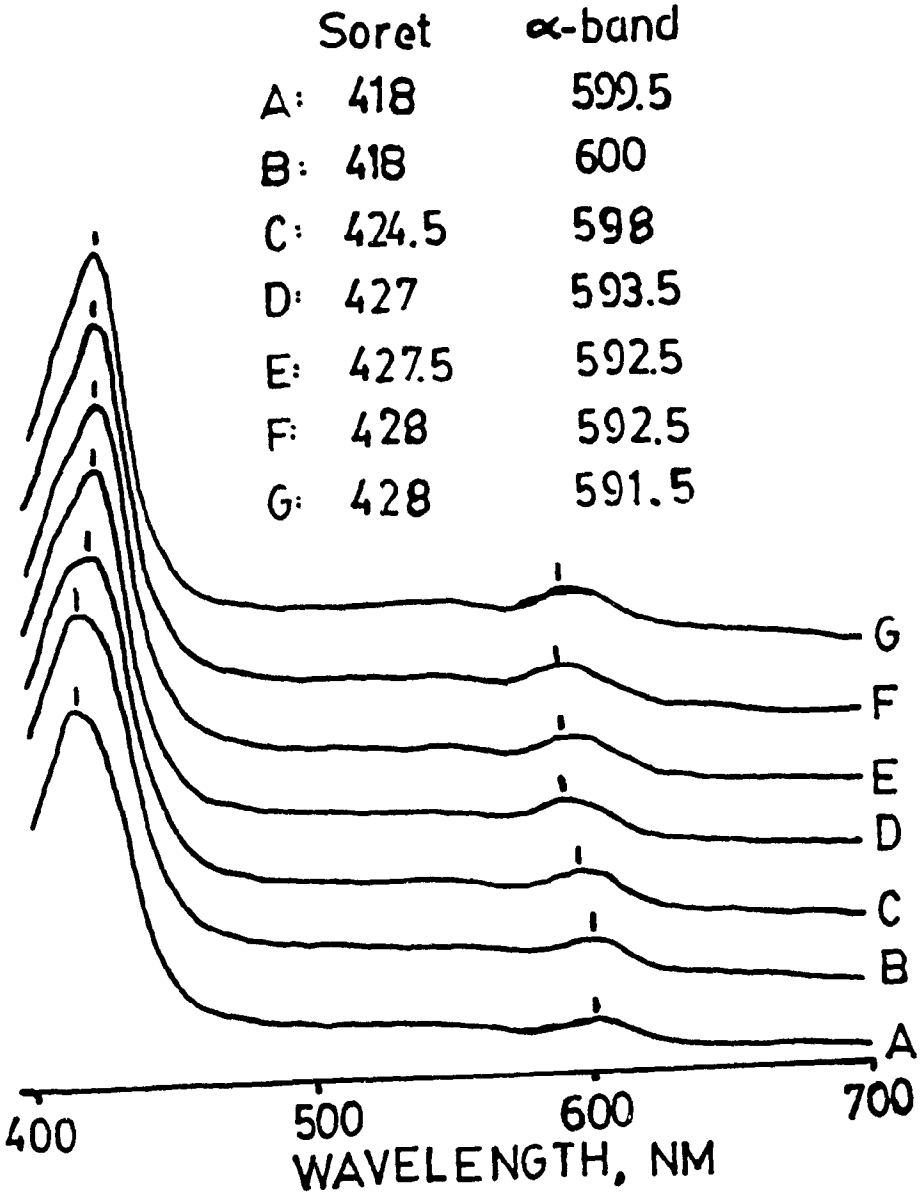
Soret α-band
A: 418 599.5
B: 418 600
C: 424.5 598
D: 427 593.5
E: 427.5 592.5
F: 428 592.5
G: 428 591.5
G
F
E
D
C
B
A
400
500
600
700
WAVELENGTH, NM

Fig.3.2: ABSORPTION DIFFERENCE SPECTRA OF CO BINDING TO aa_3 :- From the absorption spectra of the reacting aa_3 (CO-binding) was subtracted the spectrum of the fully oxidized, resting aa_3. The CO-binding aa_3 spectra were for the following time intervals:- (A) t=0 min, (B) t=30 min, (C) t=90 min, (D) t=120 min, (E) t=150 min and (F) t=3 h. Sample is 7.58 μM aa_3 in 20 mM Tris-Cl, 1 mM EDTA, 0.1 M NaCl, 1 mg/ml lauryl maltoside, pH7.8, ambient temperature.

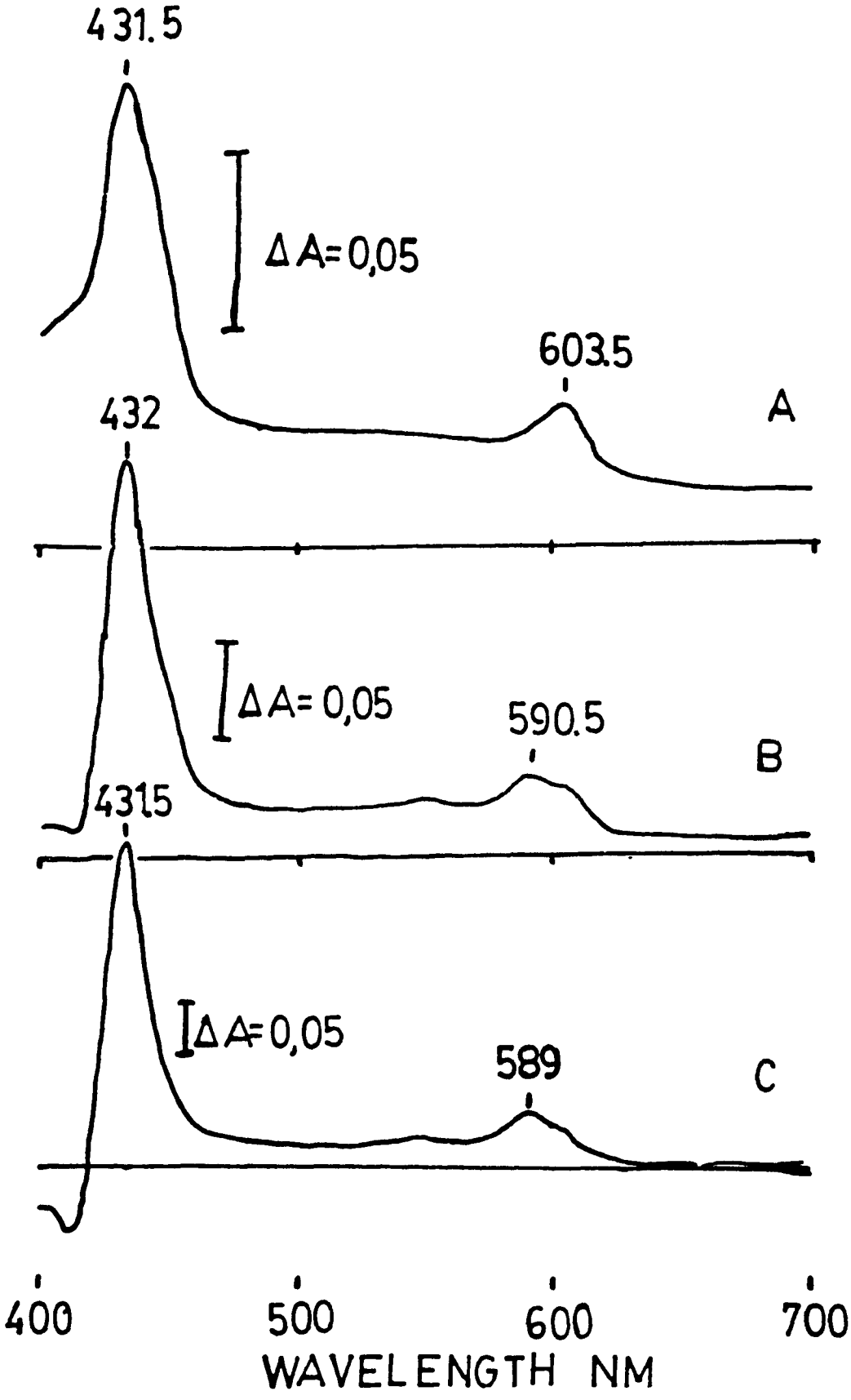
431.5
ΔA=0,05
603.5
A
432
ΔA=0,05
590.5
B
431.5
ΔA=0,05
589
C
400
500
600
700
WAVELENGTH NM

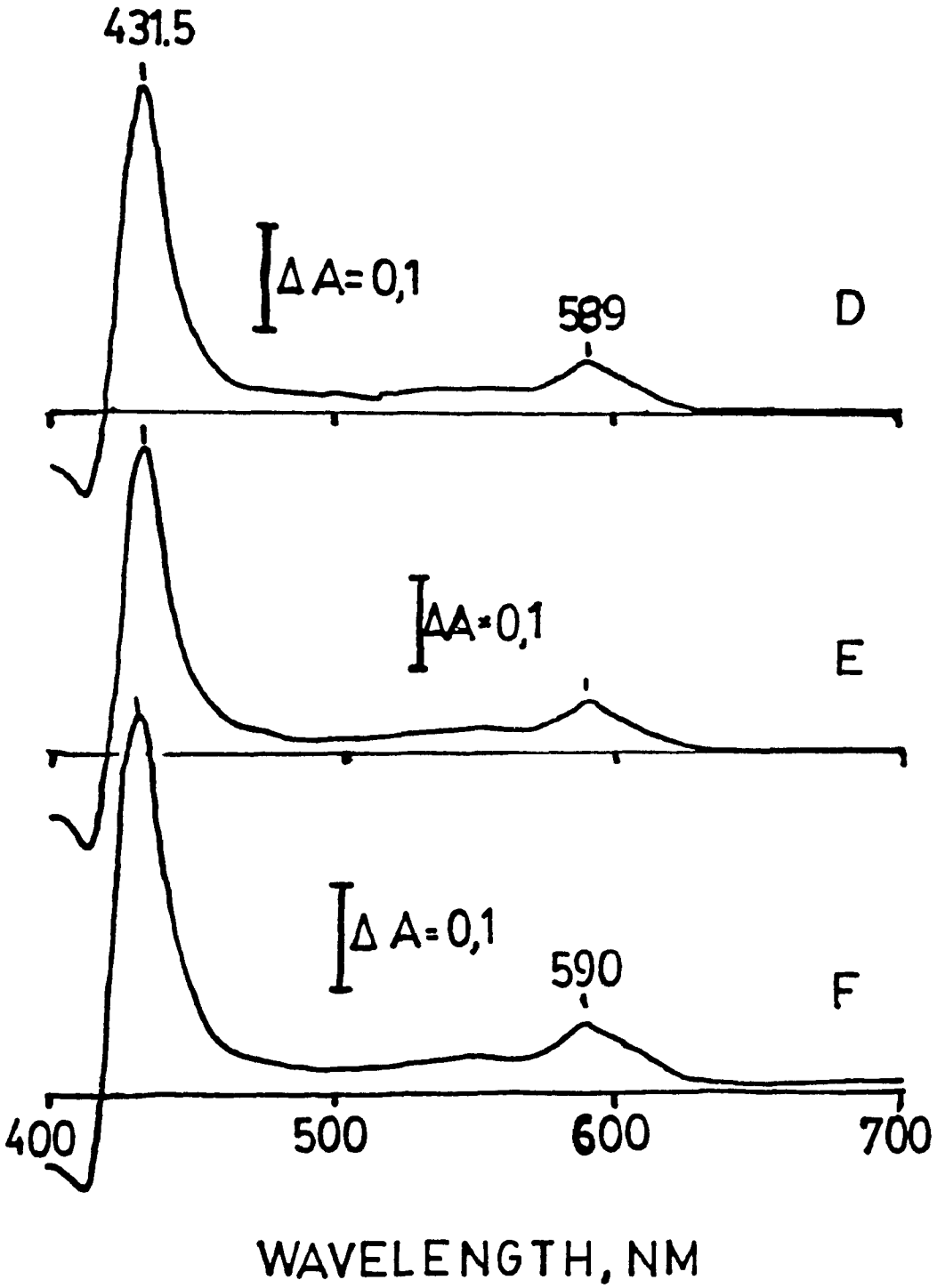
431.5
ΔA=0,1
589
D
ΔA=0,1
E
ΔA=0,1
590
F
400
500
600
700
WAVELENGTH, NM

undergoes a blue-shift from the typical 600 nm to 592 nm, commonly seen in the mixed-valence CO-bound enzyme. The changes observed upon addition of CO, as seen from the difference spectrum (figure 3.2A), are subtle but a distinct increase is observed at 431.5 nm and 603.5 nm. Although with time a gradual increase is observed in the 432 nm band, the 603.5 nm band readily shifts to lower wavelengths and a constant increase at 590 nm is observed past 30 min of incubation. The difference spectra observed are consistent with the formation of the mixed-valence CO-bound enzyme as when compared to several published results (Nicholls & Chanady, 1981; Bickar et al, 1984).

The concentration of enzyme may vary in different experimental set-ups as may the total CO incubation time. The extent of the mixed-valence CO-bound $\underline{aa_3}$ formed is dependent on the enzyme concentration. Decreased concentrations (<0.5 μM) of $\underline{aa_3}$ do not form the mixed-valence CO-bound $\underline{aa_3}$ as readily as higher concentrations of enzyme. In any case, the sample is highly anaerobic and the levels of dithionite required to fully reduce the enzyme are greatly diminished. The dithionite levels used are usually in 100-fold excess over the enzyme, therefore, whether one requires 2 or 4 reducing equivalents to fully reduce the enzyme is insignificant considering the amounts used.

3.1.3 REDUCTION OF CYTOCHROME OXIDASE USING DITHIONITE

Cytochrome oxidase was reduced in an open air cuvette by sodium dithionite (sodium hydrosulfite, Fisher, purified grade). The absorption spectra of oxidized and reduced $\underline{aa_3}$ were

obtained on a Shimadzu UV-160, UV-VIS spectrophotometer. The fluorescence spectra were obtained on a Perkin-Elmer, Model MBF-44B fluorescence spectrophotometer. Fluorescence spectra were digitized manually every 2 nm between 300 nm and 400 nm. Corrected fluorescence spectra were obtained using Eq. 3.1.

The fluorescence emission maximum of dithionite-reduced samples of $\underline{aa}_3$ was followed in time course experiments. Two time course experiments were set up. The first monitored dithionite levels, reduction state of the enzyme and the fluorescence emission maximum. Dithionite depletion was monitored at 315 nm, while the reduction level of the enzyme was monitored at 445 nm and 605 nm. All monitored changes are stated as percentages of the maximum changes observed. The difference between the basal level of absorbance or fluorescence emission maximum and the maximal level observed, in each case, was taken as 100% total change. The second time course experiment was used to monitor the relationship of the reduction level of Cu_A and dithionite levels. The levels of dithionite were monitored at 315 nm and those of the reduction level of $\underline{aa}_3$ at 445 nm using a 0.5 cm path length. The reduction level of Cu_A was monitored at 820 nm using a 1 cm path length. The total absorbance change at 820 nm upon reduction of Cu_A was 0.011.

Carboxypeptidase A is a non-heme containing protein with a tryptophan fluorescence emission maximum at 332 nm. The effect of the presence of dithionite on the fluorescence spectrum of carboxypeptidase A was monitored as a control for reductant induced changes in tryptophan fluorescence. The tryptophan

fluorescence of carboxypeptidase A (Boehringer Mannheim) having an absorbance of 0.065 at 280 nm was obtained in the absence and presence of 1 mM sodium dithionite. Fluorescence spectra were corrected as previously mentioned.

The effect of the presence of dithionite on the tryptophan fluorescence of aa_3 was established using a split cell experiment. Two 2 mm wide quartz cuvettes were positioned at 45° angles to both the excitation beam and the emission detector in the spectrofluorophotometer and back-to-back in the spectrophotometer light path (Diagram 3.1). The sample cuvette contained the

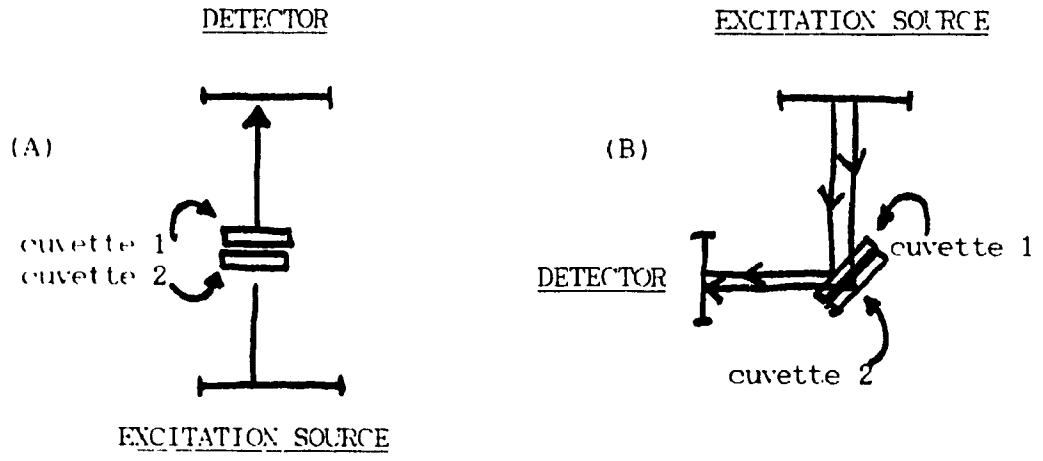

Diagram 3.1: SPLIT CELL EXPERIMENTAL SET-UP:- (A) depicts the orientation of the sample (1) and reference (2) cells in the spectrophotometer, (B) depicts the orientation of the sample (1) and reference (2) cells in the fluorimeter.

cytochrome oxidase. Absorption and fluorescence spectra were obtained in the presence and absence of dithionite in the reference cell. Spectra were corrected as before.

In order to decrease the amount of dithionite required to obtain stable, fully reduced oxidase, the fully reduced enzyme was obtained starting from the mixed-valence CO-bound state. Cytochrome $\underline{aa_3}$ was incubated overnight under CO. To the mixed-valence CO-bound $\underline{aa_3}$ was added an aliquot of dithionite. Changes in the 280 nm to 400 nm region of the absorption spectra were negligible. The percent difference in the correction factors used for the oxidized, mixed-valence CO-bound enzyme and the fully reduced CO-bound enzyme was less than 5% and was distributed evenly through out the region in question. The absorbance at 280 nm was kept within 0.2 O.D. in all cases. Spectra were corrected as previously mentioned.

3.1.4 CYTOCHROME OXIDASE REDUCTION BY DEAZAFLAVIN

The photocatalyst 3,10-dimethyl-5-deazaisoalloxazine, deazaflavin, was a generous gift from Dr.Vincent Massey (University of Michigan Medical School). Deazaflavin was chosen as an appropriate alternive reductant to dithionite, due to its optical properties. The absolute absorption spectrum of deazaflavin in the 280 nm to 500 nm region is shown in figure 3.3. Absorption maxima are at 322 nm and 388 nm. The absorbance of these peaks under these conditions was 0.02 O.D.

Reduction of cytochrome oxidase using deazaflavin was carried out in the following manner. 0.52 µM $\underline{aa_3}$, 9 mM EDTA,

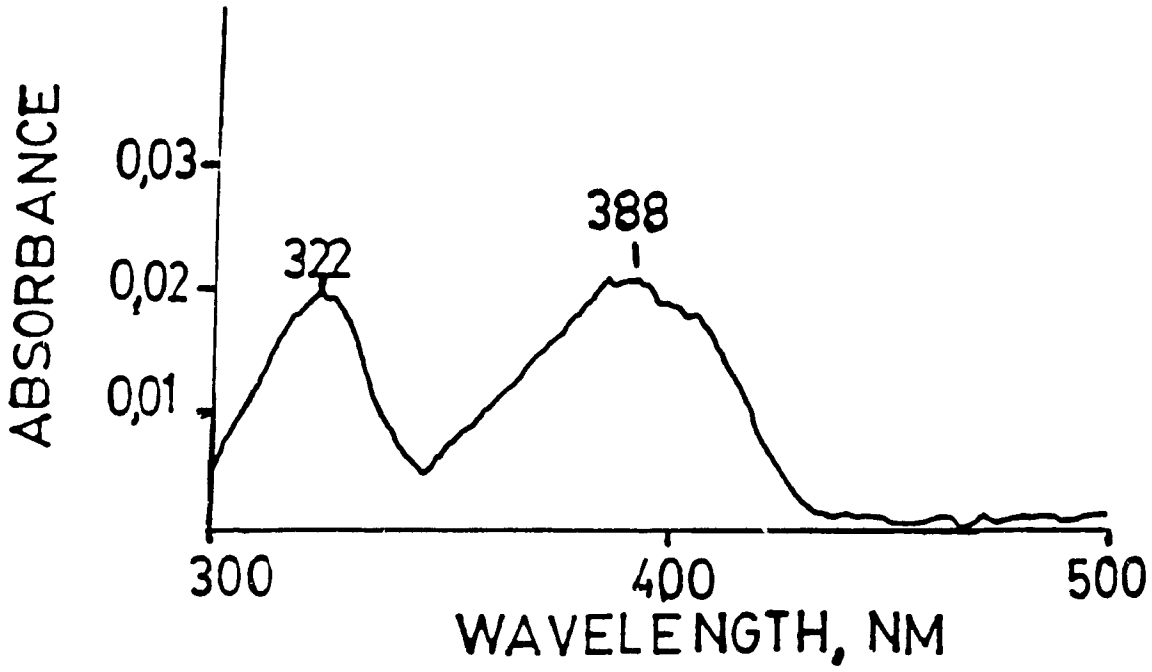

Fig.3.3: ABSOLUTE ABSORPTION SPECTRUM OF DEAZAFLAVIN :- sample consisted of 1.65 µM deazaflavin, 9 mM EDTA, 20 mM Tris-Cl, 0.1 M NaCl, 1 mg/ml lauryl maltoside, pH7.8, dearated and under CO.

1.65 µM deazaflavin, 20 mM Tris-Cl, 1 mg/ml lauryl maltoside, 0.1 M NaCl, pH 7.8 was dearated and put under an atmosphere of CO in a septum-sealed 1.5 ml quartz fluorescence cuvette. The sample was left standing in the dark overnight. Reduction of cytochrome oxidase was achieved by irradiation using the lamp of a Kodak slide projector. During irradiation, the sample was kept in a cold water bath at a distance of 5 cm from the projector. The control used consisted of 9 mM EDTA, 1.65 µM deazaflavin, 20 mM Tris-Cl, 1 mg/ml lauryl maltoside, 0.1 M NaCl pH 7.8, dearated and under CO in a septum-sealed quartz fluorescence cuvette. The irradiation procedure was identical for the sample and the control since it was done simultaneously . The irradiation procedure was done until a stable, reduced oxidase spectrum was obtained. The irradiation times were between 1-2 minutes each. The total irradiation time required, hereby denoted as t_{irr}, was 18 min. Absorption spectra were obtained on a Shimadzu UV-160, UV-VIS spectrophotometer. Fluorescence spectra were obtained on a Perkin-Elmer fluorescence spectrophotometer Model MBF-44B. Fluorescence spectra were digitized manually every 2 nm from 300 nm to 500 nm and corrected for inner filter effects. The excitation wavelength was 280 nm and both emission and excitation slit widths were set at 10 nm. A 5 µl aliquot of a concentrated dithionite solution was injected into the sealed sample cuvette in order to check that the oxidase had been fully reduced by deazaflavin.

3.1.5 PREPARATION OF CYTOCHROME OXIDASE VESICLES

Cytochrome oxidase vesicles were prepared using a

slightly modified version of the procedure described by Casey (Casey, 1986). 40 mg/ml of α-lecithin (Soya bean, Sigma) was incubated in 100 mM Hepes buffer, pH=7.5 containing 1.5% cholate, overnight. The temperature for all preparatory procedures was 4°C unless otherwise specified. The lipid was suspended by vortexing. The suspension was subsequently sonicated with 30 s pulses with 1 min intervals between pulses for a total number of 6 pulses. Sonicated vesicles were centrifuged in a MSE MicroCentaur centrifuge at 13000 rpm for 20 min. To 4.75 ml of vesicles was added 250 µl of 76 µM cytochrome oxidase. The protein-vesicle mixture was dialyzed against 1 l of 100 mM Hepes buffer, pH=7.5 for 20 h. A second dialysis was against 2 l of 50 mM Hepes buffer, 20 mM KCl, 30 mM sucrose pH=7.75 for 6 h. A final dialysis against 4 l of 50 mM Hepes, 20 mM KCl and 30 mM sucrose, pH=8.0, was performed for 30 h. 3 ml of vesicles were dialyzed by the same procedure in the absence of cytochrome oxidase. These liposomes, hereby termed "empty" vesicles, were used as the blank for the proteoliposomes in spectral corrections for background interference due to the presence of the lipid vesicles.

3.1.6 CHARACTERIZATION OF CYTOCHROME OXIDASE VESICLES

Cytochrome oxidase vesicles were characterized by their respiratory control ratios (RCR) and their accessibility to reduced cytochrome c. The respiratory control ratio of the cytochrome oxidase vesicles is determined polarographically using a Clark oxygen electrode. This ratio is simply the rate of electron transfer from cytochrome c to oxygen in the presence of the

uncoupler, CCCP, and the K^+ translocator, valinomycin divided by the rate of electron transfer in their absence (in the presence of reduced cytochrome c only) (Muller et al, 1986). The rate obtained subsequent to c addition is termed the background rate and is due to oxygen consumption by ascorbate, TMPD and cytochrome c autooxidation. Rates were monitored for 5 min. All rates are corrected for the background rate and are in $\mu M\ O_2$/min. The RCR value is determined by dividing the corrected rate after addition of CCCP by the corrected rate prior to addition of valinomycin. The polarographic trace obtained can be seen in figure 3.4.

Cytochrome c accessibility was determined spectrophotometrically on a Shimadzu UV-160 UV-VIS recording spectrophotometer. Spectra were obtained between 400 nm and 650 nm. 700 µl of oxidized cytochrome oxidase vesicles were positioned in both the reference and sample cell holders. A blank difference spectrum was thus obtained. To the vesicles in the sample cell were added 12 µl of 0.67 M ascorbate, pH=7.1 and 2 µl of 100 µM cytochrome c. Difference spectra were obtained with time between the sample and reference cuvettes. When no further change was seen (all possible oxidase reduced by c), 2 µl of 0.2 M TMPD was added to completely reduce all of the oxidase positioned in the sample cell holder. The percentage of the cytochrome oxidase molecules in the vesicles which have their cytochrome c binding site accessible to cytochrome c is proportional to the percent reduction of cytochrome oxidase observed prior to the addition of TMPD.

Fig.3.4: POLAROGRAPHIC TRACE OF VESICULAR CYTOCHROME OXIDASE RESPIRATION :- The polarographic assay was conducted as follows:- To 1.4 ml of 50 mM Hepes, 25 mM KCl, pH=7.5 was added 10 µl of 0.67 M ascorbate, pH=7.1, 2µl of 250 mM EDTA, 2 µl of 0.2 M TMPD and 15 µl of 1 mM cytochrome c. Followed by the addition of 10 µl of vesicles containing 3.8 µM $\underline{aa_3}$. Total oxidase concentration was 27 nM. 2 µl of 2 mg/ml valinomycin in ethanol was added followed by the addition of 2 µl of 2 mM CCCP in ethanol. Arrows denote addition of specified reagents. Rates are expressed in terms of the consumption of O_2 with units of µM O_2/min.

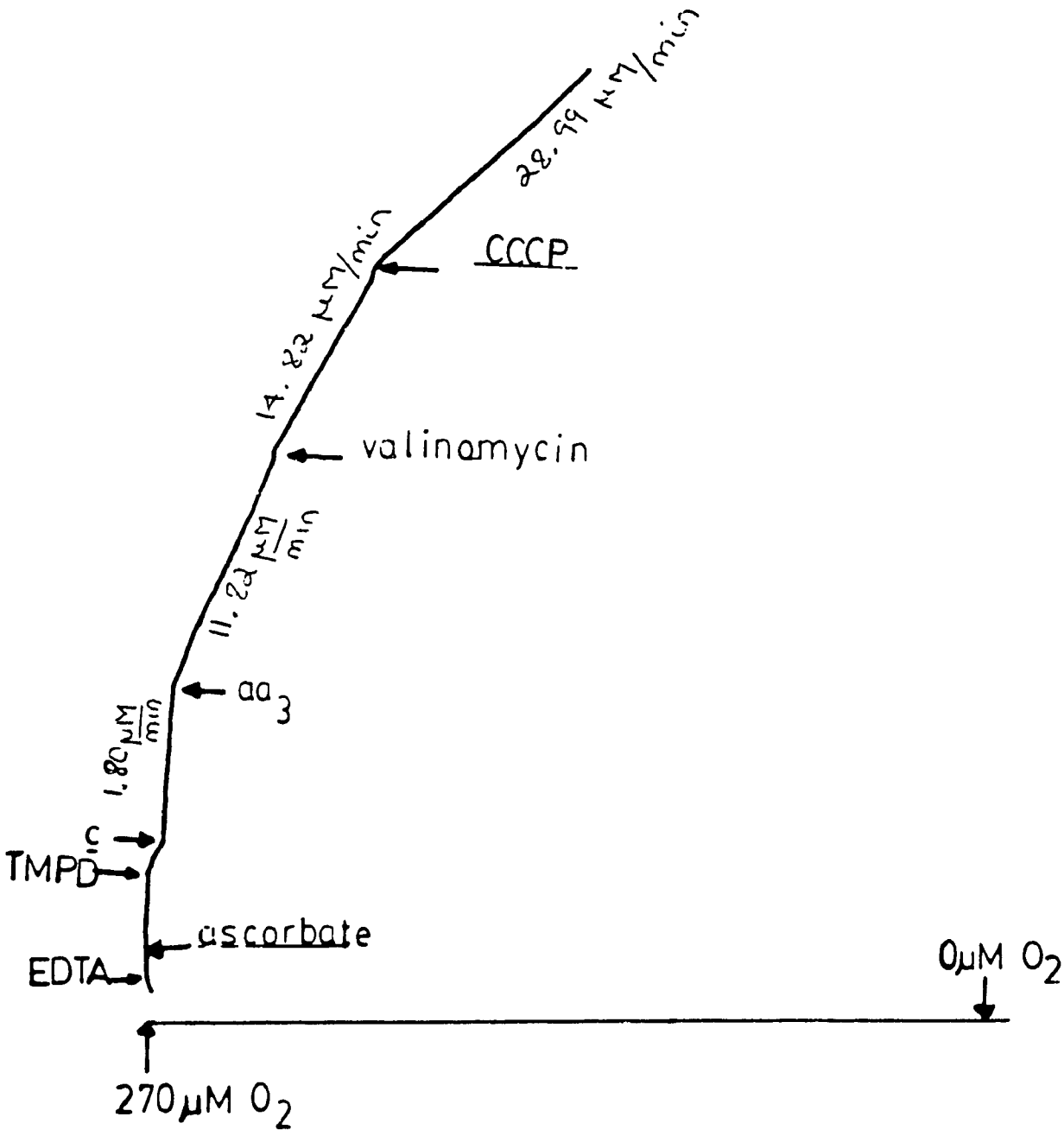
28.99 μM/min
CCCP
14.82 μM/min
valinomycin
11.24 μM/min
aa3
1.80 μM/min
c
TMPD
ascorbate
EDTA
0μM O2
270μM O2

3.1.7 TRYPTOPHAN FLUORESCENCE OF CYTOCHROME OXIDASE VESICLES

Tryptophan fluorescence of cytochrome oxidase vesicles was monitored on a Shimadzu RF-5000 spectrophotometer. To 950 µl of 100 mM Hepes, 25 mM KCl, pH=8.0 was added either 50 µl of proteoliposomes or 50 µl of "empty" vesicles. The absorption and fluorescence spectra of the "empty" vesicles were used as the blanks for the proteoliposome spectra.

Cytochrome oxidase vesicles with a pH gradient of 3.0 units were prepared by adding 50 µl of cytochrome oxidase vesicles (pH=8.0) to 950 µl of 50 mM citrate, 20 mM KCl, 30 mM sucrose pH=4.96. The appropriate blank was set up using "empty" vesicles. Spectra were obtained immediately after preparation in order to minimize the dissipation of the gradient. Fluorescence spectra were corrected for inner filter effects due to excessive absorbance in the UV region by the vesicles. For comparative purposes the tryptophan fluorescence spectrum of 360 nM cytochrome oxidase in 20 mM Tris, 1 mM EDTA, 1 mg/ml lauryl maltoside, pH=7.8 was also obtained. The 280/420 ratio for this protein sample was 2.44.

3.2 FLUORESCENCE OF CYTOCHROME c PEROXIDASE AND $Ru(NH_3)_5$-His(60)-CYTOCHROME c PEROXIDASE

3.2.1 PROTEIN SAMPLES

Cytochrome c peroxidase and its His-60 ruthenated complex were a kind gift from Mr. Ted Fox and Dr. A.M.English (Concordia University, Department of Chemistry and Biochemistry). Peroxidase samples were made up from crystals. An equimolar sample of cytochrome c peroxidase and pentaamminehistidineruthenium(III)

trichloride was used as a control. Absorption spectra were obtained on a Shimadzu UV-160, UV-Vis recording spectrophotometer. The purity index of the peroxidase samples was determined by the ratio of the heme band at 408 nm to the protein band at 280 nm. A purity index of approximately 1.3 was found for all samples (Fig.3.5) used. Fluorescence spectra were recorded on a Shimadzu RF-5000 spectrofluorometer.

3.2.2 QUANTUM YIELD

The quantum yield of a fluorophore expresses the ratio of photons emitted to photons absorbed. Excitation of a fluorophore from its ground state level, S_g, to an excited state, S^*_{ex}, is followed by decay processes which return the fluorophore to its ground state, S_g (Diagram 3.2). These processes may be

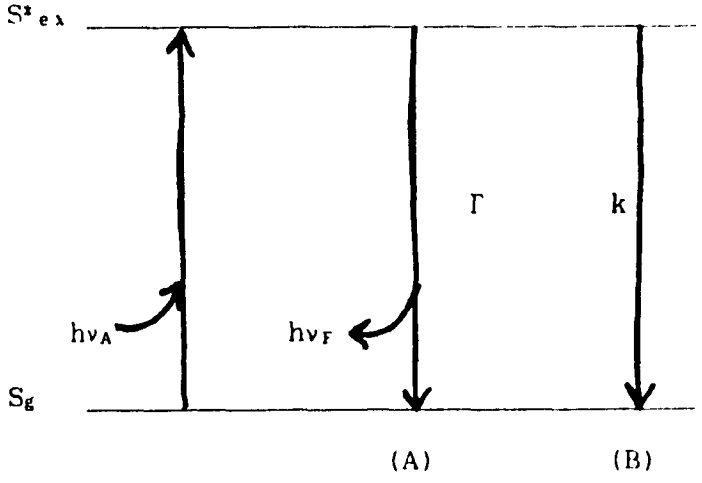

Diagram 3.2: SIMPLIFIED JABLONSKI DIAGRAM ILLUSTRATING DECAY PROCESSES FROM AN EXCITED SINGLET STATE. The decay processes from an excited state of a fluorophore may be (A) radiative or (B) non-radiative.

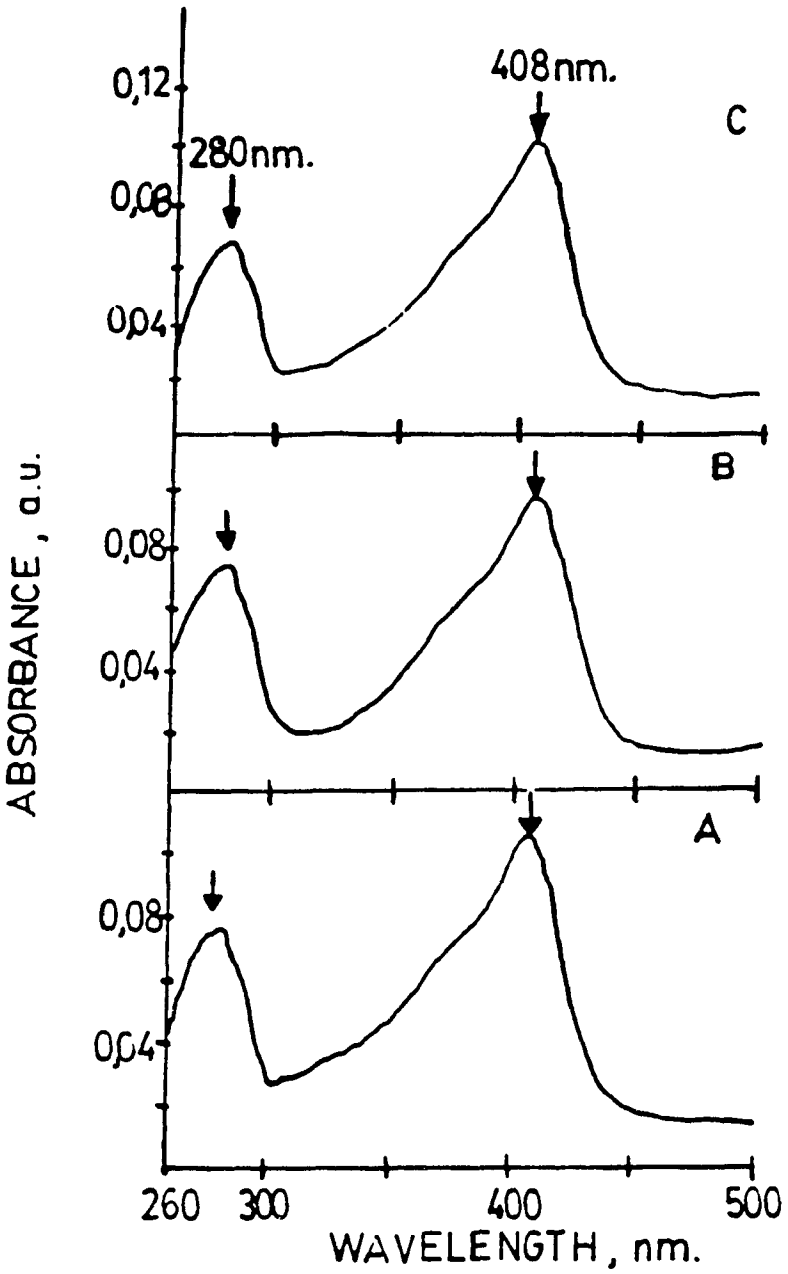

Fig.3.5: ABSORPTION SPECTRA OF CcP SAMPLES - (A) 1 μM native CcP, (B) 1 μM Ru-CcP and (C) 1 μM CcP/Ru-His. All samples were in 0.1 M Na-Pi buffer, pH=7, ambient temperature.

radiative or non-radiative in nature and their sum will equal the amount of energy absorbed by the fluorophore in the ground state. The radiative process gives rise to the measured fluorescence of the fluorophore. The quantum yield of a fluorophore may be expressed in terms of the rate constants of the decay processes involved.

Γ, is the rate constant for the radiative decay process while **k** is the rate constant of the sum total of the non-radiative processes. The ratio of Γ to the sum of Γ and **k** is the quantum yield of the fluorophore, denoted Φ (Lakowicz, 1983).

$$\Phi = \Gamma/(\Gamma + k) \qquad \text{Eq.3.2}$$

An quantum yield of 100% is assigned to the fluorescence of a standard, standardized at its excitation wavelength. For tryptophan fluorescence, the standard used in this work was N-acetyltryptophanamide (N-ATA, Sigma). In the determination of quantum yields, fluorescence spectra were obtained for N-ATA and CcP samples by excitation at 280 nm with emission and excitation slits set at 3 nm. Emission spectra were standardized using the 280 nm absorbance of the sample and corrected for inner filter effects. The average of the greatest and smallest correction factor determined in the 300 nm to 400 nm region of the absorption spectrum was used to correct fluorescence emission spectra. The average did not deviate by more than 4% in any of the samples. Quantum yield values were determined by

integrating the standardized and corrected fluorescence emission spectrum of each sample.

3.2.3 FLUORESCENCE EMISSION AND EXCITATION SPECTRA OF CcP AND RU-CcP

Fluorescence emission spectra of CcP and Ru-CcP were obtained upon excitation at various wavelengths in the ultra-violet range. The blank, 0.1 M Pi pH=7 or 0.1 M MOPS pH=7, fluorescence emission spectrum was in each case subtracted from the emission spectrum of the protein samples. Emission spectra were further corrected for possible inner filter effects. In all cases the absorbance at the excitation wavelength was kept under 0.2 O.D. units in order to minimize the correction involved. Excitation spectra of protein samples at various emission wavelengths were obtained under identical fluorimeter settings as those of emission spectra. No manipulations of excitation spectra were performed. Emission and excitation wavelengths are specified in each case.

3.2.1 FLUORESCENCE QUENCHING OF CcP AND Ru-CcP

Fluorescence quenching in biochemistry is usually used as a means of determining 1) the accessibility and localization of fluorophores in proteins, either soluble or membrane-bound, as well as 2) the permeabilities of proteins and membranes to these quenchers and their respective diffusion rates. Fluorescence quenching is any process which decreases the fluorescence of a fluorophore. The four main classes demonstrating these processes are 1) excited state reactions between the fluorophore in its excited state, F^*, and the quencher, Q, 2) energy transfer between the fluorophore, F, and Q, 3) complex formation between F and Q

(static quenching) and 4) collisional quenching between F and Q (dynamic quenching). Static quenching, due to complex formation between fluorophore and quencher at high quencher concentrations, causes distortions in the analysis of collisional quenching.

Fluorescence quenching of CcP, Ru-CcP and CcP/Ru-His was performed using the fluorescence quenchers, acrylamide, iodide and cesium. Acrylamide quenching of CcP fluorescence was determined by monitoring fluorescence emission spectral changes as a function of acrylamide (Schwartz/Mann Biotech, Ultrapure) concentration. From each spectrum was subtracted the background fluorescence of 0.1 M Pi pH=7. The resulting spectra were further corrected for inner filter effects, as well as dilution and subsequently standardized in terms of total amount of protein using the O.D. at 408 nm as the reference.

Fluorescence quenching of peroxidase samples by iodide was monitored in 820 µl samples consisting of 700 µl of 1 µM peroxidase, 1 mM sodium thiosulfate (Anachemia) and compensating amounts of 5 M NaCl and/or 5M KI (ACP Chemicals Inc.) with 1 mM sodium thiosulfate, resulting in a constant added volume of 120 µl. Thiosulfate functions primarily in maintaining iodide in the I^- form. The ionic strength was kept constant at 0.732 M (i.e. in 820 µl). The concentration range of iodide was from 0 M to 0.732 M. Spectral corrections and standardization are the same as for the acrylamide quenching experiment. Fluorescence spectra in the absence and presence of 0.732 M KI were also obtained using an excitation wavelength of 280 nm. Spectra were corrected as

previously stated.

Cesium quenching of peroxidase fluorescence was performed exactly the same as the quenching experiment using iodide except that no sodium thiosulfate was present. The quencher stock was 5 M cesium chloride (Aldrich) in 0.1 M Pi pH=7. Spectral corrections were identical to those established in the iodide experiment. Fluorescence spectra in the presence and absence of 0.732 M CsCl were also obtained upon excitation at 295 nm. Similar corrections apply.

Analysis of fluorescence quenching is achieved using the Stern-Volmer equation (Eq.3.3),

$$F_o/F = 1 + K_{SV}[Q] \qquad \text{Eq.3.3}$$

where F_o is the fluorescence in the absence of quencher, F is the fluorescence in the presence of quencher, [Q] is the quencher concentration and K_{SV} is the Stern-Volmer quenching constant. A plot of F_o/F versus [Q] will give rise to a slope equal to K_{SV}.

Stern-Volmer constants, K_{SV}, of fluorescence quenching of peroxidase were determined from Stern-Volmer plots based on equation 3.3. F_o and F can be simply the fluorescence intensity of the particular sample at a chosen maximal emission wavelength or the area under the emission spectrum. Due to the change in spectral shape of the fluorescence spectrum of the peroxidase samples under certain conditions of high quencher concentrations, integration values were chosen to be more representative of F_o and F.

Determination of the Stern-Volmer constant, K_{SV}, is used to identify the quencher as a dynamic and/or static quencher and its magnitude is used, in relation to a standard, as a measure of the effectiveness of the quencher on the fluorophore in question.

3.2.5 DENATURATION OF CYTOCHORME c PEROXIDASE USING UREA

Fluorescence spectra of CcP were obtained as a function of urea (Bio-Rad Electrophoresis Purity Reagent) concentration in order to monitor the denaturing process. The urea concentration scale ranged from 0 to 8 M. The 1 ml samples were incubated for 10 min, the time it took for t e absorption spectrum of the sample to stabilize. Spectra were digitized and corrected for possible inner filter effects using the method previously stated.

The reversibility of the denaturation process was briefly investigated by incubating 2.5 µM CcP in 8 M urea, 0.1 M phosphate buffer, pH=7.0 for 10 min. From this incubation mixture a 200 µl aliquot was added to either 800 µl of 10 M urea stock solution or 800 µl of 0.1 M phosphate buffer, pH=7.0. These samples were incubated for 15 min, the time it took to stabilize the absorption spectrum of the sample diluted with phosphate buffer. Spectra were digitized and corrected as previously mentioned.

4. RESULTS

4.1 TRYPTOPHAN FLUORESCENCE OF CYTOCHROME OXIDASE

4.1.1 REDUCTION OF CYTOCHROME OXIDASE BY DITHIONITE

Dithionite has an absorption spectrum at 315 nm with an extinction of 8000 $M^{-1}cm^{-1}$ (Dawson et al., 1986) (Fig.4.1A). The absorbance decreases sharply near 280 nm which allows for excitation of chromophores such as tryptophan. The tryptophan fluorescence spectrum of cytochrome oxidase, reduced by sodium dithionite, was first reported by Copeland et al. (1987). Fig.4.1 shows optical spectra of oxidized (resting) and dithionite-reduced cytochrome oxidase. The Soret maxima are 417 nm and 414 nm, respectively. The tryptophan fluorescence emission spectra of cytochrome oxidase in the resting and fully reduced forms are shown in figure 4.2. The uncorrected spectra indicate emission maxima of 328 nm, for the resting form of the enzyme consistent with reports by Hill et al. (1986) and Copeland et al. (1987) and 346 nm, for the fully, dithionite reduced enzyme, consistent with the report of Copeland et al. (1987). No observable change is seen in the corrected fluorescence spectrum of the resting oxidase, except for an increase in the intensity. A marked decrease in the position of the emission maximum is observed in the corrected fluorescence spectrum of the fully reduced form. The 18 nm red-shift initially observed in the uncorrected fluorescence spectrum of reduced aa_3 is blue-shifted back to 326 nm upon correction for the inner filter effects caused by the presence of the reductant. Upon aeration of the sample the absorbance at 315 nm, due to dithionite, disappears. It is also observed that the magnitude of the

Fig.4.1: ABSORPTION SPECTRA OF OXIDIZED AND FULLY REDUCED CYTOCHROME OXIDASE :-(A) absolute absorption spectra of resting, oxidized aa_3 (0.59 μM) (solid line) and fully reduced aa_3 using 1 mM dithionite (dashed line), inset demonstrates the contribution of dithionite to the optical spectrum (dotted line), (B) visible spectra of oxidized aa_3 (solid line) and fully reduced aa_3 (dashed line). Samples are in 20 mM Tris-Cl, 1mM EDTA, 0.1M NaCl, 1mg/ml lauryl maltoside, pH7.8, in an open air cuvette, at ambient temperature.

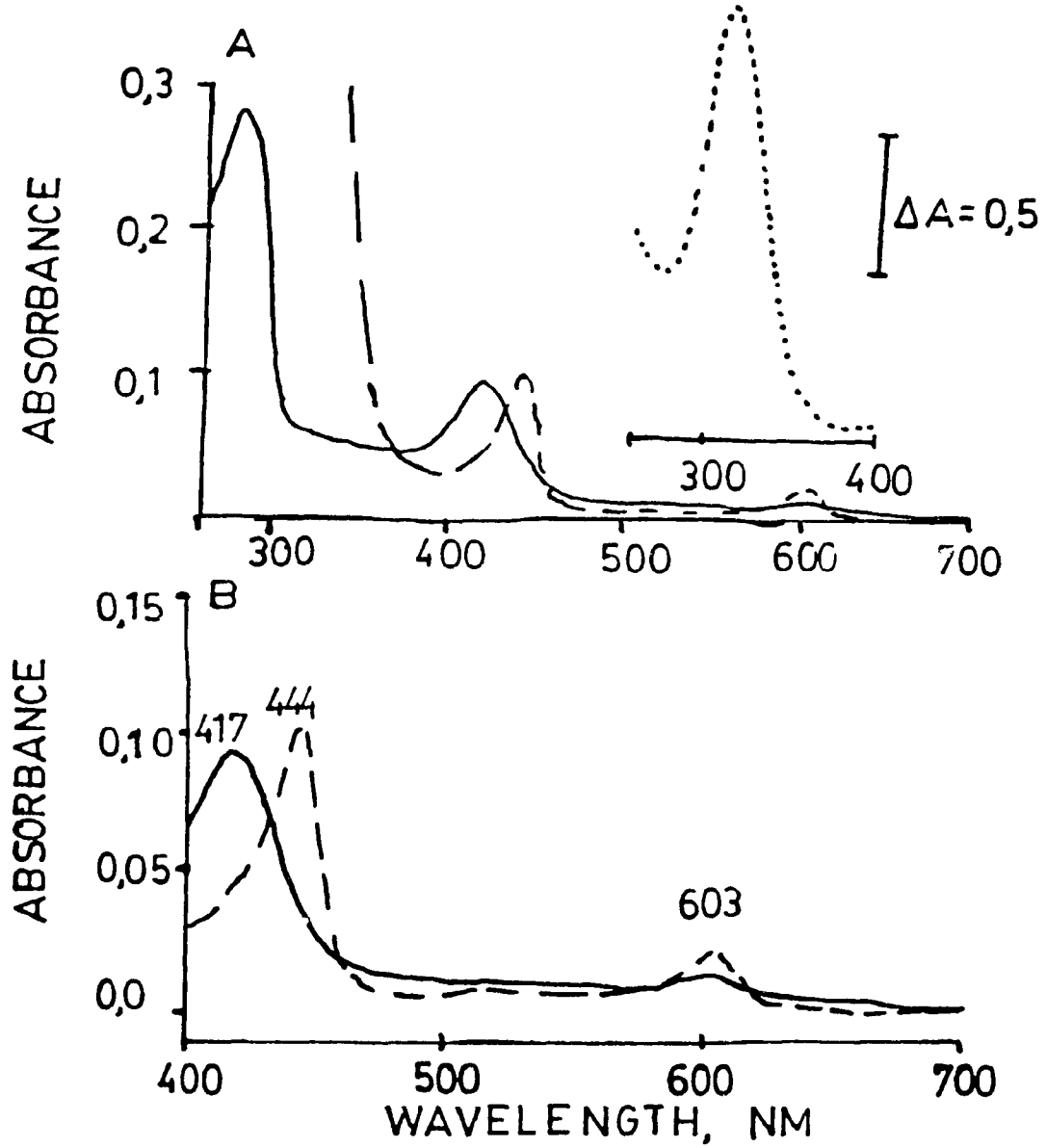
A
0,3
0,2
0,1
ABSORBANCE
ΔA=0,5
300
400
300
400
500
600
700
B
0,15
0,10
0,05
0,0
417
444
603
ABSORBANCE
400
500
600
700
WAVELENGTH, NM

Fig.4.2: TRYPTOPHAN FLUORESCENCE EMISSION SPECTRA OF OXIDIZED AND FULLY REDUCED CYTOCHROME OXIDASE :- oxidized aa_3 (0.59 μM) (circles), fully reduced aa_3 with 1 mM dithionite (triangles). Uncorrected spectra are denoted by the open symbols, corrected spectra by the closed symbols. Excitation wavelength was 280 nm. Emission and excitation slits were set at 10 nm.Samples are in 20 mM Tris-Cl, 1mM EDTA, 0.1M NaCl, 1mg/ml lauryl maltoside, pH7.8, in an open air cuvette, at ambient temperature.

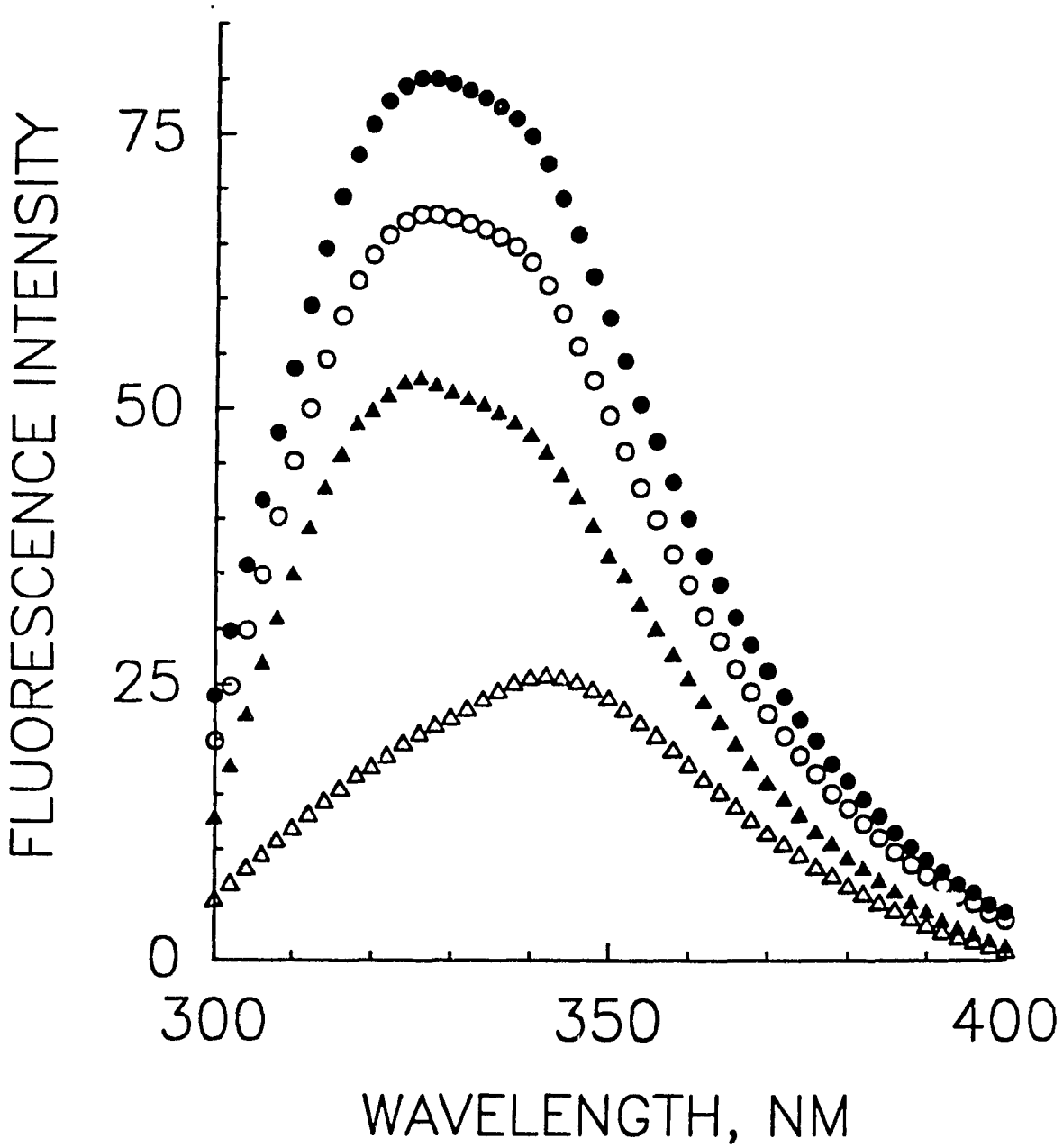
FLUORESCENCE INTENSITY
75
50
25
0
300
350
400
WAVELENGTH, NM

315 nm dithionite band is directly related to the extent of red-shift observed in the fluorescence emission maxima. Figure 4.3 is the time course of dithionite depletion as monitored by the absorbance value at 315 nm. The effect of this depletion on the fluorescence emission maximum and the redox state of the enzyme, as monitored spectrophotometrically at 605 nm and 445 nm, is also shown. Time zero is immediately following addition of dithionite to an open cuvette containing resting, oxidized oxidase. The fluorescence emission maximum is red-shifted maximally immediately upon addition of dithionite, while the enzyme only achieves complete reduction at ca. 70 minutes after dithionite addition. It can also be seen that the enzyme is still fully reduced at 90 minutes but both the dithionite levels and the fluorescence emission maximum have almost completely reverted back to levels typical for the oxidase in the absence of dithionite. The time course experiment clearly shows that the shift in the fluorescence emission maximum is a direct consequence of the dithionite levels in the sample in question and not a consequence of the redox state of the enzyme. The red-shift to 348 nm had been attributed specifically to the reduction of Cu_A (Copeland et al., 1987; 1988). A similar time course as the one above, at higher concentrations of cytochrome oxidase is used to monitor the relationship of the redox state of Cu_A (Fig.4.4), as monitored spectrophotometrically at 820 nm and the fluorescence shift . It is shown that the redox state of Cu_A has a time course similar to that observed for reduction of heme a and a_3. Reoxidation of Cu_A occurs at a

Fig.4.3: TIME COURSE OF DITHIONITE DEPLETION:- Dithionite levels were monitored at 315 nm (open circles), the redox level of aa_3 was monitored at 415 nm (closed circles) and 605 nm (open triangles), red-shift of the fluorescence emission maximum (closed triangles). The concentration of oxidase used was 3.4 µM in 20 mM Tris-Cl, 1mM EDTA, 0.1 M NaCl, 1 mg/ml lauryl maltoside pH7.8. The concentration of sodium dithionite was 0.8 mM. The optical path length was 1 cm. Excitation was 280 nm with both slit widths at 10 nm. Samples were at ambient temperature and open to air.

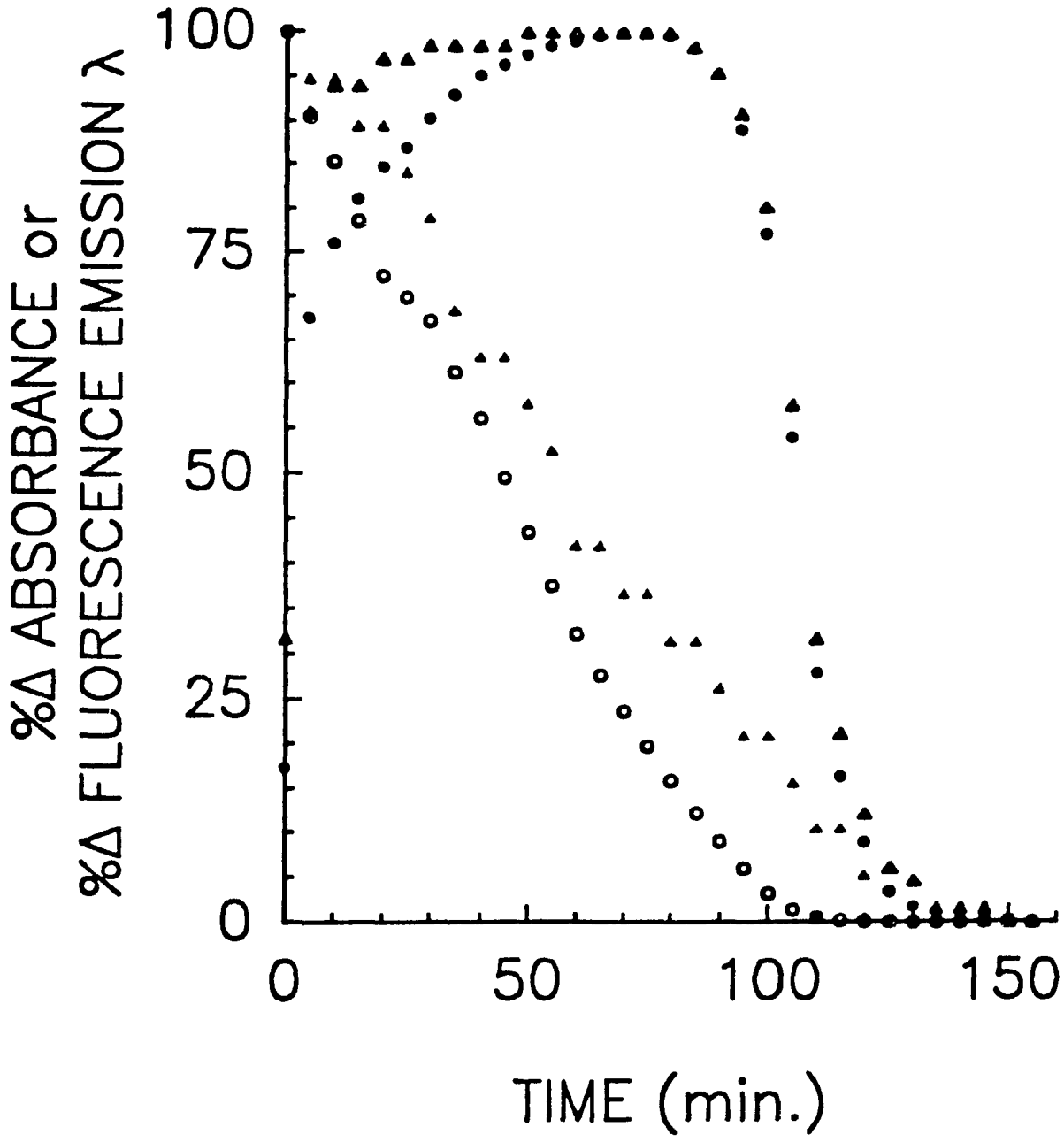
%Δ ABSORBANCE or
%Δ FLUORESCENCE EMISSION λ
100
75
50
25
0
0
50
100
150
TIME (min.)

Fig.4.4: TIME COURSE OF Cu_A RE-OXIDATION:- Dithionite levels were monitored at 315 nm (open circles), redox state of aa_3 was monitored at 445 nm (closed circles), redox state of Cu_A was monitored at 820 nm (closed triangles). The oxidase concentration was 5.36 μM in 20 mM Tris-Cl, 1mM EDTA, 0.1 M NaCl, 1 mg/ml lauryl maltoside pH7.8. The concentration of dithionite used was 1 mM. The optical path length was 1 cm for the 820 nm determination and 0.5 cm for the determinations at 315 nm and 445 nm. Samples were at ambient temperature and open to air.

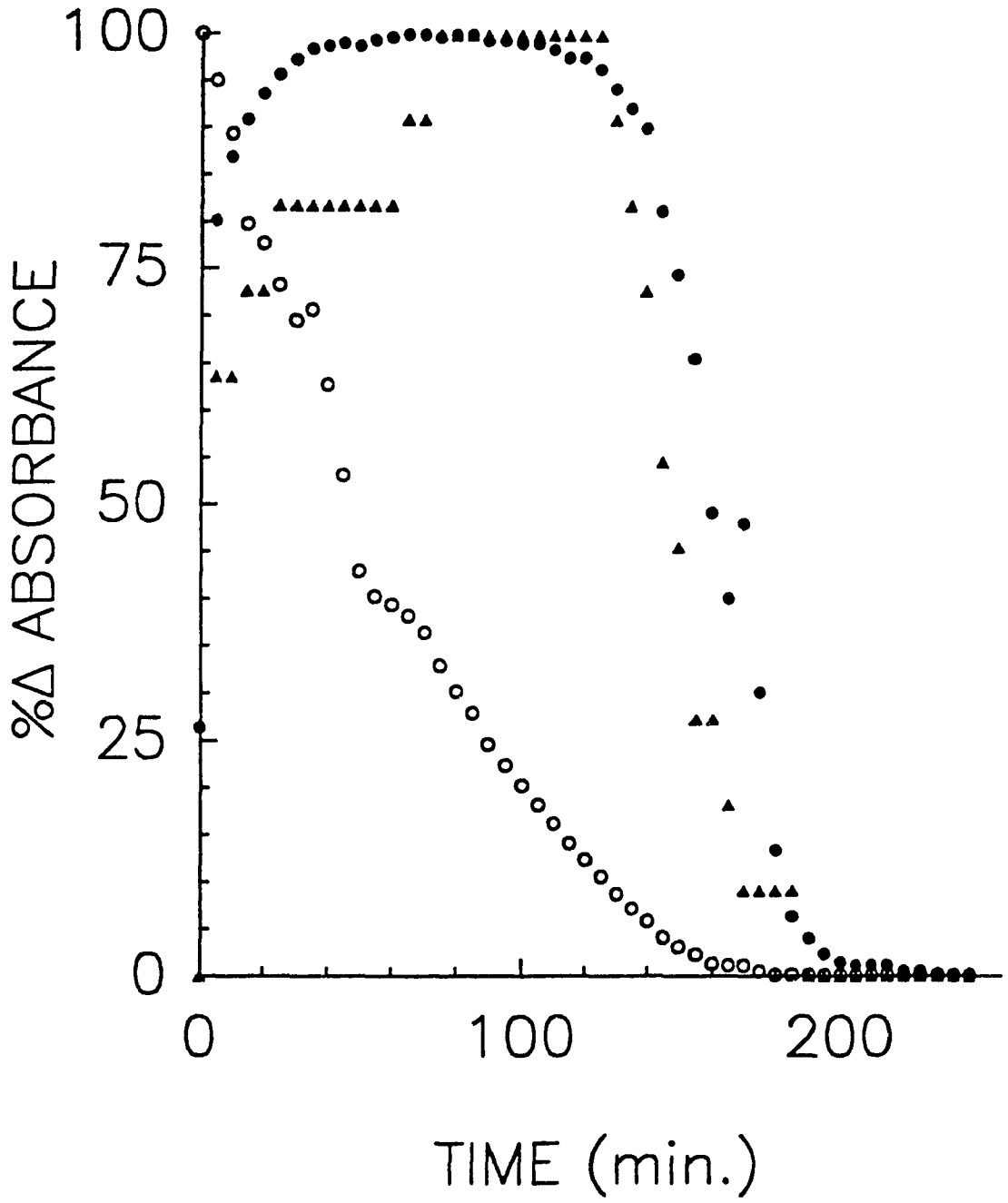
100
75
50
25
0
%Δ ABSORBANCE
0
100
200
TIME (min.)

time when the dithionite levels are almost nil. By direct reference to the time course shown in figure 4.3 it can be concluded that the 20 nm red-shift in fluorescence emission maximum can not be attributed to Cu_A reduction since they obviously have strikingly different time courses.

Carboxypeptidase A is an enzyme which is not involved in redox processes and is not a hemoprotein. It was chosen because its tryptophan fluorescence emission maximum, i.e. 332 nm, is comparable to that observed for cytochrome oxidase. Since no redox reaction is possible, the presence of dithionite in a carboxypeptidase A sample should not influence the enzyme in a way expected of dithionite for cytochrome oxidase. Figure 4.5 depicts the optical spectra of carboxypeptidase A in the absence and presence of dithionite. The spectrum in the presence of dithionite is on a restricted scale and the 280 nm absorbance band of carboxypeptidase A is camouflaged by the dithionite spectrum. The uncorrected and corrected fluorescence emission spectra of carboxypeptidase A in the absence and presence of dithionite are shown in figure 4.6. In the absence of dithionite the fluorescence emission maxima of both corrected and uncorrected spectra of carboxypeptidase A are at 332 nm, consistent with the published report of Lakowicz and Weber (1973). By contrast the uncorrected fluorescence spectrum of carboxypeptidase A in the presence of dithionite has an emission maximum red-shifted to 350 nm. Correction of this spectrum for the inner filter effects due to dithionite gives rise to a spectrum with an emission maximum

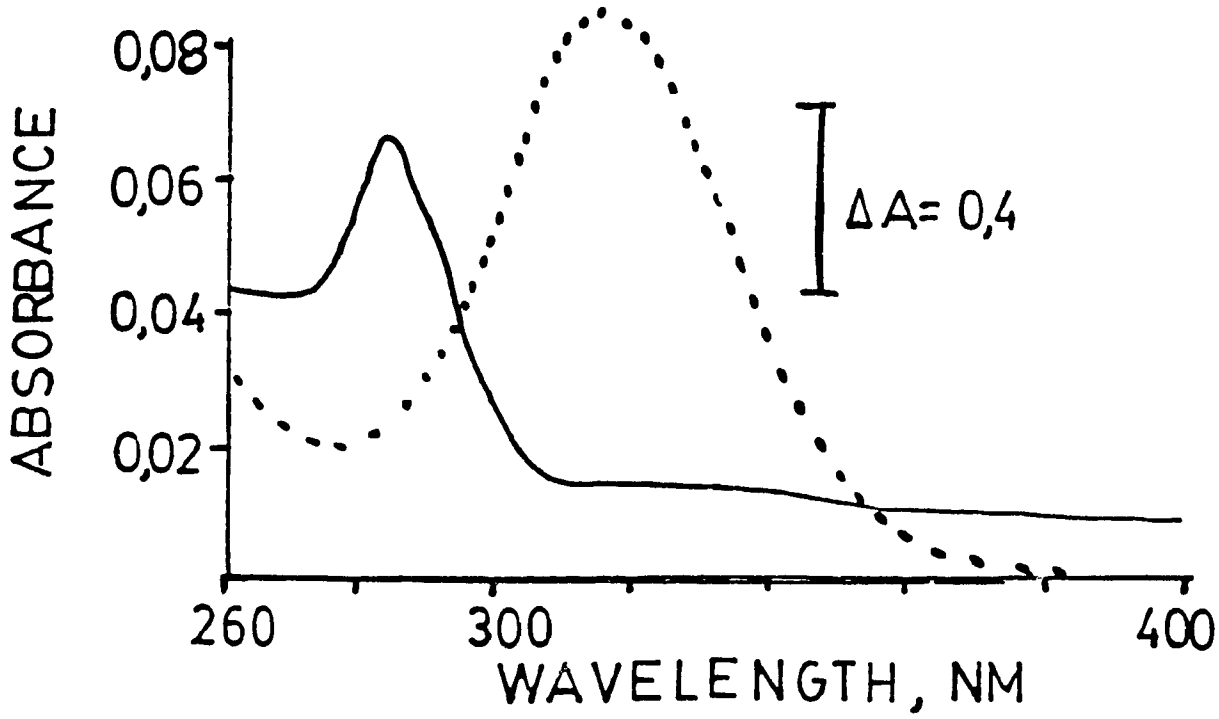

Fig.4.5: ABSORPTION SPECTRA OF CARBOXYPEPTIDASE A:- Carboxypeptidase A in the absence (solid line) and presence of 1 mM dithionite (dotted line). Note: dotted line is on a restricted scale with the marker set at ΔA=0.4 O.D. units. Ambient temperature, open to air.

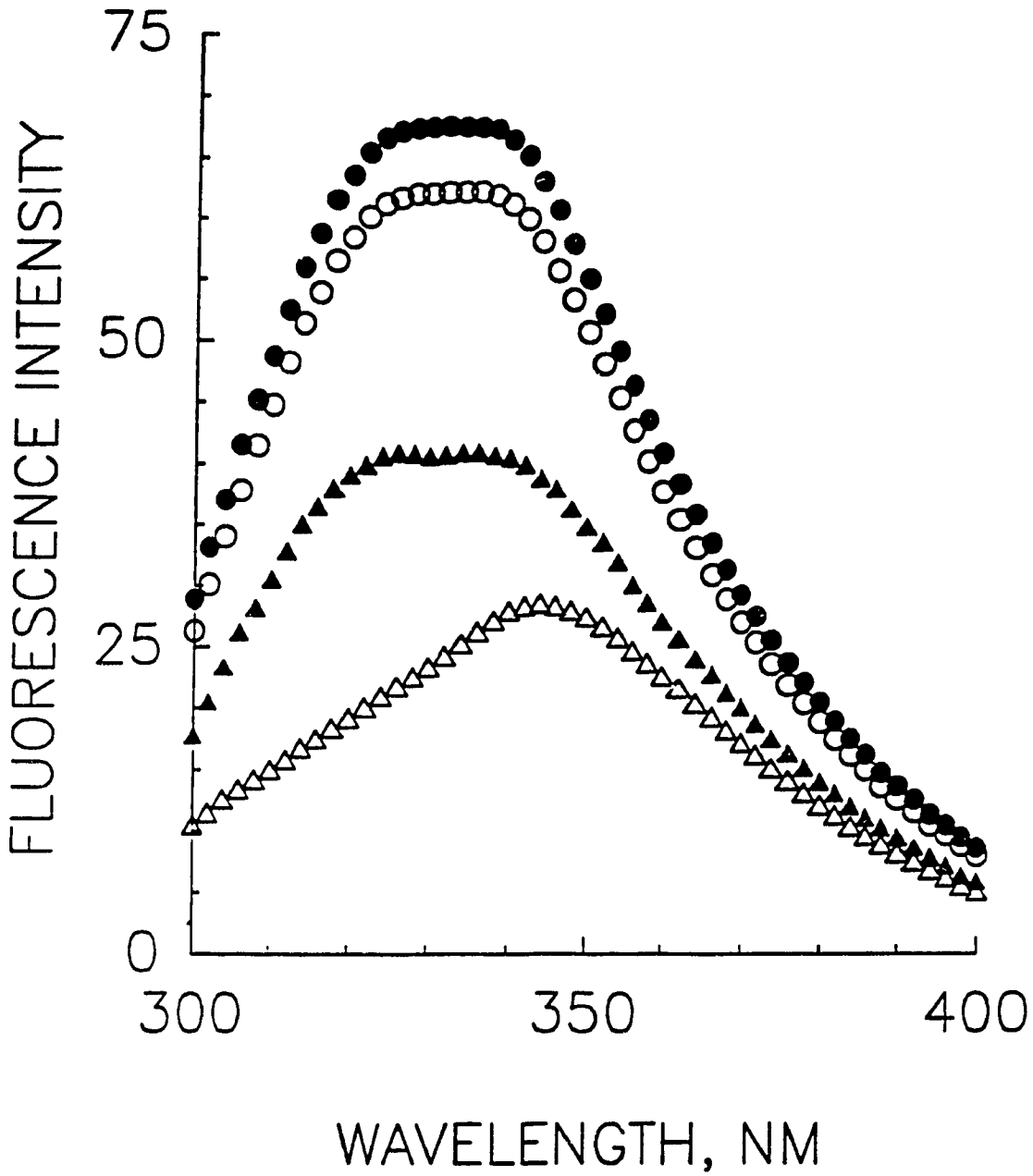

Fig.4.6: TRYPTOPHAN FLUORESCENCE EMISSION SPECTRA OF CARBOXYPEPTIDASE A:- Carboxypeptidase A in the absence (circles) and presence of 1 mM dithionite (triangles). Uncorrected spectra (open symbols), corrected spectra (closed symbols). Excitation wavelength was 280 nm. Emission and excitation slit widths set at 10 nm. Ambient temperature, open to air.

consistent with that observed for carboxypeptidase A, i.e. ca. 332 nm.

A split cell experiment demonstrates that the red-shift in the fluorescence emission maximum observed is a direct consequence of the optical qualities of the reductant used. Figure 4.7 depicts the optical spectrum of a two-cell system, where one cell contains a sample of cytochrome oxidase and the other has either buffer or buffer with the addition of dithionite. It is observed that the Soret band of the oxidase in either case is unchanged. The increase in the optical background intensity is due to dithionite, as well as the absorption band at 315 nm. The fluorescence results (Fig.4.8) show that the uncorrected spectrum obtained in the presence of dithionite in the reference cell is red-shifted to 345 nm. The corrected spectra have the usual 328 nm emission maxima regardless of the presence of dithionite as does the uncorrected spectrum obtained in the absence of dithionite in the reference cell. Since no interaction is possible between cytochrome oxidase and dithionite, the red-shift observed in the fluorescence spectra of dithionite-reduced cytochrome oxidase is attributed to the optical properties of the reductant.

In order to study the redox dependence of the oxidase's conformation using tryptophan fluorescence care must be taken that optical properties of the sample are not drastically changed by the reductant to be used, as is observed in the case of dithionite. In order to minimize this effect, a decrease in the dithionite level used to produce a stable, fully reduced cytochrome oxidase is

Fig.4.7: ABSORPTION SPECTRA OF RESTING, OXIDIZED CYTOCHROME OXIDASE - SPLIT CELL EXPERIMENT:- Absorption spectra were obtained in the absence (solid line) and presence (dashed line) of a dithionite filter. Dotted line denotes dithionite contribution to the optical spectrum. Both cuvettes contained 0.5 ml of 20 mM Tris-Cl, 1 mM EDTA, 0.1 M NaCl, 1 mg/ml lauryl maltoside, pH7.8. To one (sample cuvette) was added 5 µl of 125.89 µM $\underline{aa_3}$. To the other (reference cuvette), was added an aliquot of dithionite solution giving rise to a final concentration of 1 mM. Ambient temperature, open to air.

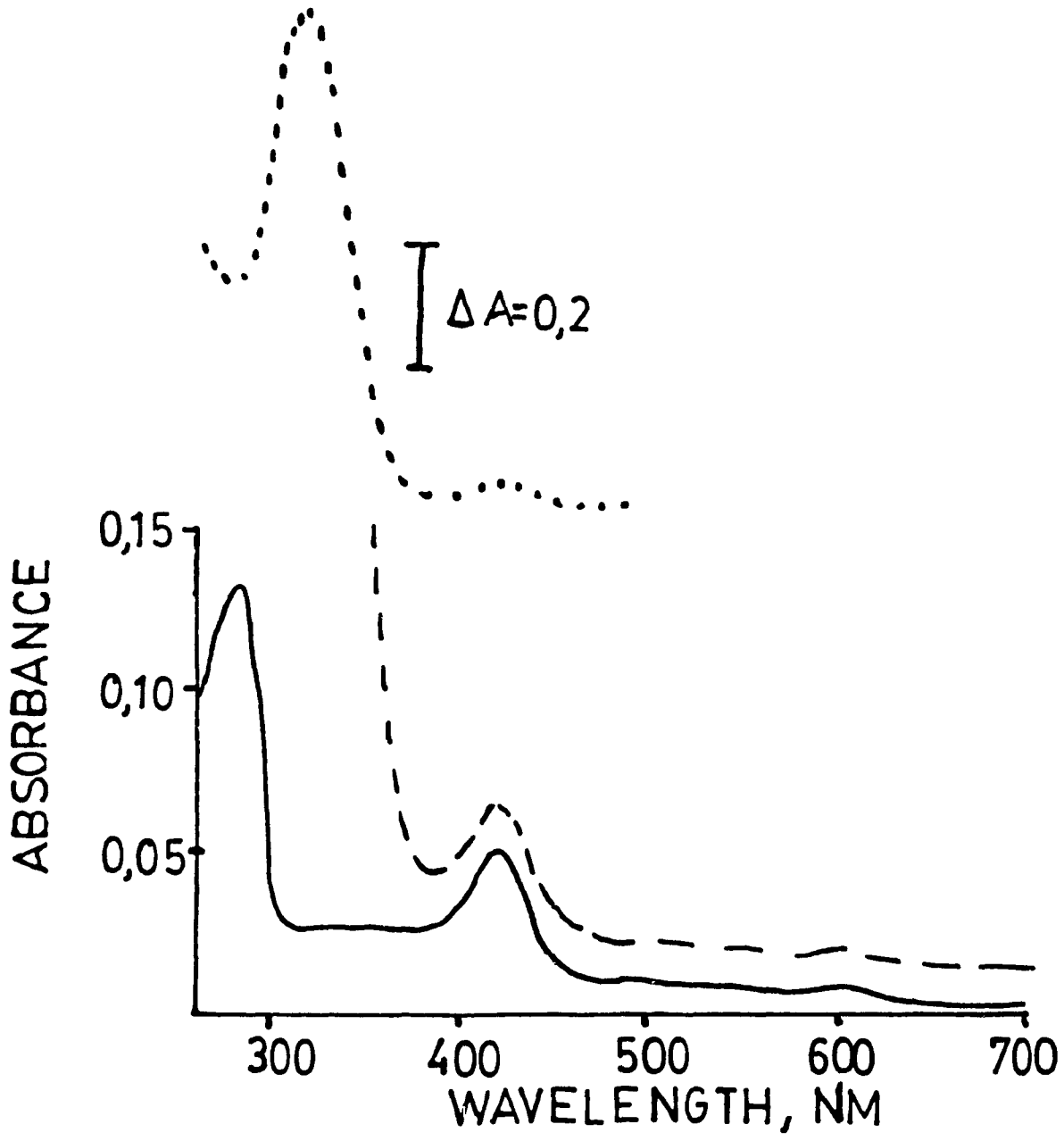
ΔA=0,2
0,15
0,10
0,05
ABSORBANCE
300
400
500
600
700
WAVELENGTH, NM

Fig.4.8: TRYPTOPHAN FLUORESCENCE EMISSION SPECTRA OF OXIDIZED CYTOCHROME OXIDASE - SPLIT CELL EXPERIMENT:- Spectra were obtained in the absence (circles) and presence of a dithionite filter (triangles). Corrected spectra (closed symbols), uncorrected spectra (open symbols). Both cuvettes contained 0.5 ml of 20 mM Tris-Cl, 1 mM EDTA, 0.1 M NaCl, 1 mg/ml lauryl maltoside, pH7.8. To one (sample cuvette) was added 5 µl of 125.89 µM $\underline{aa_3}$. To the other (reference cuvette), was added an aliquot of dithionite solution giving rise to a final concentration of 1 mM. Excitation wavelength was 280 nm. Emission and excitation slits were set at 10 nm. Ambient temperature, open to air.

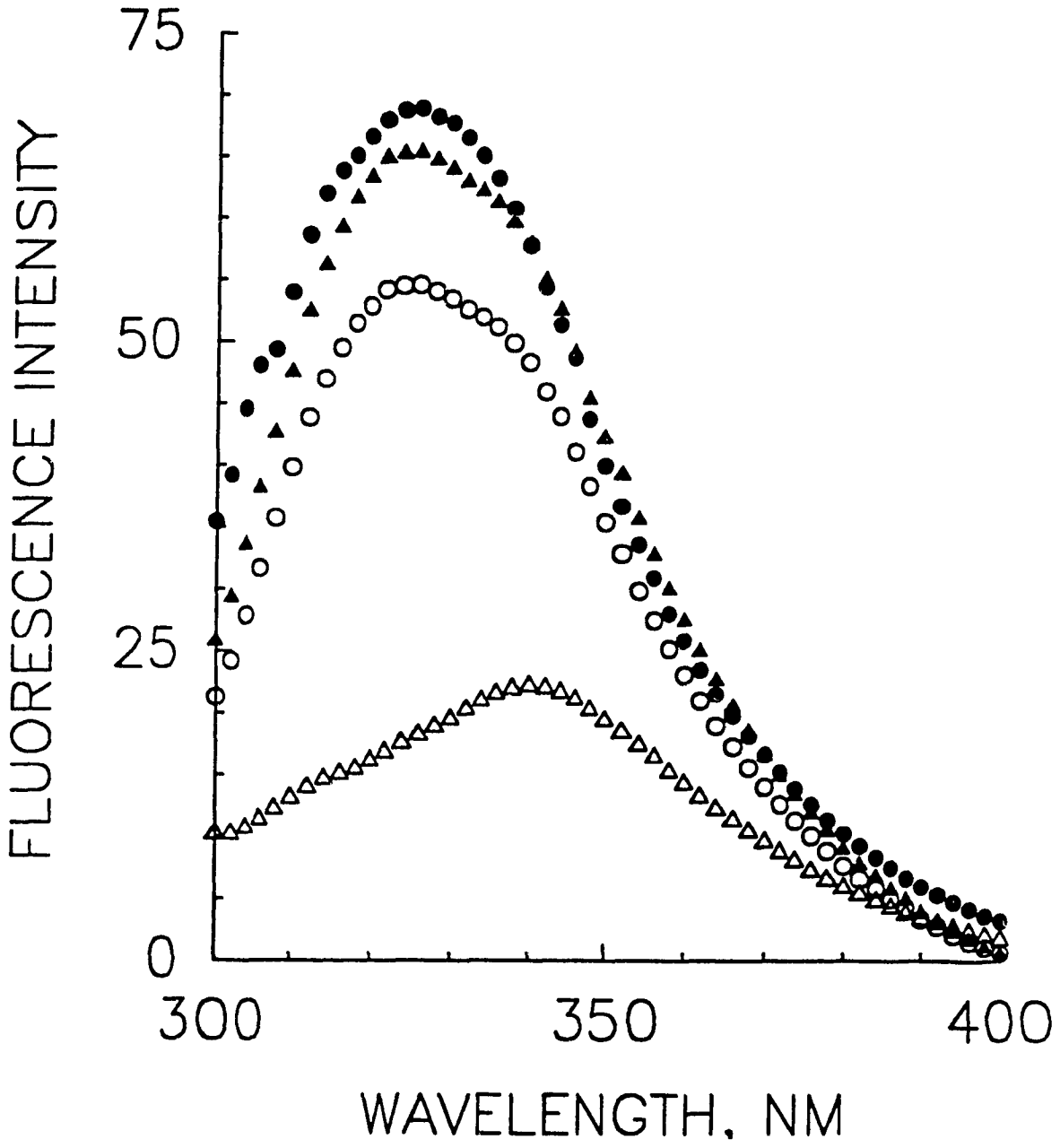
75
50
25
0
FLUORESCENCE INTENSITY
300
350
400
WAVELENGTH, NM

desired. Much lower concentrations may be used when the enzyme is placed in a strictly anaerobic environment so that when it is reduced it cannot be reoxidized. This is achieved by generating mixed-valence, CO-bound cytochrome oxidase. When CO is added to oxidized cytochrome oxidase CO and O_2 are turned over until the solution is anaerobic at which point cytochrome $\underline{a}_3$ is ferrous and CO bound. Cu_B is also reduced in the formation of the mixed-valence, CO-bound species while cytochrome $\underline{a}$ and Cu_A remain oxidized. Thus, the mixed-valence, CO-bound enzyme is generated anaerobically and therefore requires only two further electrons to become fully reduced. This has the net effect of decreasing the amount of reductant required to reduce the enzyme. The visible spectra of cytochrome oxidase in the oxidized, resting form, mixed-valence CO-bound form and the fully reduced CO-bound form are shown in figure 4.9. The Soret values for these three forms were 419 nm, 429 nm and 432 nm, respectively. The difference spectrum between the fully-reduced CO-bound form and the oxidized, resting form is also shown, with maximal optical differences at 410 nm and 603 nm. The optical Soret values determined, as well as spectral shapes, and the values determined from the difference spectrum are consistent with published results (Greenwood et al., 1971). The tryptophan fluorescence emission spectra of these species are shown in figure 4.10. From the uncorrected spectra it is clear that the decreased levels of reductant used has the effect of shifting the emission maximum by only a few nanometers to the red. The mixed-valence CO-bound enzyme has the same fluorescence emission

Fig.4.9: ABSORPTION SPECTRA OF RESTING, OXIDIZED $\underline{aa}_3$, MIXED-VALENCE CO-BOUND $\underline{aa}_3$ AND FULLY REDUCED CO-BOUND $\underline{aa}_3$:- (A) represents 0.51 μM $\underline{aa}_3$ in the resting, oxidized form (dotted line), mixed-valence CO-bound form (solid line) and fully reduced CO-bound form (dashed line). The reductant was 51 μM dithionite. (B) the difference spectrum obtained between the fully reduced CO-bound $\underline{aa}_3$ and the resting, oxidized $\underline{aa}_3$. Samples are in 20 mM Tris-Cl, 1 mM EDTA, 0.1 M NaCl, 1 mg/ml lauryl maltoside, pH7.8. Ambient temperature, anaerobic.

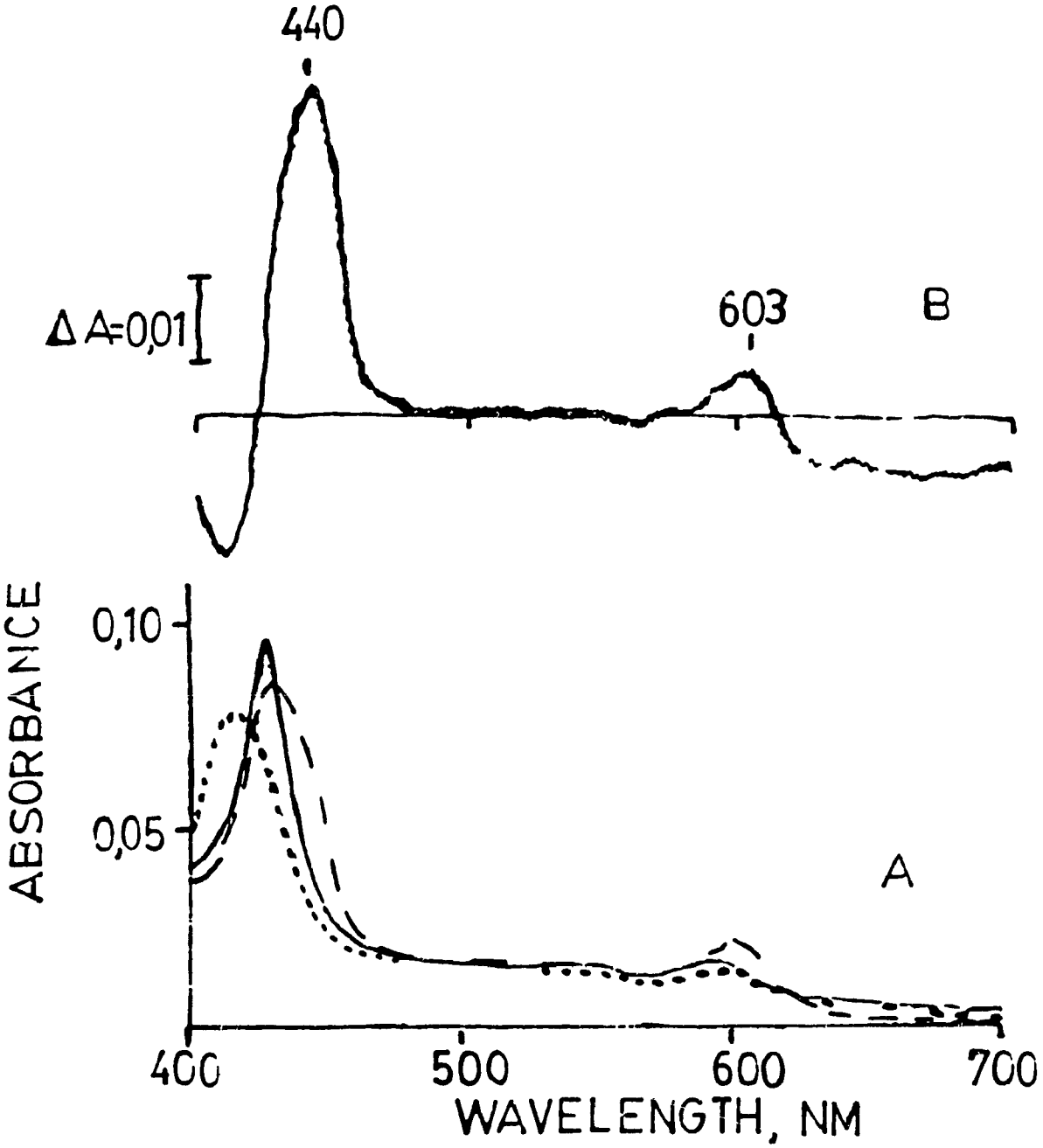
440
ΔA=0,01
603
B
AESORBANCE
0,10
0,05
A
400
500
600
700
WAVELENGTH, NM

Fig.1.10: TRYPTOPHAN FLUORESCENCE EMISSION SPECTRA OF RESTING, OXIDIZED $\underline{aa_3}$, MIXED-VALENCE CO-BOUND $\underline{aa_3}$ AND FULLY REDUCED CO-BOUND $\underline{aa_3}$:- Uncorrected spectra (open symbols), corrected spectra (closed symbols). 0.51 μM resting, oxidized $\underline{aa_3}$ (circles), mixed-valence CO-bound $\underline{aa_3}$ (triangles) and fully reduced CO-bound $\underline{aa_3}$ (squares). Excitation wavelength is 280 nm. Emission and excitation slits are set at 10 nm. Samples are in 20 mM Tris-Cl, 1 mM EDTA, 0.1 M NaCl, 1 mg/ml lauryl maltoside, pH7.8. Ambient temperature, anaerobic.

maximum properties as the resting form of the enzyme consistent with reports by Copeland et al., (1987). The corrected fluorescence spectra of these species are essentially identical in terms of their emission maxima.

4.1.2 REDUCTION OF CYTOCHROME OXIDASE USING DEAZAFLAVIN

The photoreductant deazaflavin may be used in catalytic amounts to reduce cytochrome oxidase. The low absorbance of deazaflavin under these conditions does not significantly alter the absorption spectrum of cytochrome oxidase, thereby contributing very little to the overall inner filter effect. In this respect deazaflavin is different from the reductant sodium dithionite which produces a large inner filter effect in a 20 nm red-shift of the tryptophan emission. The use of deazaflavin minimizes the absorbance of reduced enzyme samples in the UV spectral region such that correction of the fluorescence spectrum will be small.

At the concentration of photoreductant used the contribution of deazaflavin to the the optical spectrum is 0.02 absorbance units at 322 nm and 388 nm (Fig.3.3). This contribution is negligible compared to the absolute spectrum of cytochrome aa_3 used in these experiments. Figure 4.11 is the absolute absorption spectrum of $\underline{aa_3}$ under one atmosphere of CO prior to irradiation. The Soret band is at 419 nm. Due to the low concentration of aa_3, the mixed-valence carbonmonoxy-bound species, $a^{3+}a_3^{2+}$-CO, is not formed to a large extent. The Soret maximum at 419 nm indicates that the enzyme is mostly in the oxidized state (i.e. $a^{3+}a_3^{3+}$). The fluorescence spectrum of this sample is shown in figure 4.12.

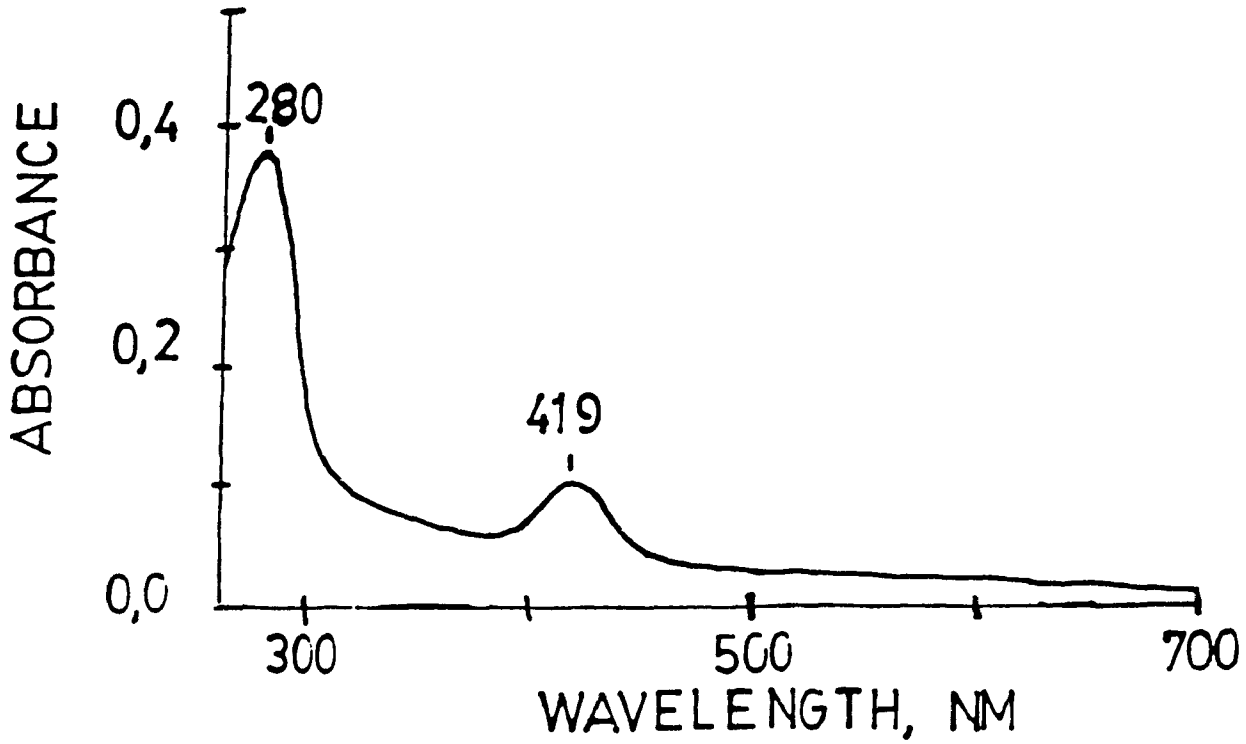

Fig.4.11: ABSOLUTE ABSORPTION SPECTRUM OF NON-IRRADIATED CYTOCHROME OXIDASE :- cytochrome oxidase concentration is 520 nM. Sample is under an atmosphere of CO with 1.65 µM deazaflavin, 9 mM EDTA, 20 mM Tris-Cl, 1 mg/ml lauryl maltoside, 0.1 M NaCl, pH 7.8. Ambient temperature.

Fig.4.12: CORRECTED FLUORESCENCE EMISSION SPECTRA OF NON-IRRADIATED SAMPLES:- 0.52 μM cytochrome oxidase, 1.65 μM deazaflavin, 9mM EDTA, 20 mM Tris-Cl, 1 mg/ml lauryl maltoside, 0.1 M NaCl, pH7.8 under CO (open circle) - 1.65 μM deazaflavin, 9 mM EDTA, 20 mM Tris-Cl, 1 mg/ml lauryl maltoside, 0.1 M NaCl, pH7.8 under CO (closed circle) - Net fluorescence due to aa$_3$/CO corrected for deazaflavin contribution (open triangle). Excitation at 280 nm. Emission and excitation slit widths set at 10 nm. Ambient temperature.

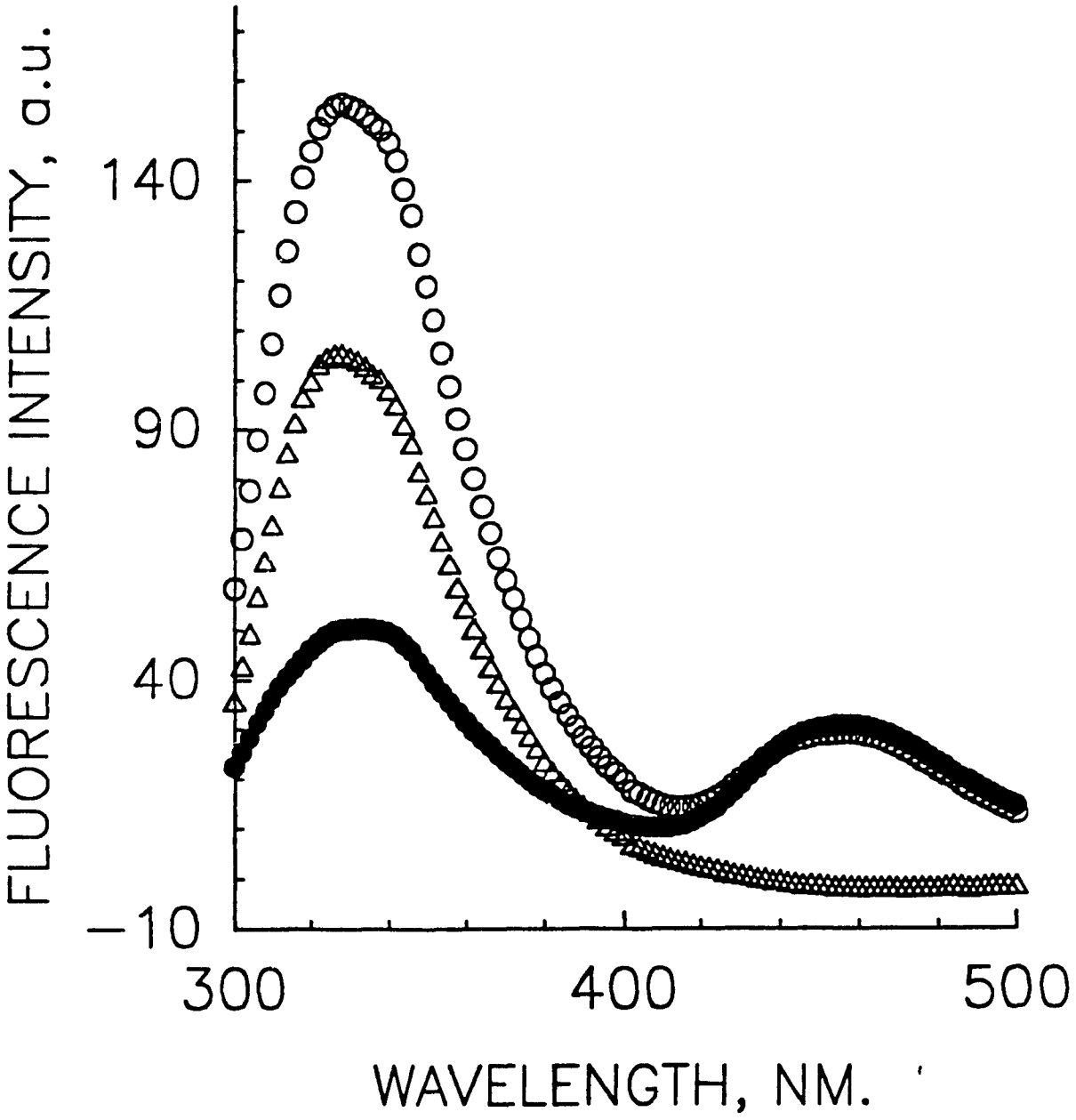
FLUORESCENCE INTENSITY, a.u.
140
90
40
−10
300
400
500
WAVELENGTH, NM.

Cytochrome oxidase under CO and in the presence of deazaflavin, prior to irradiation, has a corrected fluorescence spectrum with emission maxima at 328 nm and 456 nm. The same concentration of deazaflavin under the same conditions as the enzyme sample above, shows a broad fluorescence emission band at 330 nm and 458 nm. The fluorescence intensity observed at 330 nm for the control is ca. 33% of that observed for the $\underline{aa}_3$:CO sample. The fluorescence emission due solely to $\underline{a}^{3+}\underline{a}_3{}^{3+}$/CO (under CO) is determined from the difference spectrum of the $\underline{aa}_3$ sample and the deazaflavin control. The 458 nm peak is abolished and a decrease of ca. 33% in the fluorescence intensity at 328 nm is observed in the $\underline{a}^{3+}\underline{a}_3{}^{3+}$/CO difference spectrum, which corresponds to the contribution of deazaflavin.

After a total irradiation time, t_{irr}, of 18 min, cytochrome oxidase is fully reduced by deazaflavin (Fig. 1.13). Figure 4.14A depicts the visible absorption spectra of $\underline{a}^{3+}\underline{a}_3{}^{3+}$/CO and $\underline{a}^{2+}\underline{a}_3{}^{2+}$-CO (bound CO). A Soret maximum at 430 nm is indicative of fully reduced CO-bound cytochrome oxidase. The difference spectrum of the reduced CO-bound enzyme and the oxidized is shown in figure 4.14B. The maximum difference is observed at 443 nm and 605 nm, typical of reduced minus oxidized $\underline{aa}_3$ spectra under normal conditions (no CO, plus dithionite). The extinction coefficients were determined for each band. $\varepsilon_{443-479\ nm}$(red.-ox.) was determined to be 69.23 $mM^{-1}cm^{-1}$ and $\varepsilon_{605-620\ nm}$(red.-ox.) was 17.31 $mM^{-1}cm^{-1}$. The respective extinction coefficients for non-ligated, fully reduced $\underline{aa}_3$ are 164.1 $mM^{-1}cm^{-1}$ and 21.42 $mM^{-1}cm^{-1}$. The fully

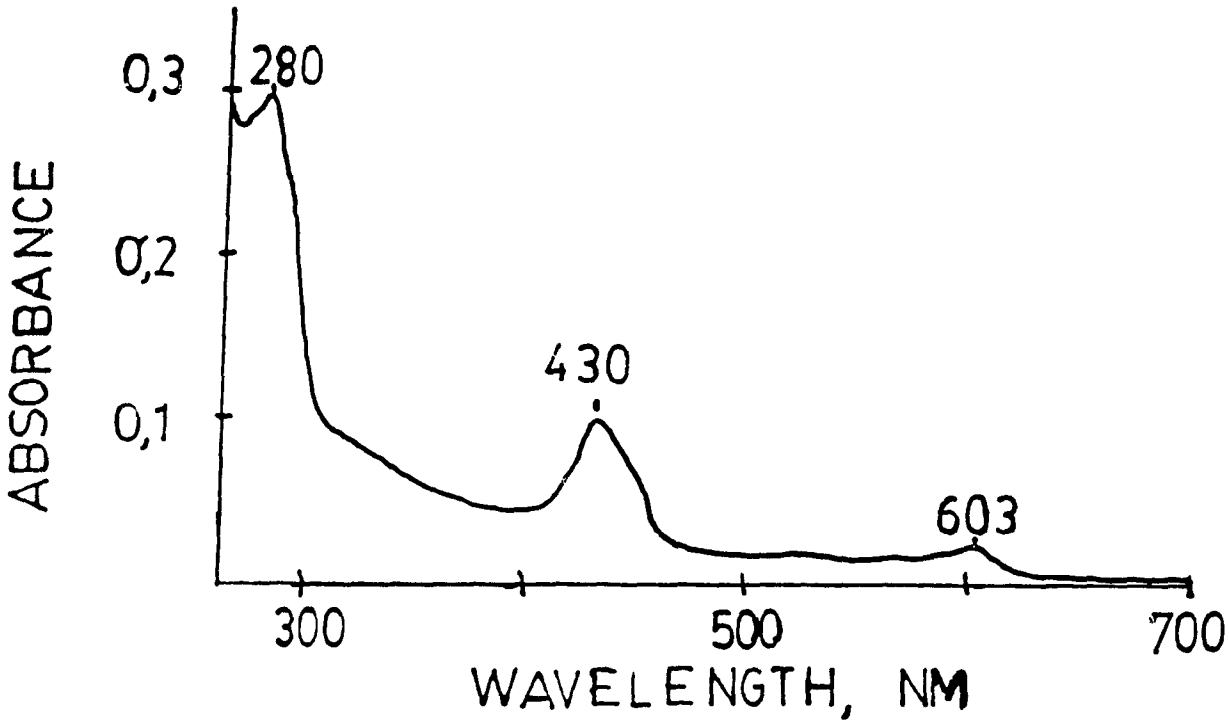

Fig.4.13: ABSOLUTE ABSORPTION SPECTRUM OF FULLY DEAZAFLAVIN REDUCED CYTOCHROME OXIDASE:- 0.52 µM cytochrome oxidase, 1.65 µM deazaflavin, 9mM EDTA, 20 mM Tris-Cl, 1 mg/ml lauryl maltoside, 0.1 M NaCl, pH7.8 under CO at ambient temperature. Total irradiation time was 18 min.

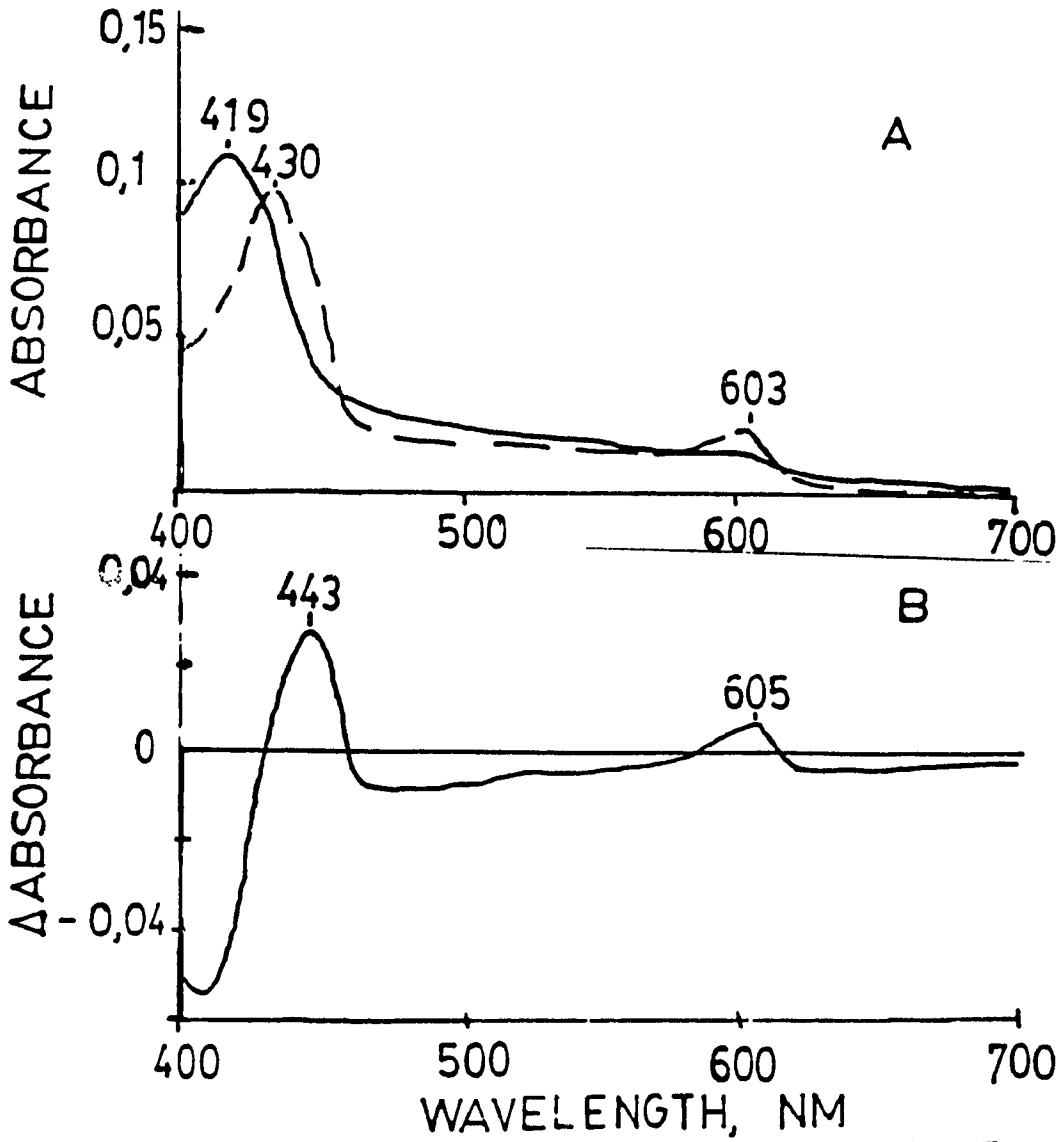

Fig.4.14: ABSORPTION SPECTRA OF NON-IRRADIATED AND IRRADIATED CYTOCHROME OXIDASE:- (A) depicts the absorption spectra of $\underline{a}^{3+}\underline{a}_3{}^{3+}$/CO (solid line) and $\underline{a}^{2+}\underline{a}_3{}^{2+}$-CO (dashed line), (B) represents the difference spectrum obtained between $\underline{a}^{2+}\underline{a}_3{}^{2+}$-CO and $\underline{a}^{3+}\underline{a}_3{}^{3+}$/CO. 0.52 μM cytochrome oxidase, 1.65 μM deazaflavin, 9mM EDTA, 20 mM Tris-Cl, 1 mg/ml lauryl maltoside, 0.1 M NaCl, pH7.8 under CO at ambient temperature. Total irradiation time was 18 min.

reduced $\underline{aa}_3$-CO using deazaflavin gave rise to extinction coefficients which were 42.2% and 80.8% of those cited for the 443-479 nm and 605-620 nm pair, respectively. These values are comparable to the contribution of reduced cytochrome $\underline{a}$ to the reduced spectrum of $\underline{aa}_3$. Furthermore, subsequent addition of dithionite induces no change in the visible spectrum except for a consistent increase in the background absorbance (Fig.4.16A). Figure 4.16B demonstrates the difference spectrum of deazaflavin reduced $\underline{aa}_3$ prior and subsequent to the addition of dithionite. No appreciable difference is observed implying that the cytochrome oxidase is fully reduced by irradiation in the presence of deazaflavin. The corrected fluorescence spectra of the irradiated samples are shown in figure 4.15. Fully reduced cytochrome $\underline{aa}_3$ has an emission maximum at 326 nm. The irradiated control has a fluorescence spectrum similar to that observed for the non-irradiated control except for a decrease in the fluorescence intensity, ca. 33%, in the 450 nm region. The 457 nm band is no longer present in the oxidase sample spectrum but is still visible in the control spectrum consisting of deazaflavin in the absence of oxidase. The process giving rise to this band is not clear, but its possible origin will be addressed.

The difference spectrum of non-irradiated $\underline{aa}_3$ ($\underline{a}^{3+}\underline{a}_3{}^{3+}$/CO) and irradiated $\underline{aa}_3$ ($\underline{a}^{2+}\underline{a}_3{}^{2+}$-CO) is shown in figure 4.17. A net increase in fluorescence intensity is observed at 328 nm for the non-irradiated sample. The difference in the 450 nm region is due to the discrepancy between the irradiated control and

Fig.4.15: CORRECTED FLUORESCENCE EMISSION SPECTRA OF IRRADIATED SAMPLES:- 0.52 μM aa_3, 1.65 μM deazaflavin, 9 mM EDTA, 20 mM Tris-Cl, 1 mg/ml lauryl maltoside, 0.1 M NaCl, pH7.8 under CO (open circle) - 1.65 μM deazaflavin, 9 mM EDTA, 20 mM Tris-Cl, 1 mg/ml lauryl maltoside, 0.1 M NaCl, pH7.8 under CO (closed circle)- Net fluorescence due to fully reduced aa_3-CO corrected for deazaflavin contribution (open triangle). Excitation at 280 nm. Emission and excitation slits at 10 nm. Ambient temperature.

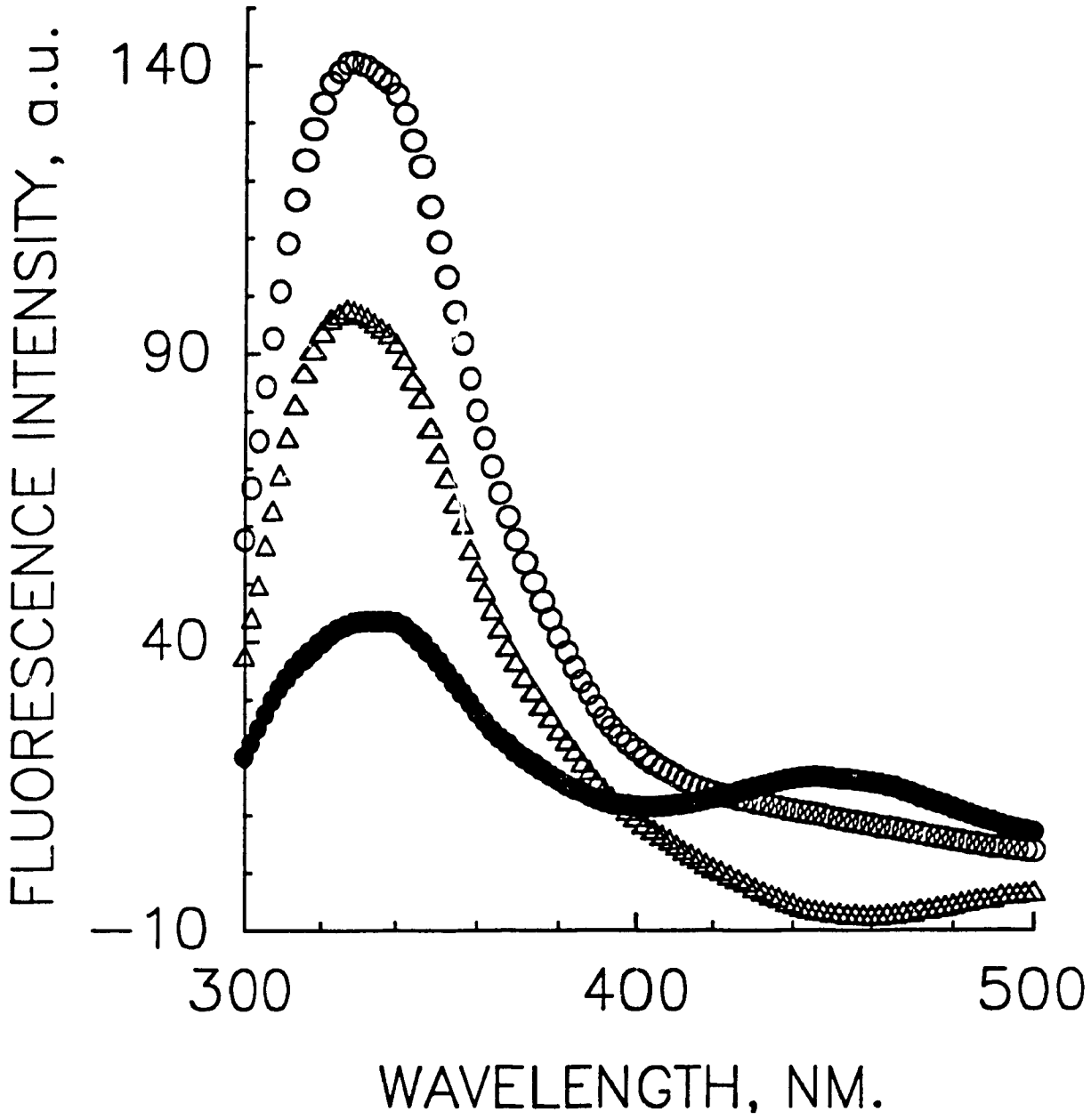
FLUORESCENCE INTENSITY, a.u.
140
90
40
−10
300
400
500
WAVELENGTH, NM.

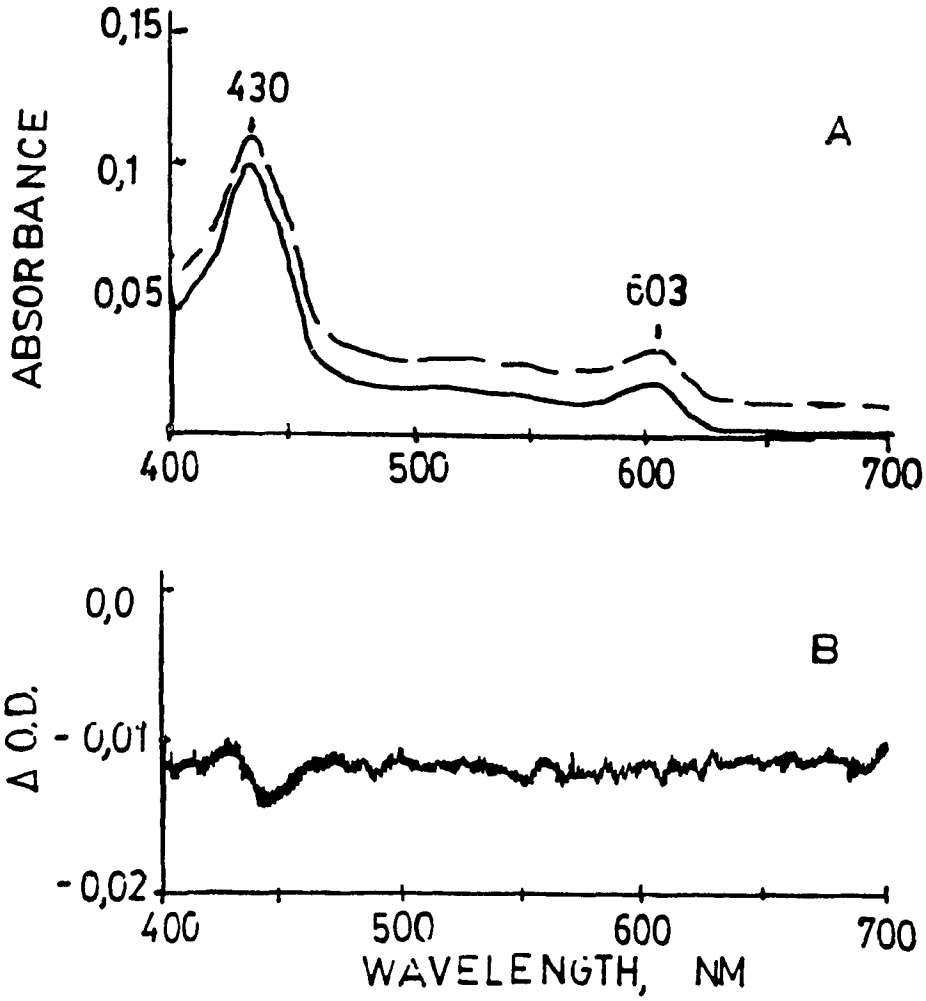

Fig.4.16: ABSORPTION SPECTRUM OF FULLY DEAZAFLAVIN REDUCED aa_3-CO UPON DITHIONITE ADDITION:- (A) demonstrates the absorption spectra of fully reduced aa_3-CO prior to (solid line) and subsequent to (dashed line) the addition of excess dithionite. (B) the difference spectrum obtained for fully reduced aa_3-CO after minus before addition of dithionite. 0.52 μM aa_3, 1.65 μM deazaflavin, 9 mM EDTA, 20 mM Tris-Cl, 1 mg/ml lauryl maltoside, 0.1 M NaCl, pH7.8 under CO at ambient temperature.

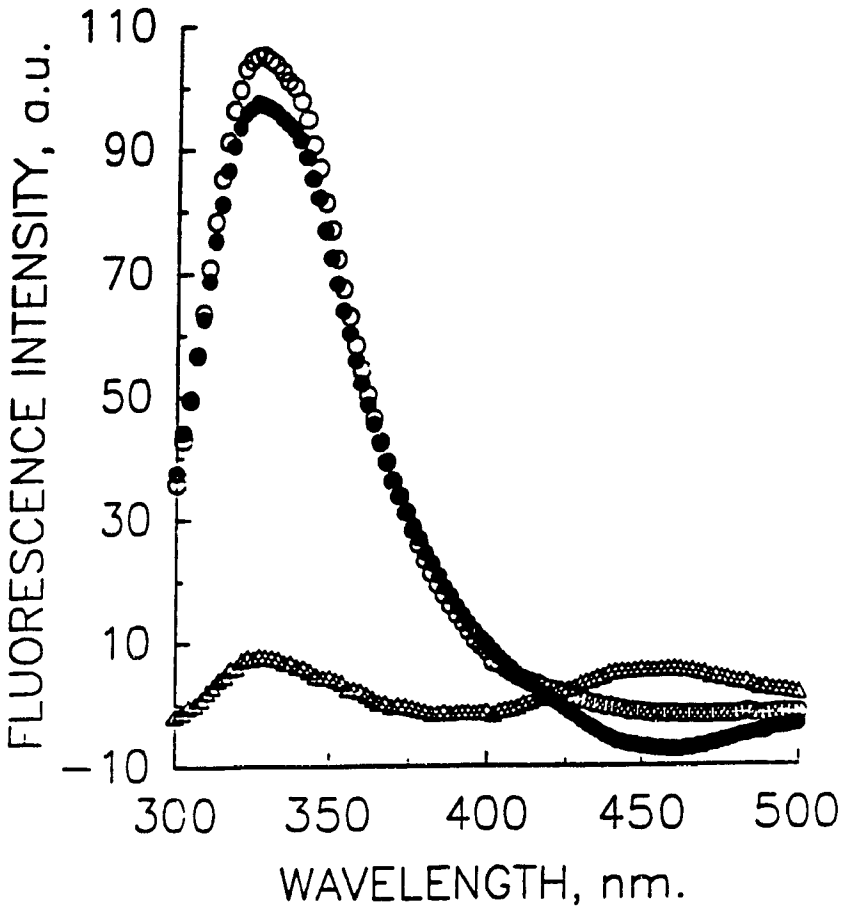

Fig.4.17: CORRECTED FLUORESCENCE EMISSION SPECTRA FOR MIXED-VALENCE CO-BOUND $\underline{aa_3}$ AND FULLY REDUCED CO- BOUND $\underline{aa_3}$:- mixed-valence CO-bound $\underline{aa_3}$ (open circle), fully reduced CO-bound $\underline{aa_3}$ (closed circle), difference spectrum between the mixed-valence and fully reduced enzyme (open triangle). 0.52 µM $\underline{aa_3}$, 1.65 µM deazaflavin, 9 mM EDTA, 20 mM Tris-Cl, 1 mg/ml lauryl maltoside, 0.1 M NaCl, pH7.8 under CO at ambient temperature. No dithionite present.

the irradiated sample in this region. Since this region of the spectrum is due solely to deazaflavin, the observed difference has no direct consequence on the $\underline{aa}_3$ tryptophan fluorescence. The difference spectrum obtained between the mixed-valence CO-bound $\underline{aa}_3$ and the fully reduced CO-bound $\underline{aa}_3$ has two emission maxima, 328 nm and 458 nm. The 458 nm fluorescence intensity is equal to the decrease observed upon irradiation of the control. The 328 nm band in the irradiated control was unaltered so the 10% increase observed in this band for the mixed-valence enzyme as compared to its fully reduced counterpart is a consequence of the differences in the tryptophan fluorescence of the two cytochrome oxidase species. It should be noted that a 10% difference is within the realm of possible experimental error and in the procedure used for data correction.

4.1.3 TRYPTOPHAN FLUORESCENCE OF VESICULAR CYTOCHROME OXIDASE

Cytochrome oxidase vesicles are prepared and characterized as stated in the Methods and Materials section. A relative measure of the inherent permeability of this membrane system to protons can be obtained by determining the respiratory control ratio. The respiratory control ratio for these vesicles is 2.7. Cytochrome oxidase incorporated into phospholipid vesicles may be oriented so that its cytochrome c binding site faces towards the cytosolic side or the matrix side of the lipid membrane. To determine how much of each orientation is present, the cytochrome c reducibility of the oxidase is determined (Fig.4.18). The maximum absorbance change observed in the presence of ascorbate and

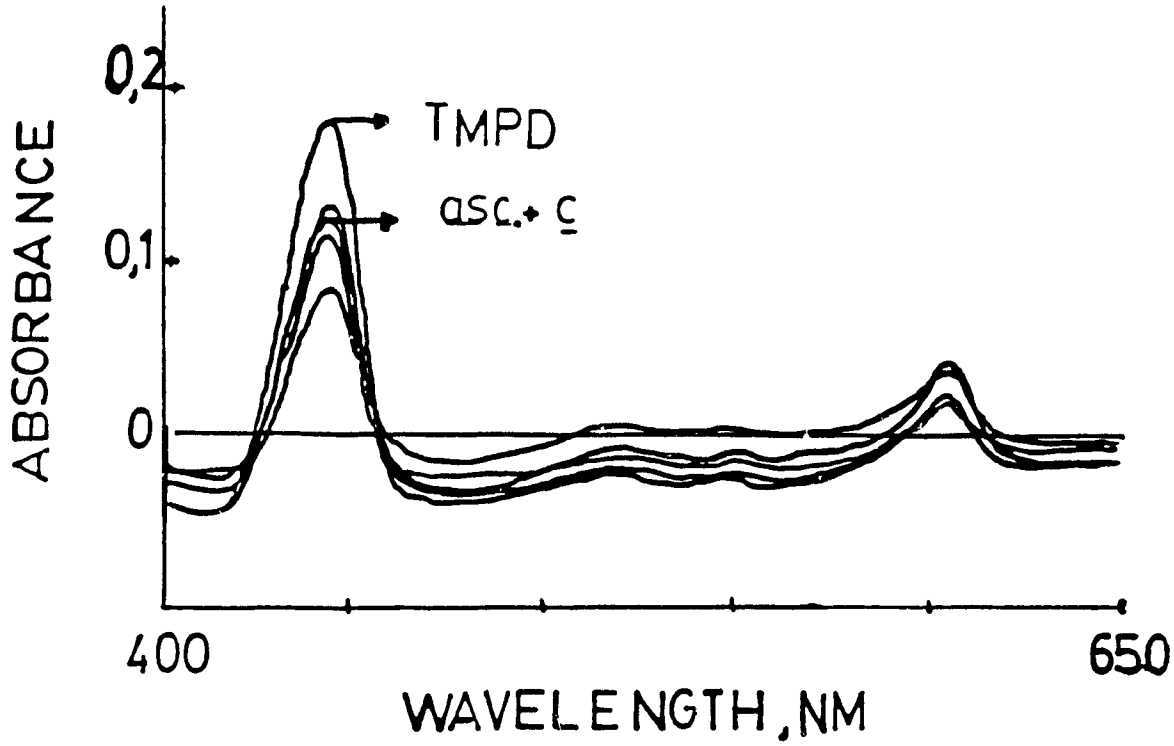

Fig.4.18: CYTOCHROME c ACCESSIBILITY OF CYTOCHROME OXIDASE VESICLES :- the cytochrome oxidase concentration was 3.8 µM. Reduced minus oxidized difference spectra were obtained at various times during a 2 hour assay period. Maximal reduction of cytochrome oxidase by 11.5 mM ascorbate and 0.28 µM cytochrome c is denoted by arrow (asc. + c). Complete reduction of cytochrome oxidase is achieved with 0.57 mM TMPD and is indicated by arrow (TMPD).

cytochrome c, and in the presence of a membrane permeable artificial substrate, TMPD, is shown for the 445 nm band. The percentage of $\underline{aa_3}$ in the vesicle preparation having the cytochrome c binding site oriented towards the cytosolic side is 81% using an $\varepsilon_{(442-475)}$= 153.04 $mM^{-1}cm^{-1}$ (reduced minus oxidized) and 86% using an $\varepsilon_{(605-477)}$= 32.55 $mM^{-1}cm^{-1}$ (reduced minus oxidized). Figure 4.19 represents the absorption difference spectrum of $\underline{aa_3}$ vesicles with a cytosolic and matrix pH of 8.0. The reference sample was an equal concentration of vesicles containing no protein. The uncorrected tryptophan fluorescence emission spectrum for the proteoliposomes with a $\Delta pH=0$ across the membrane is shown in figure 4.20. Liposomes containing no cytochrome oxidase are shown to have a fluorescence peak at 359 nm. The 359 nm fluorescence peak is also observed for the proteoliposomes but is eliminated when the difference spectrum between the proteoliposomes and the liposomes (no $\underline{aa_3}$) is taken. The emission maxima for the proteoliposomes as determined from the uncorrected spectrum is 330 nm.

No significant change in the absorption spectrum of proteoliposomes having a matrix pH=8.0 and a cytosolic pH=1.96 is observed when compared to proteoliposomes with a $\Delta pH=0$ (Fig.4.21). By contrast, the absorption spectra of proteoliposomes is broadened compared to that observed for $\underline{aa_3}$ free in a lauryl maltoside solution (Fig.4.22). This phenomenon is probably due to the light scattering properties of the vesicles. The inability to properly reference this region of the spectrum in order to obtain an unperturbed $\underline{aa_3}$ spectrum is most probably due to differences in the

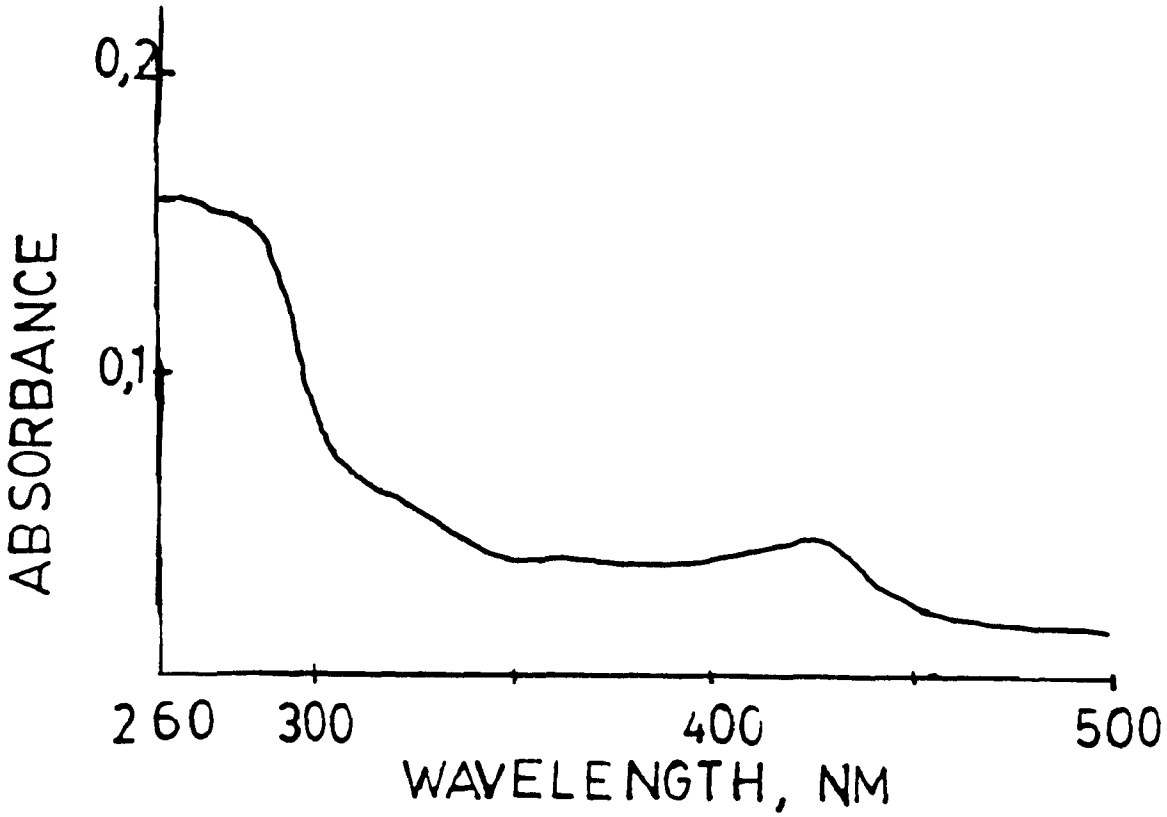

Fig.4.19: DIFFERENCE SPECTRA OF CYTOCHROME OXIDASE VESICLES, ΔpH=0 :- sample consisted of 190 nM cytochrome oxidase in phospholipid vesicles. Reference was the same concentration of vesicles containing no protein. Cytosolic pH=8.0, matrix pH=8.0.

Fig.4.20: UNCORRECTED FLUORESCENCE SPECTRA OF CYTOCHROME OXIDASE VESICLES :- the cytochrome oxidase concentration was 190 nM. Cytosolic pH=8.0, matrix pH=8.0. Reference was similar concentration of vesicles containing no protein. (open circles) reference, (closed circles) proteoliposomes, (open triangles) difference spectra (proteoliposomes-liposomes). Excitation was at 280 nm. Excitation and emission slits were 5 nm. Ambient temperature, open to air.

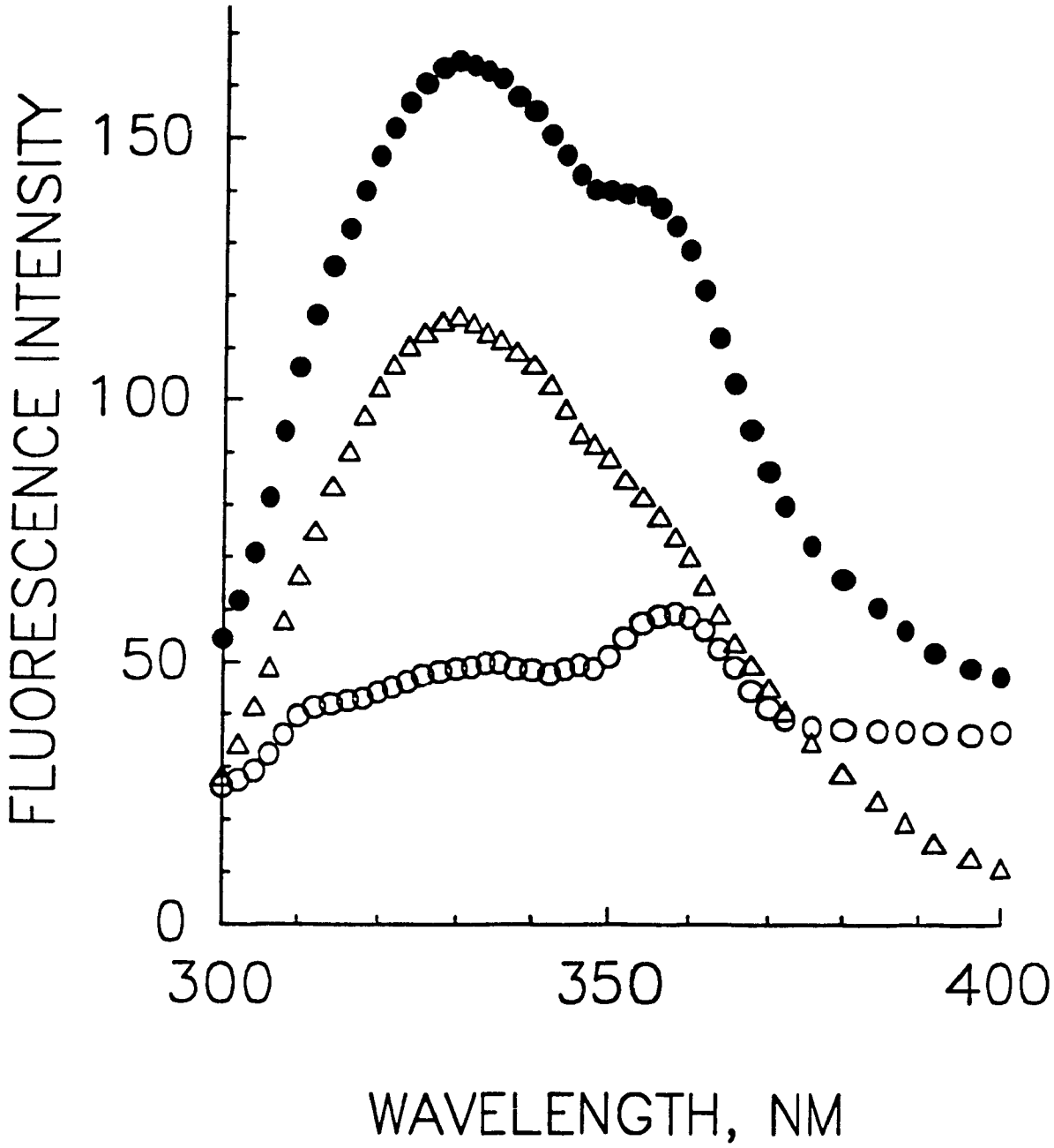
FLUORESCENCE INTENSITY
150
100
50
0
300
350
400
WAVELENGTH, NM

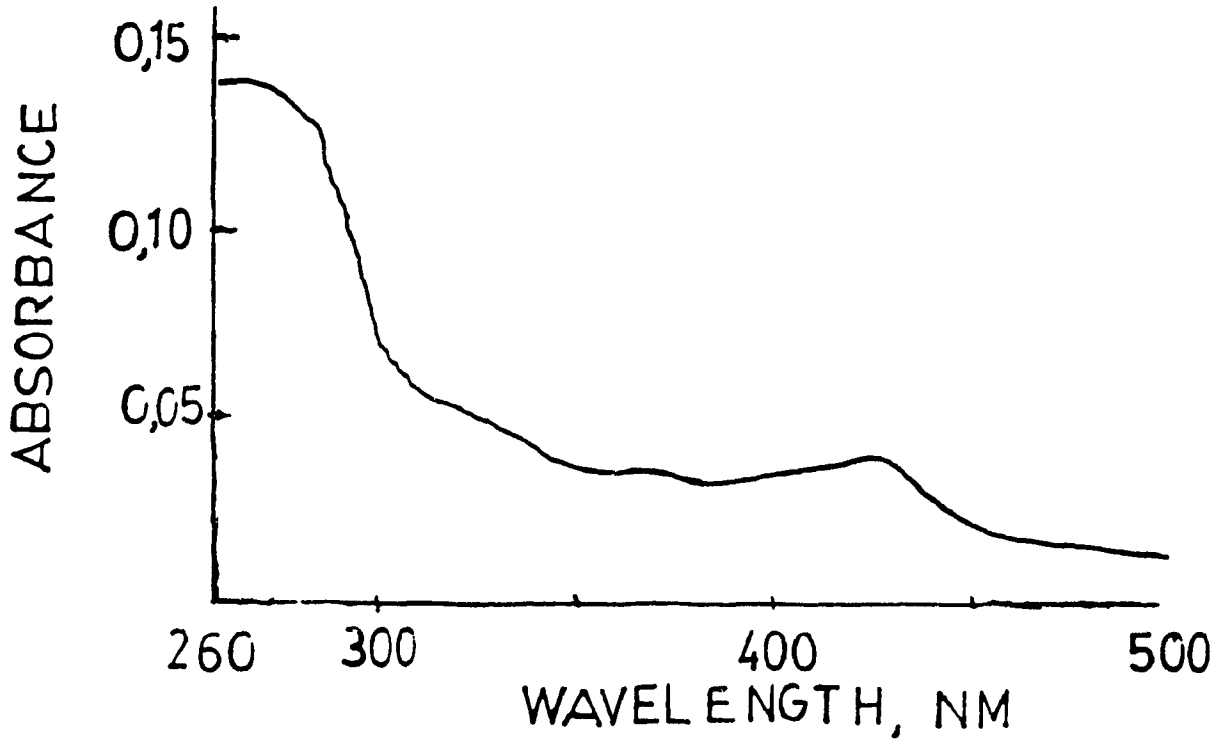

Fig.4.21: ABSORPTION DIFFERENCE SPECTRUM OF CYTOCHROME OXIDASE VESICLES, ΔpH=3.0 :- cytochrome oxidase concentration was 190 nM. Reference was equal concentration of liposomes (no protein). Cytosolic pH=4.96, matrix pH=8.0. Ambient temperature, open to air.

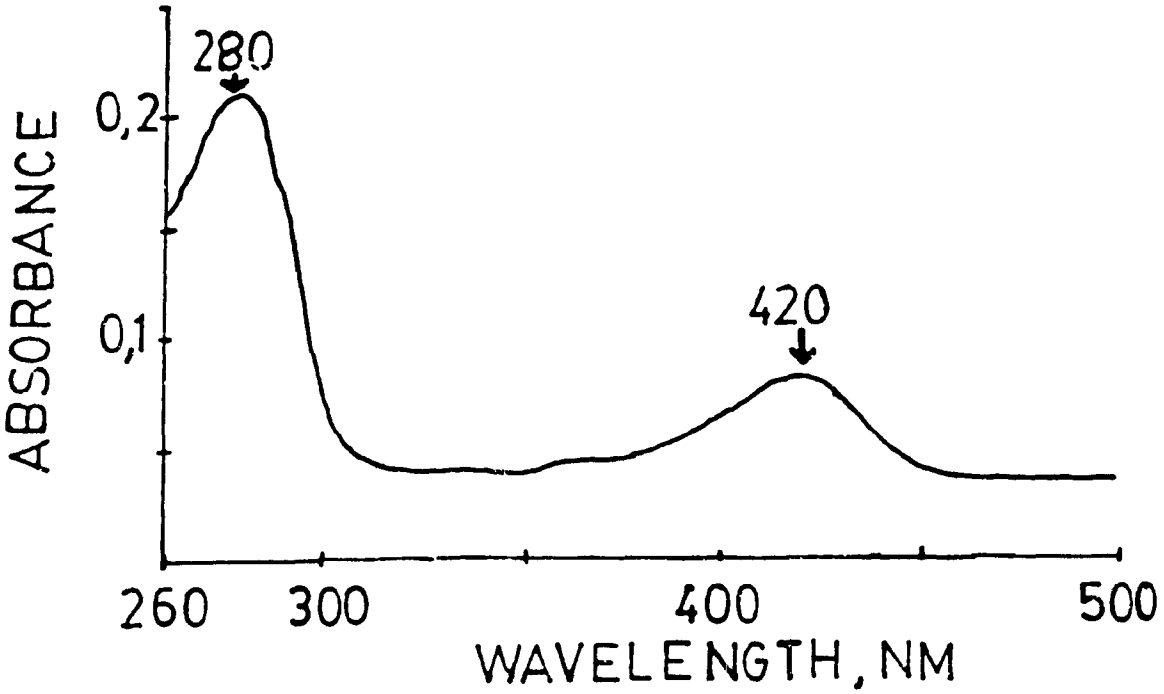

Fig.4.22: ABSOLUTE ABSORPTION SPECTRUM OF CYTOCHROME OXIDASE :- cytochrome oxidase was 360 nM in 20 mM Tris-Cl, 1 mM EDTA, 1 mg/ml lauryl maltoside, pH=7.8. Ambient temperature, open to air.

light scattering properties of vesicles containing no protein and those containing $\underline{aa}_3$.

The corrected tryptophan fluorescence emission spectra of $\underline{aa}_3$ vesicles in the presence and absence of a pH gradient, as well as that for free $\underline{aa}_3$ in solution is shown in figure 4.23. The increase in the fluorescence intensity of free $\underline{aa}_3$ as compared to vesicular $\underline{aa}_3$ is due mainly to its greater concentration in the sample. The corrected fluorescence intensity of the vesicular $\underline{aa}_3$ is overestimated due to the increased magnitude in the correction factors used, ca. 2.9 for vesicular $\underline{aa}_3$ and ca. 1.3 for free $\underline{aa}_3$. Comparing the fluorescence intensities of the liposomal $\underline{aa}_3$ in the presence and absence of a pH gradient across the vesicle membrane, it is observed that the fluorescence intensity of $\underline{aa}_3$ vesicles in the presence of a pH gradient of 3.0 units is decreased by 20% at its maximum. In order to visualize the effect of these conditions on the fluorescence emission wavelength maxima the spectra were normalized with regards to the maximum fluorescence emission intensity (Fig.4.24). The fluorescence emission maximum for vesicular $\underline{aa}_3$ is consistent with that for free $\underline{aa}_3$ and is centered at 330 nm. A slight blue-edge broadening is observed in the vesicular $\underline{aa}_3$. By contrast, a fluorescence emission maximum of 326 nm is observed for vesicular $\underline{aa}_3$ in the presence of a pH gradient. This blue-shift and decrease in fluorescence intensity may be attributed to various processes:- 1) increased quenching of relatively exposed tryptophans resulting in a decrease in total fluorescence intensity and a net increase in the

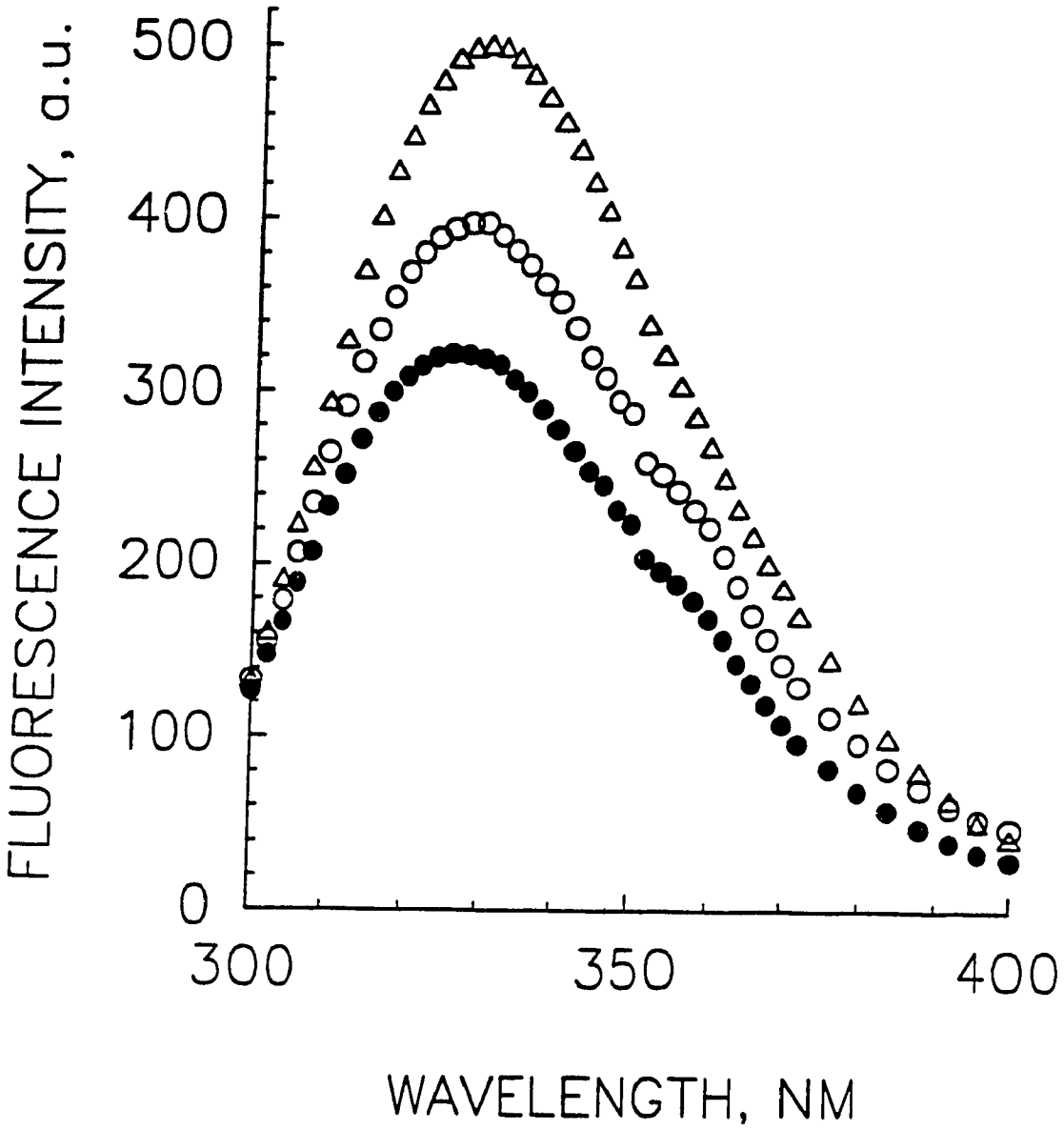

Fig.4.23: CORRECTED TRYPTOPHAN FLUORESCENCE EMISSION SPECTRA OF VESICULAR AND FREE CYTOCHROME OXIDASE :- Vesicular cytochrome oxidase concentration was 190 nM and the pH gradient across the vesicle membrane was ΔpH=0 (open circles) or ΔpH=3 (closed circles). Cytochrome oxidase in lauryl maltoside was 360 nM (open triangles), pH=7.8. Ambient temperature, open to air.

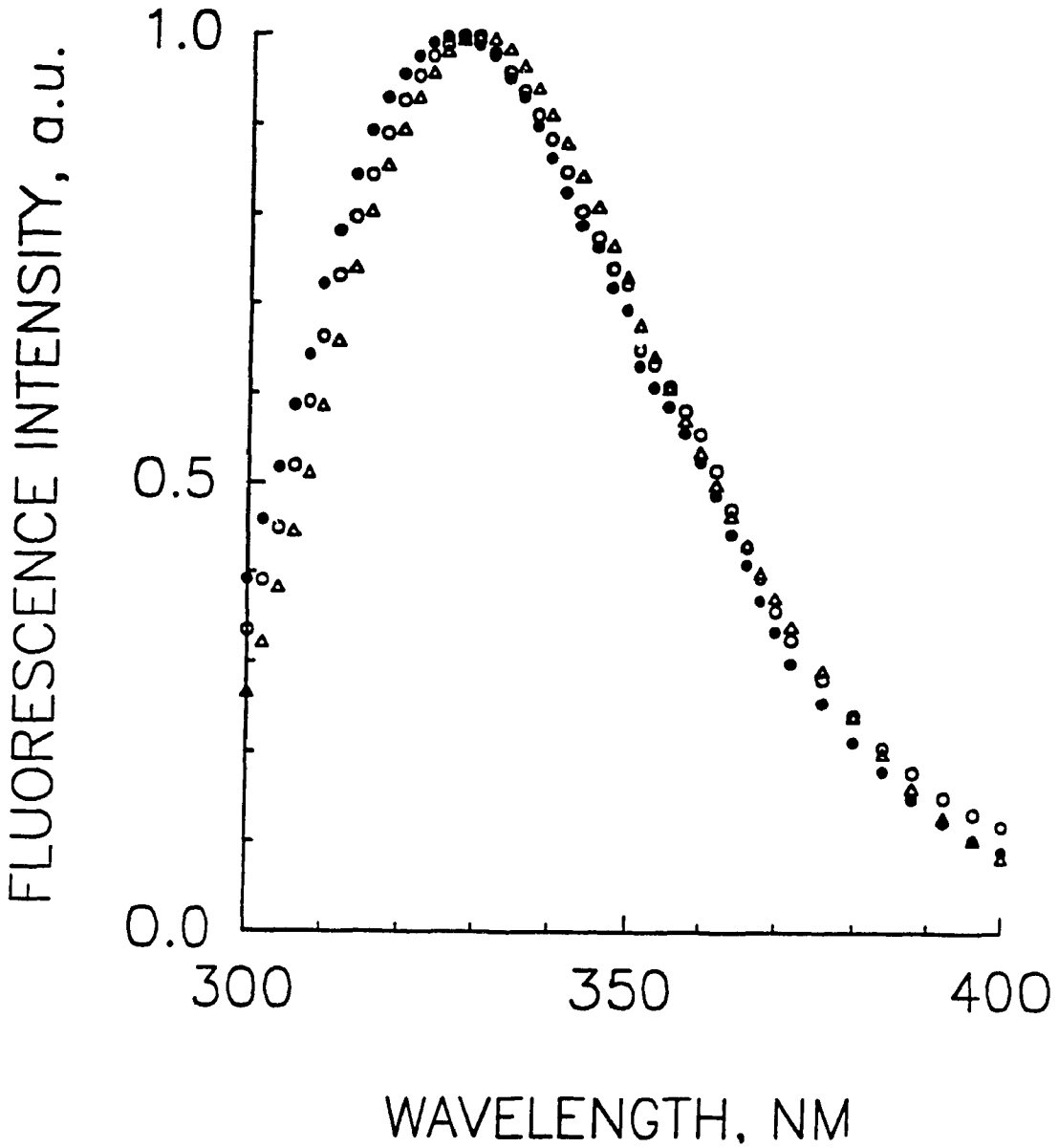

Fig.4.24: NORMALIZED FLUORESCENCE EMISSION SPECTRA OF VESICULAR AND FREE CYTOCHROME OXIDASE :- vesicular aa_3 was 190 nM. The pH gradient across the vesicle membrane was $\Delta pH=0$ (open circles) or $\Delta pH=3$ (closed circles). Free oxidase concentration was 360 nM (open triangles), pH=7.8.

contribution of internal fluorophores to the total observable intensity, 2) a conformational change inducing the exposure of a percentage of fluorescing tryptophans such that these species are rendered significantly less fluorescent possibly by the process stated in (1), and 3) a conformational change inducing internalization of a small percentage of fluorescent tryptophans giving rise to the observed blue-shift in the emission spectrum. In the latter case the decrease in fluorescence intensity may be attributed to an increase in the efficiency of quenching the tryptophans by the heme.

The fluorescence emission difference spectrum of vesicular $\underline{aa_3}$ and free $\underline{aa_3}$ is shown in figure 4.25B. A net increase in fluorescence intensity occurs in the lower wavelength region of the spectrum. The slight increase observed in the fluorescence intensity difference is most probably due to the increased relative intensity of buried tryptophans due to increased shielding from the external environment by way of the phospholipid coat. Since the emission maximum is unchanged the percentage of buried and external tryptophans is assumed to be consistent in both vesicular $\underline{aa_3}$ and free $\underline{aa_3}$.

The difference between vesicles in the presence or absence of a pH gradient is depicted in figure 4.25A. A net shift in the fluorescence intensity to lower wavelengths is observed, indicating an increase in either the relative intensity of the emitting fluorescent species in this region or a net increase in the population of fluorophores in this region. A net decrease in

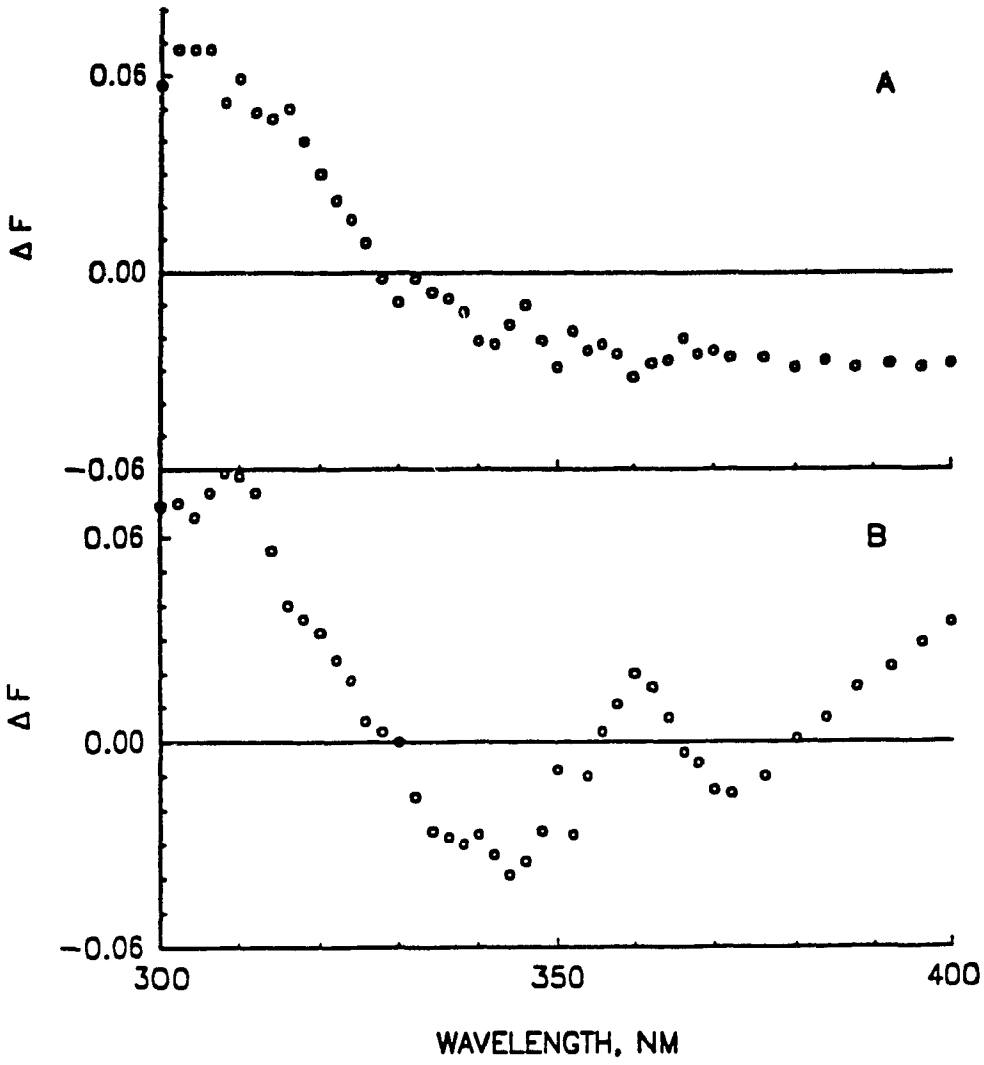

Fig.4.25: FLUORESCENCE EMISSION DIFFERENCE SPECTRA OF VESICULAR CYTOCHROME OXIDASE :- Spectra used were normalized spectra shown in figure 4.24. (A) depicts the difference spectrum obtained between $\underline{aa_3}$ vesicles with a ΔpH=3 and $\underline{aa_3}$ vesicles with a ΔpH=0 (ΔpH3-ΔpH0) (protonmotive effect). (B) portrays the difference spectrum obtained between vesicular $\underline{aa_3}$ (ΔpH=0) and free $\underline{aa_3}$ in lauryl maltoside (vesicular - free) (liposomal incorporation effect).

the fluorescence intensity is observed throughout the red-edge of the spectrum. This decrease may be attributed to either a decrease in the relative intensity of the regional fluorescent species or a decrease in the population of the regional fluorescent species. The latter point concerning both the increase in the blue-edge region with an accompanying decrease in the red-edge region, tends to indicate the presence of a conformational change arising from the influence of a pH gradient across the membrane. The relationship between protonmotive force and conformational changes shall be discussed.

4.2 FLUORESCENCE OF CYTOCHROME c PEROXIDASE

4.2.1 GENERAL CHARACTERISTICS

The fluorescence spectrum of native CcP has an emission maximum at 326 nm upon excitation at 280 nm and at 330 nm using 295 nm excitation (Fig.4.26). The bandwidths are 60.8 nm and 62.4 nm, respectively. Excitation of the ruthenated derivative at 280 nm results in an emission maximum at 323 nm, whereas emission is at 330 nm when excitation is at 295 nm (Fig.4.27). The bandwidths of each respective emission spectrum are 53.82 nm and 57.15 nm. A mixture of CcP and pentaammninehistidineruthenium(III) trichloride in equimolar quantities, displays similar fluorescence characteristics as those seen for the native protein alone, indicating that the presence of the ruthenium compound does not contribute to the fluorescence spectrum. Fluorescence emission spectra for this sample are shown in Fig.4.28.

The fluorescence emission spectrum of CcP is dependent

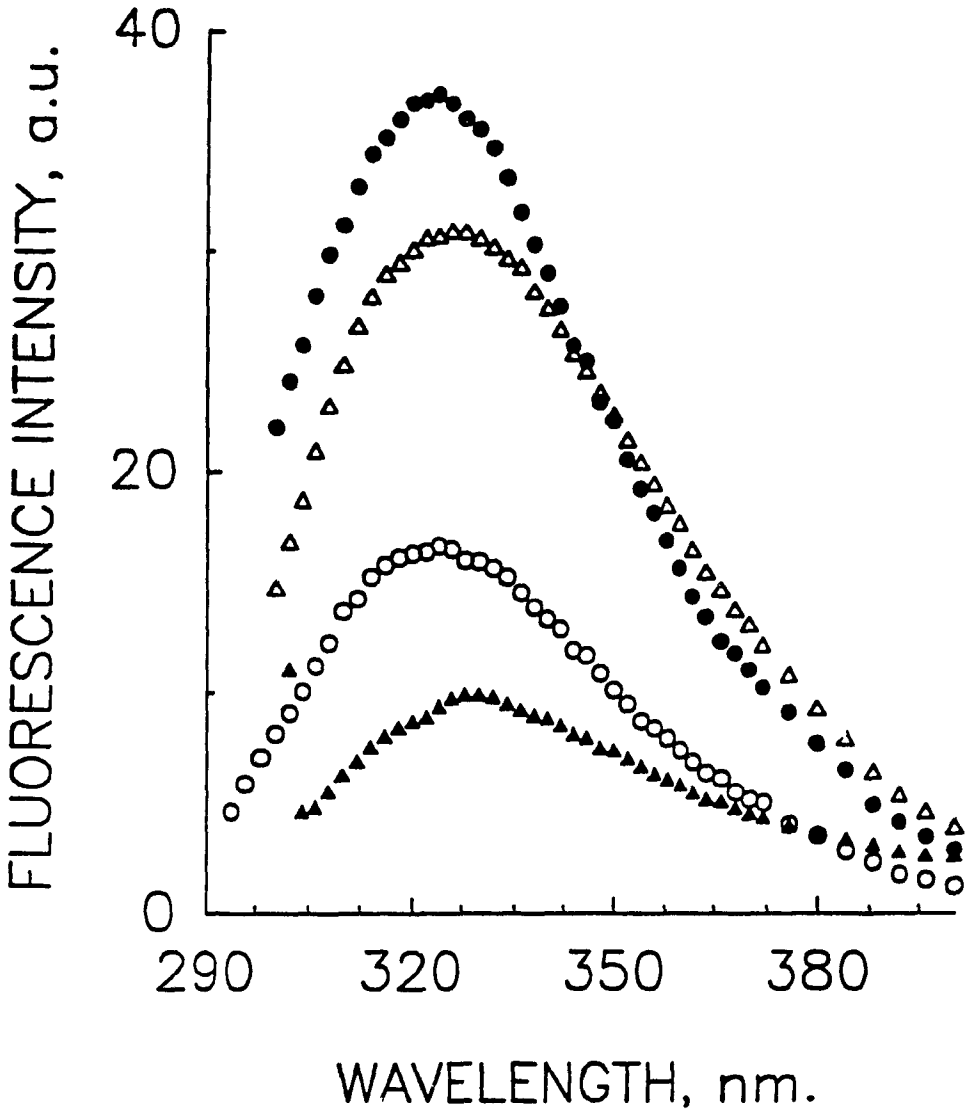

Fig.4.26: FLUORESCENCE EMISSION SPECTRA OF CcP - corrected for inner filter effects. Excitation wavelengths were 260 nm (open circles), 275 nm (closed circles), 280 nm (open triangles) and 295 nm (closed triangles). Emission and excitation slits were set at 5 nm each. Enzyme concentration was 1 μM in 0.1 M NaPi, pH7, T=19°C.

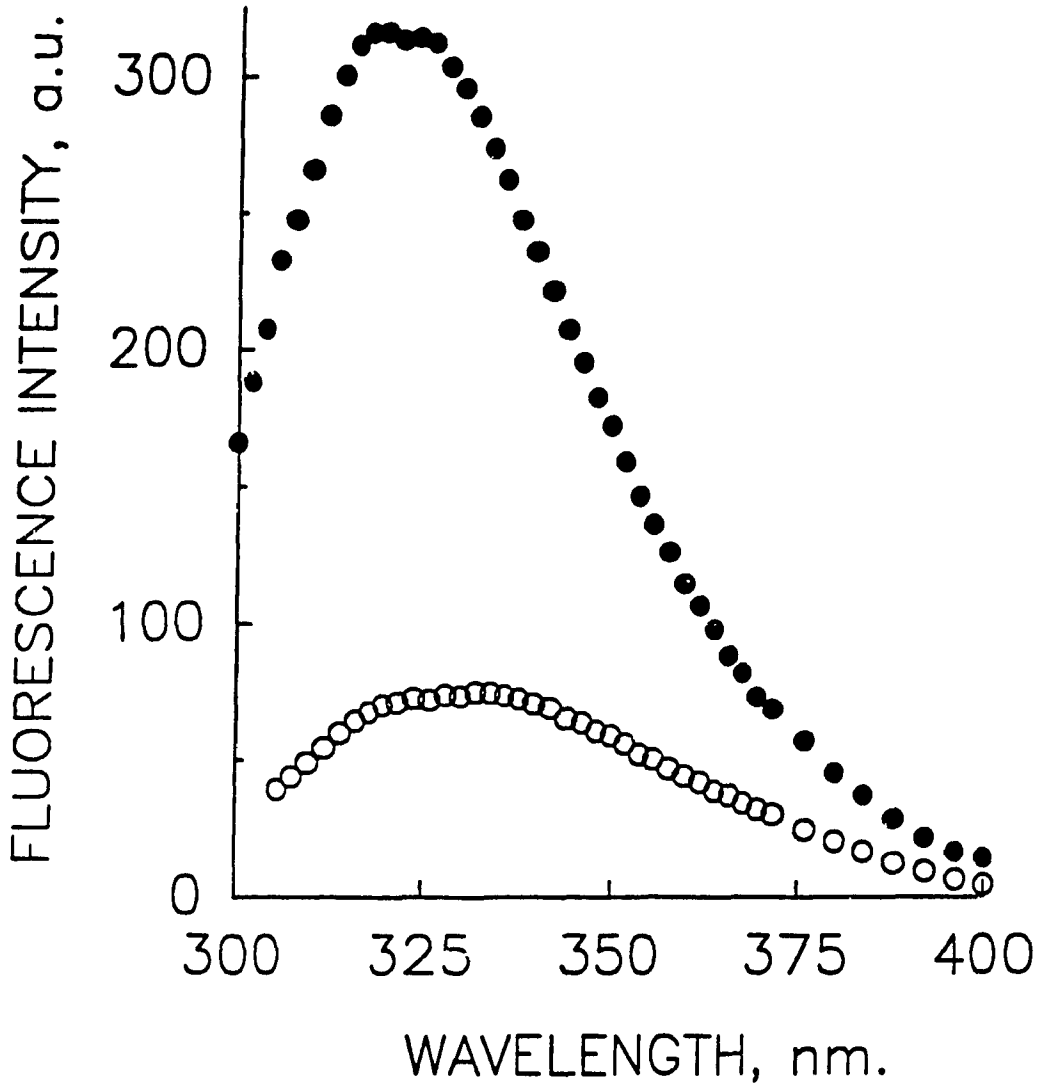

Fig.4.27: FLUORESCENCE EMISSION SPECTRA OF Ru-CcP - corrected . Excitation at 280 nm (closed circles) and 295 nm (open circles). Emission and excitation slits set at 5 nm each. Enzyme concentration was 1 μM in 0.1 M NaPi, pH7, T=19°C.

on the excitation wavelength (figures 4.26 and 4.29). Excitation of CcP at 260 nm, 275 nm, 280 nm and 295 nm give rise to fluorescence emission spectra with maxima at 323 nm, 324 nm, 326 nm and 330 nm, respectively. The gradual red-shift of the emission spectra due to excitation at longer wavelengths are more pronounced for CcP in 0.1 M MOPS buffer, pH=7 (Fig.4.29) than in 0.1 M phosphate. The emission maximum of CcP in MOPS is red-shifted from 326 nm, with 260 nm excitation, to 340 nm with 295 nm excitation. Table 4.1 lists the emission wavelength and bandwidth dependence of CcP, in Pi and MOPS buffers, as a function of excitation wavelength. The red-shift observed between excitation at 260 nm and 295 nm is 7 nm in Pi buffer and 14 nm in MOPS buffer. Likewise, the increase in bandwidth between the two extremeties in excitation wavelength is 6.4 nm in Pi and 17.6 nm in MOPS .

The excitation spectra of Ru-CcP and CcP is shown in figure 4.30. An excitation maximum at 276 nm was observed regardless of the emission wavelength monitored. The emission wavelengths monitored were 320 nm, 330 nm and 340 nm.

The quantum yields of the native protein , the ruthenated derivative and the RuHis/CcP mixture are determined against the tryptophan standard N-acetyltryptophanamide. Both the native enzyme and the Ru/His enzyme mixture had quantum yield values of ca. 5%, while the ruthenated species was 4.2%. Thus, in comparison to native CcP, the ruthenated derivative was further quenched by approximately 14%. A compilation of the general characteristics of CcP fluorescence, derivative and mixture

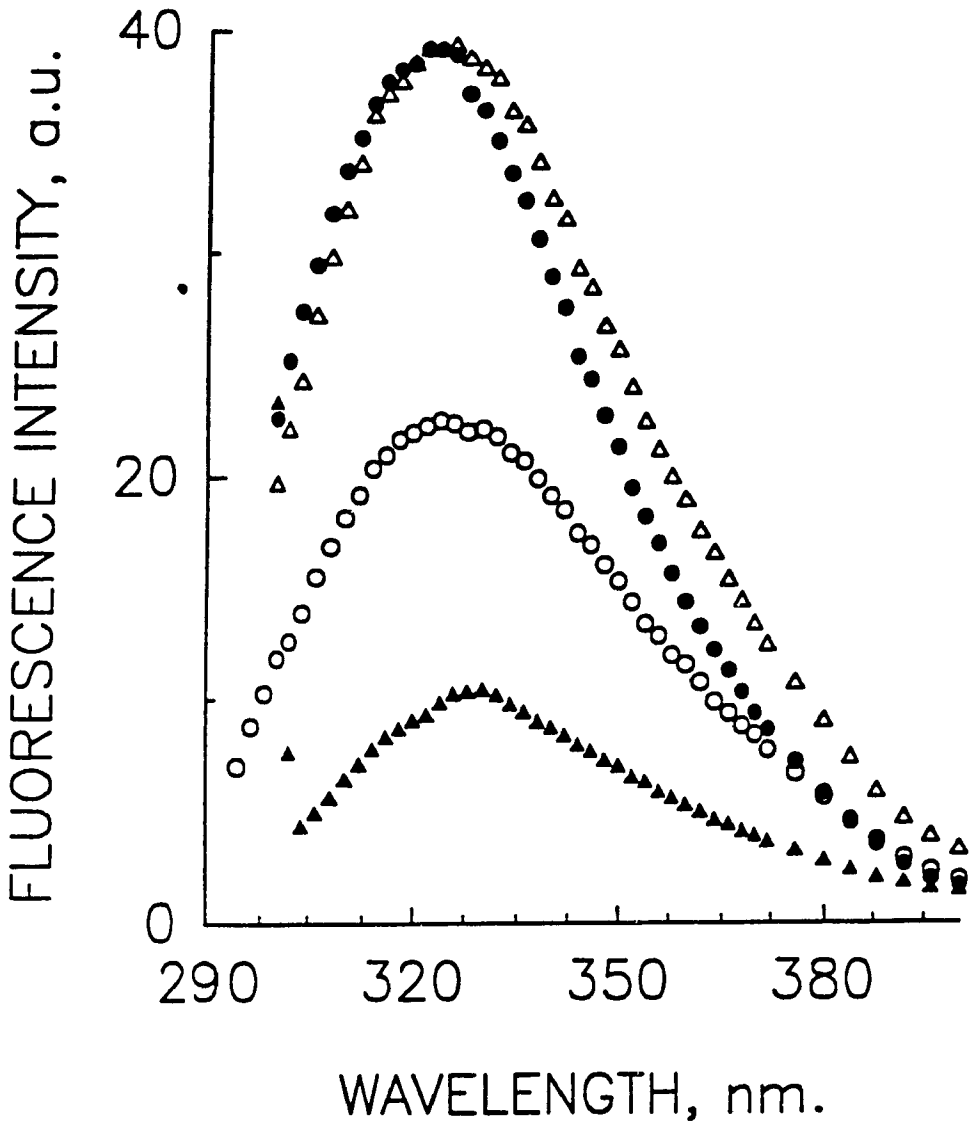

Fig.4.28: FLUORESCENCE EMISSION SPECTRA OF CcP/RuHis - corrected. Excitation wavelengths were 260 nm (open circles), 275 nm (closed circles), 280 nm (open triangles) and 295 nm (closed triangles). Emission and excitation slits were 5 nm. Enzyme concentrations were 1 μM in 0.1 M NaPi, pH7, T=19°C.

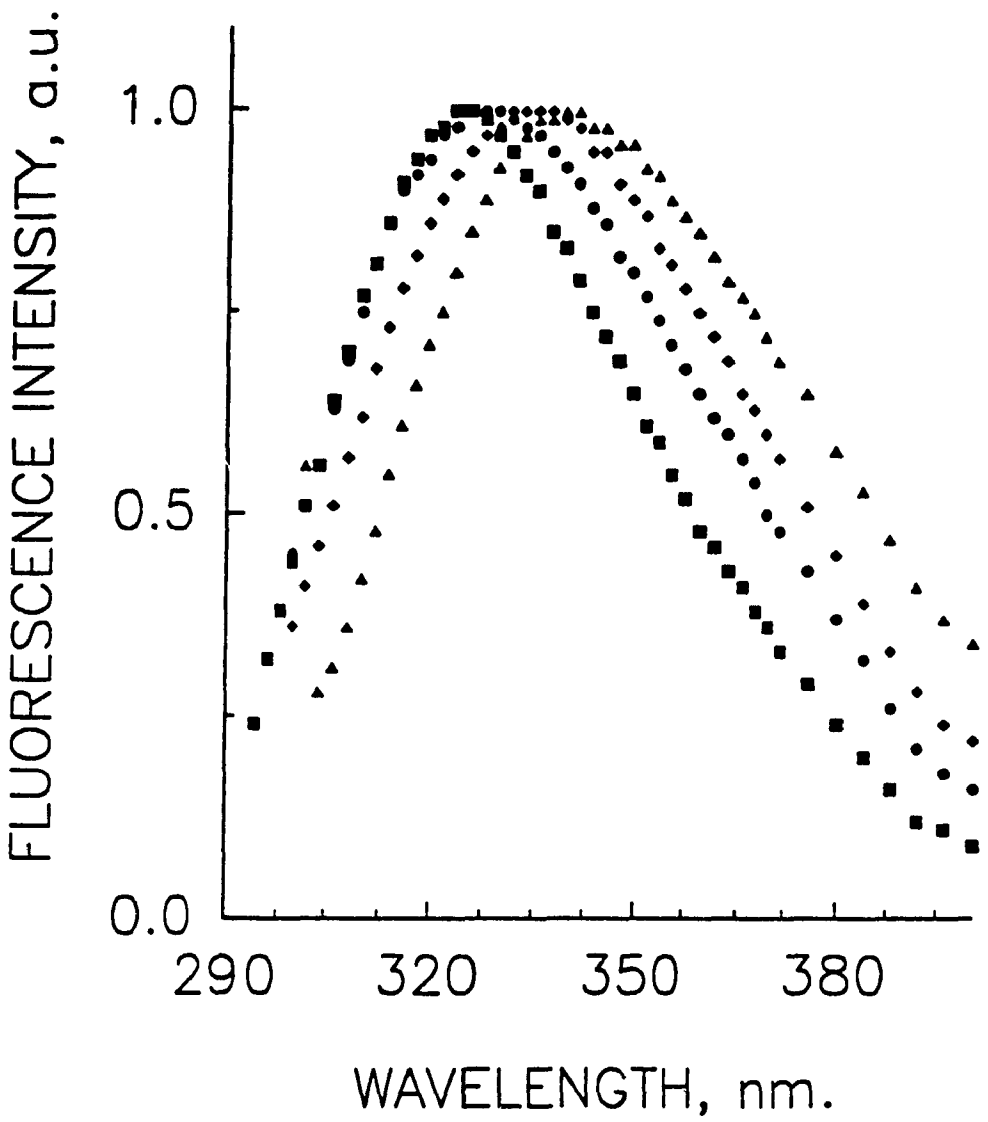

Fig.4.29: FLUORESCENCE EMISSION SPECTRA OF CcP IN MOPS BUFFER - corrected. Excitation wavelengths were 260 nm (squares), 275 nm (circles), 280 nm (diamonds) and 295 nm (triangles). Emission and excitation slits were 5 nm. Enzyme concentration was 1 μM in 0.1 M MOPS, pH7, T=19°C.

Table 4.1: Dependence of the fluorescence emission spectra of CcP on excitation wavelength and buffer .

	CcP in Pi		CcP in MOPS	
λ_{Ex} nm	λ_{Em} nm	Bw nm	λ_{Em} nm	Bw nm
260	323	56	326	57.6
275	324	60	328	68
280	326	60.8	335	70.4
295	330	62.4	340	75.2

λ_{Ex} = excitation wavelength used

λ_{Em} = emission wavelength maximum

Bw = bandwidth of emission spectrum at half height

Note: Measurements are from the spectra shown in figures 4.28 and 4.29.

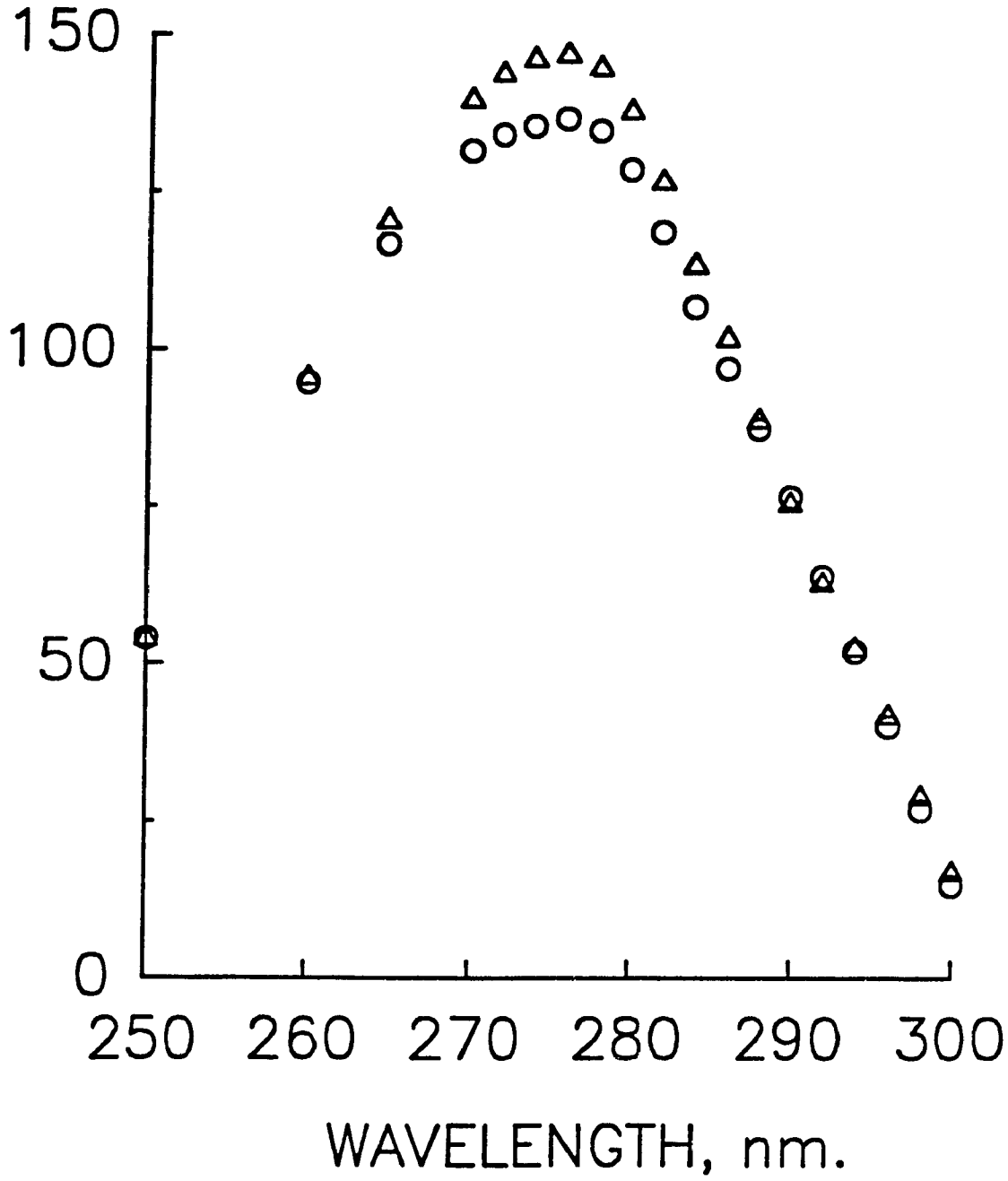

Fig.4.30: EXCITATION SPECTRA OF CcP AND Ru-CcP. The emission wavelength monitored was 330 nm for both CcP (circles) and Ru-CcP (triangles). Emission and excitation slits were 5 nm. Enzyme concentration was 1μM in 0.1 M NaPi, pH7, T=19°C.

Table 4.2: Fluorescence data for CcP, Ru-CcP and RuHis + CcP in phosphate buffer.

Protein	CcP	Ru-CcP	RuHis + CcP
Φ, % (N-ATA)[1]	4.92 ± 0.20 (10)[3]	4.24 ± 0.29 (8)[3]	5.02 ± 0.22 (4)[3]
Φ, % (CcP)[2]	100	86.18	102
$\lambda_{em,250}$, nm	326	323	325
Bw_{250}, nm	60.8	53.82	59.2
$\lambda_{em,295}$, nm	330	330	330
Bw_{295}, nm	62.4	57.45	61.6
$\lambda_{ex\ max}$, nm	276	276	276

1: the quantum yield calculated using Φ=100% for N-ATA fluorescence

2: the quantum yield calculated assuming Φ=100% for native CcP

3: numbers in bracketts represent the number of observations used to calculate an average Φ for each protein sample.

$\lambda_{em,250}$: emission wavelength maximum upon excitation at 280 nm.

$\lambda_{em,295}$: emission wavelength maximum upon excitation at 295 nm.

Bw_{250}, Bw_{295}: bandwidth observed for emission spectra due to excitation at 280 nm and 295 nm, respectively.

inclusive, is shown in Table 4.2.

4.2.2 ACRYLAMIDE QUENCHING OF CcP FLUORESCENCE

Localization and accessibility of the fluorophore may be estimated by studying the effects of different quenchers with varying chemical natures. Acrylamide and iodide are common favourites due to their quenching efficiencies, as well as their distinct chemical natures. Acrylamide is a bulky but uncharged quencher of tryptophan fluorescence which is capable of penetration into the protein matrix. Acrylamide is therefore often used as a quencher of internal or buried tryptophan residues. Iodide, on the other hand, is a negatively charged ion with a large hydration sphere which for both these reasons is unable to penetrate into the protein matrix. Iodide is a suitable quencher of surface tryptophans. Comparative quenching studies by both these quenchers reveals , firstly, the relative permeability of the protein to the specific quencher and secondly, the localization of tryptophan residues in general, as determined by the relative proportion of these which are accessible to a defined quencher.

Quenching of CcP fluorescence by the non-ionic quencher, acrylamide, is shown in figure 4.31. In the absence of acrylamide the emission maximum for CcP fluorescence is 327 nm. Increasing the concentration of acrylamide causes a gradual blue-shift in the emission maximum. At 0.091 M acrylamide definition of a smaller fluorescence peak, with a maximum at 334 nm, begins. In the presence of 0.732 M acrylamide the CcP fluorescence emission spectrum consists of two peaks, at 314 nm and the 334 nm. The major peak at 314 nm was

Fig.4.31: ACRYLAMIDE QUENCHING OF CcP FLUORESCENCE- Excitation wavelength was 295 nm. Emission and excitation slits were 5 nm. Spectra are staggered for visual purposes. Dashed line denotes the extrapolation of the 314 nm peak at 0.732 M acrylamide. Difference spectrum (original minus extrapolated) is represented by the dotted line. [CcP] was 1 μM, 0.1 M NaPi, pH7, T=19°C.

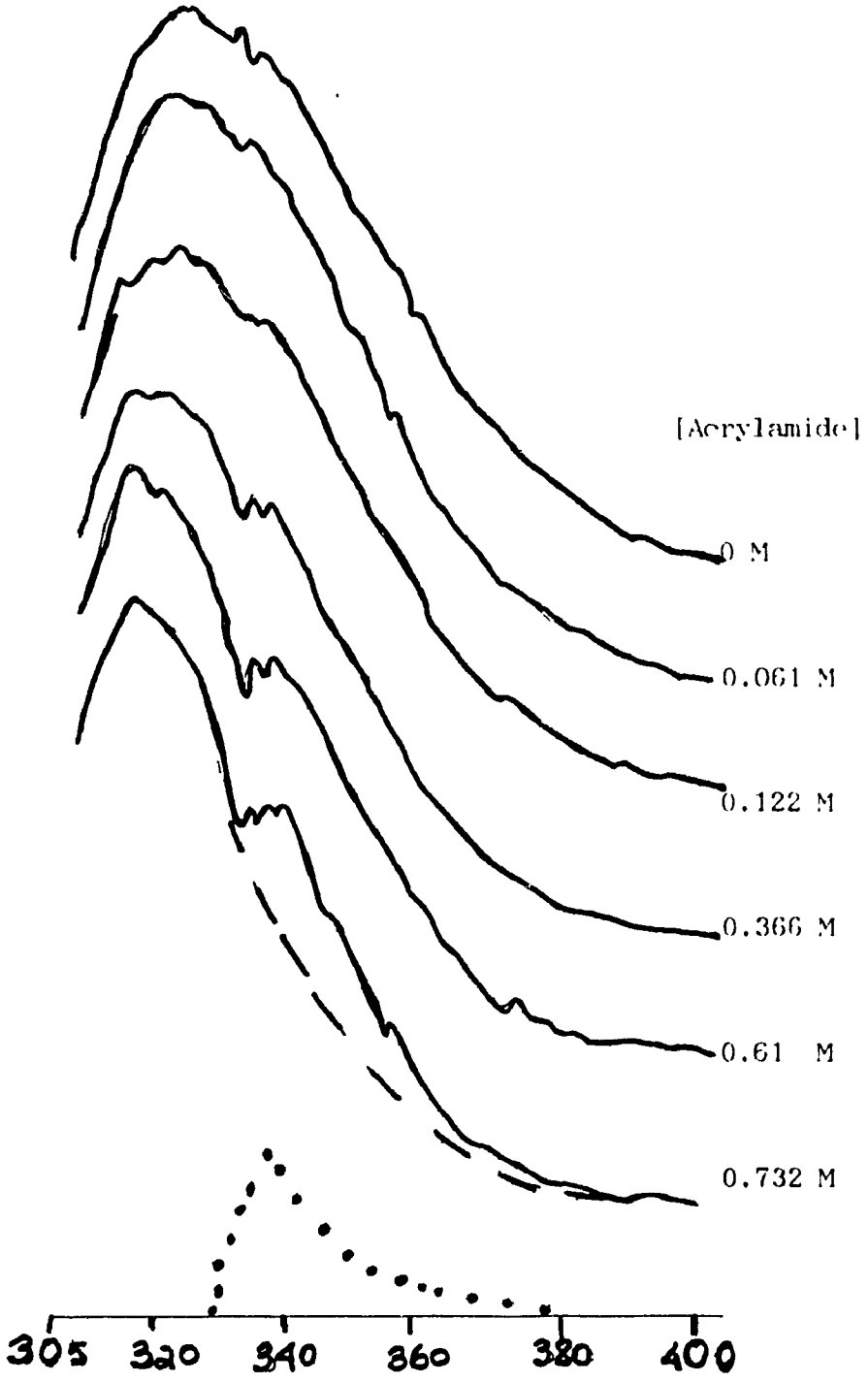
[Acrylamide]
0 M
0.061 M
0.122 M
0.366 M
0.61 M
0.732 M
305
320
340
360
380
400
WAVELENGTH, nm.

extrapolated at its red-edge to 400 nm in order to better resolve the smaller component. The resultant difference spectrum has a maximum at 340 nm.

Figure 4.32 shows the results of acrylamide quenching of Ru-CcP fluorescence. Similarly to CcP, a gradual blue-shift in the fluorescence emission spectra is observed. Resolution of the fluorescence spectrum into two distinct peaks is observed at concentrations of acrylamide greater than 0.091 M. Extrapolation of the major peak at 314 nm for Ru-CcP fluorescence in the presence of 0.732 M acrylamide gave rise to a difference spectrum with a maximum at 340 nm. The control CcP/Ru-His gave results similar to those of the native protein.

A Stern-Volmer plot for acrylamide quenching of CcP fluorescence is shown in figure 4.33. Due to overlap in the experimental points for all CcP samples, the Stern-Volmer constant was taken to be approximately the same for CcP, Ru-CcP and CcP/Ru-His with a value of 3.02 M^{-1}. Acrylamide quenching of N-ATA is observed to be non-linear and deviates towards the y-axis. Extrapolation of the initial portion of the graph gives rise to a K_{SV} value of 15.46 M^{-1} for acrylamide quenching of N-ATA. Deviation towards the y-axis is common for acrylamide quenching of N-ATA fluorescence and does not indicate, in this case, the occurrence of static quenching. This deviation has been ascribed to be due to the continual presence of quencher within the possible quenching sphere of the fluorophore, such that quenching, although dynamic, is not diffusion-controlled (Lakowicz, 1983).

Fig.4.32: ACRYLAMIDE QUENCHING OF Ru-CcP FLUORESCENCE - Spectra have been staggered for visual purposes. The extrapolated spectrum consists only of the 314 nm peak and is denoted by the dashed line. Dotted line represents the difference spectrum (original spectrum minus extrapolated spectrum). The excitation wavelength was 295 nm. Emission and excitation slits were 5 nm. [Ru-CcP] was 1 μM, 0.1 M NaPi, pH7, T=19°C.

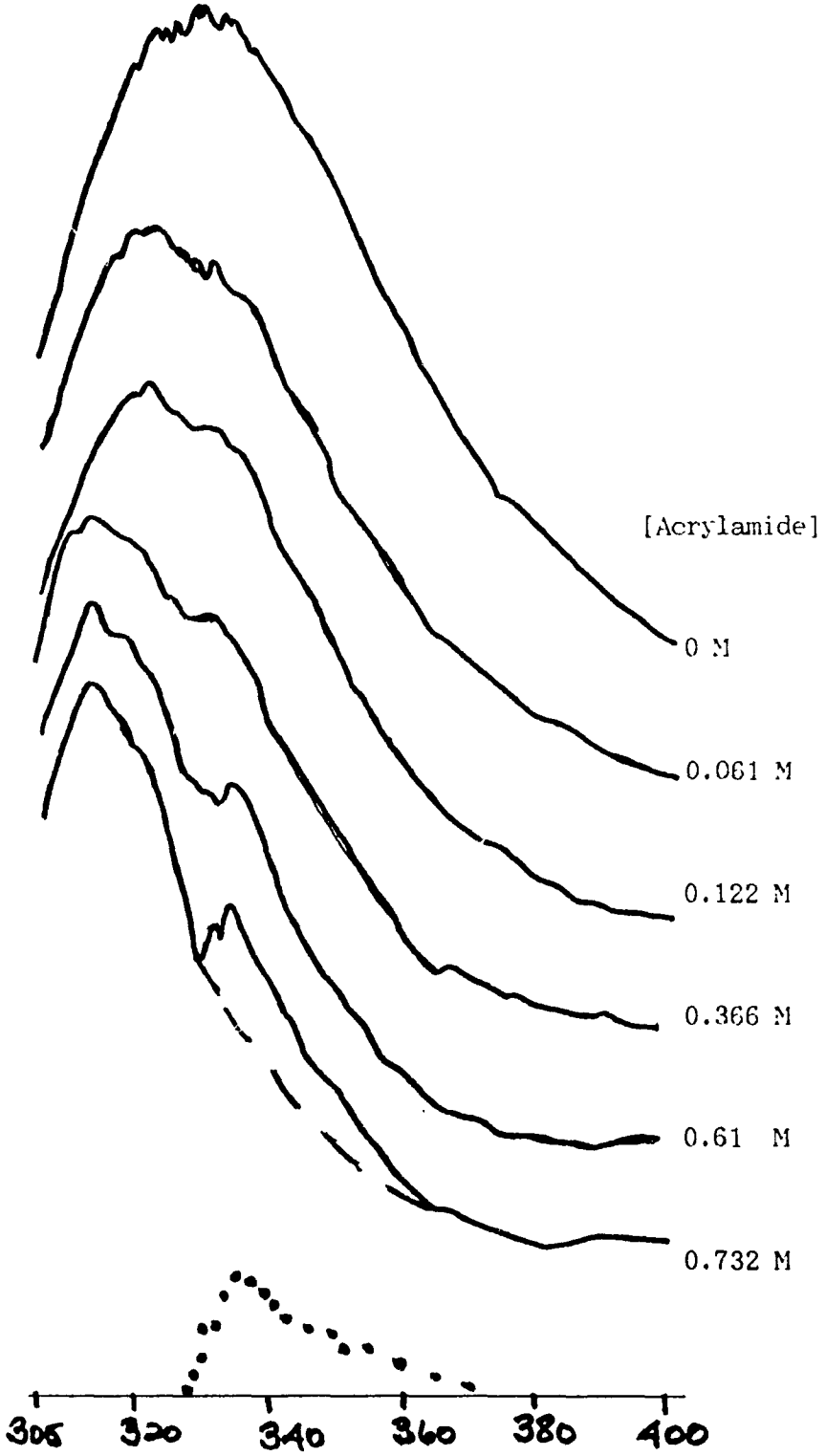
[Acrylamide]
0 M
0.061 M
0.122 M
0.366 M
0.61 M
0.732 M
305
320
340
360
380
400
WAVELENGTH, nm.

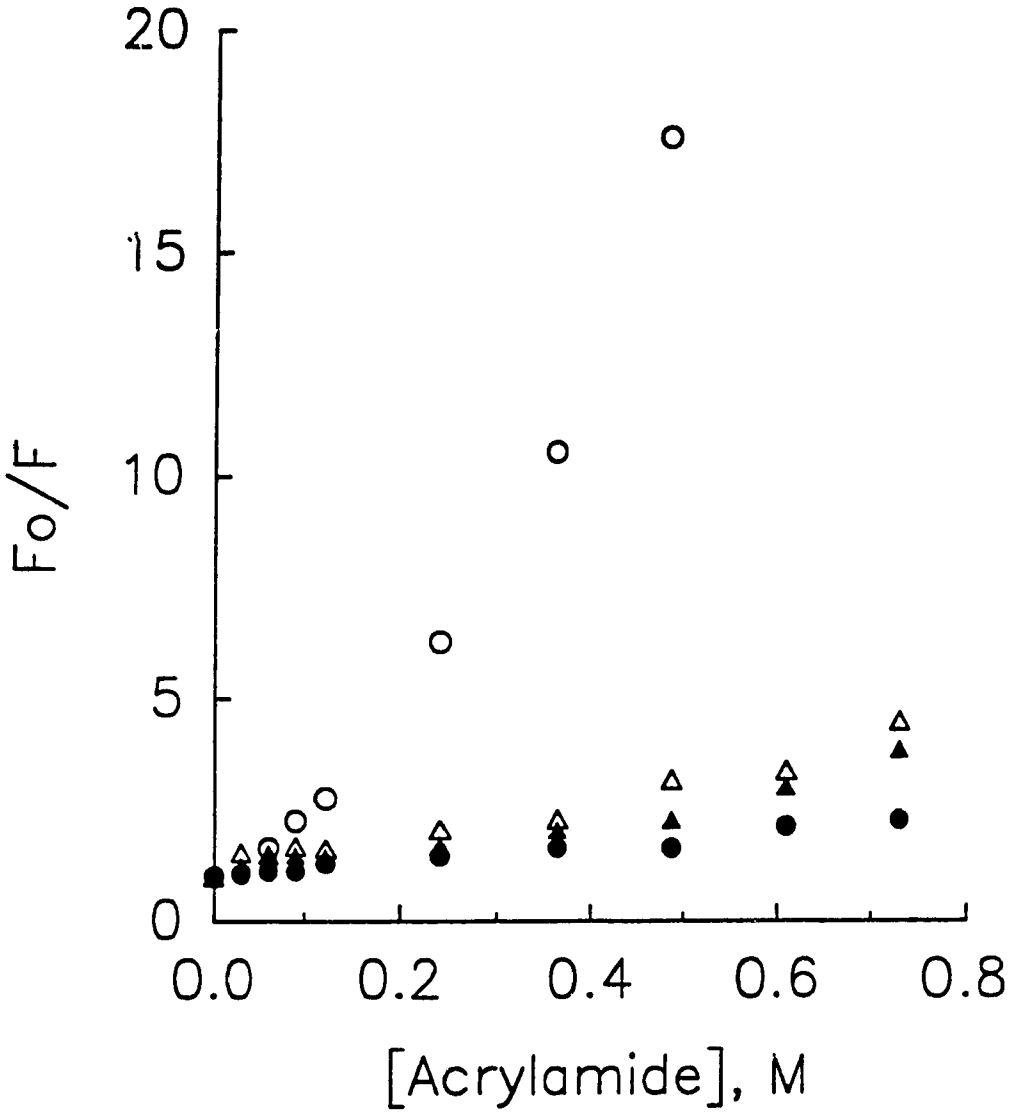

Fig.4.33: STERN-VOLMER PLOT OF ACRYLAMIDE QUENCHING OF CcP FLUORESCENCE :- Samples are N-ATA (open circles), CcP (closed circles), Ru-CcP (open triangles) and Ru-His/CcP (closed triangles). Enzyme concentrations were 1 μM in 0.1 M NaPi, pH7, T=19°C. Excitation was 295 nm. Emission and excitation slit widths were 5 nm.

4.2.3 IODIDE QUENCHING OF CcP FLUORESCENCE

Quenching of cytochrome c peroxidase fluorescence with the anionic quencher iodide is demonstrated as a function of quencher concentration in figure 4.34. At low quencher concentrations (<0.091 M) a decrease in the relative emission at the red-edge of the emission maximum is seen. Increasing quencher concentrations cause a blue-shift of the emission spectra and definition of a fluorescence peak at 332 nm which appears to be unaltered by the presence of quencher. The peak at 332 nm becomes more pronounced as quenching of long wavelength tryptophan emission is increased. The fluorescence emission maximum is blue-shifted from 326 nm to 320 nm as the KI is increased to 0.732 M. At 0.732 M KI the peak at 332 nm is the major emission peak as is shown in the normalized fluorescence emission spectra of CcP (Fig.1.35). The above spectra were obtained at an excitation of 295 nm. Fluorescence emission spectra of CcP in phosphate buffer using an excitation wavelength of 280 nm are shown in Fig.1.36. The second peak at 332 nm, seen with excitation at 295 nm, in the presence of 0.732 M KI is not seen when the excitation wavelength is 280 nm. Figure 1.36 illustrates that in the presence of KI, quenching is observed at the red-edge of the spectrum but the spectral shape remains similar to that observed in the absence of quencher. The emission maximum is only slightly blue-shifted (2-4 nm). Similar results are obtained for CcP in MOPS buffer at an excitation of 280 nm as are shown in figure 4.37. Figure 4.38 demonstrates the fluorescence emission spectra of CcP in MOPS buffer in the presence and absence of KI using an excitation of 295 nm. From the normalized

Fig.4.34: IODIDE QUENCHING OF CcP FLUORESCENCE - The excitation wavelength was 295 nm. Emission and excitation slits were 5 nm. Spectra were staggered for visual purposes. The dashed line represents the extrapolated spectrum. The dotted line represents the difference spectrum. [CcP] was 1 μM, 0.1 M NaPi, 1 mM Na-thiosulphate pH7, T=19°C. Ionic strength constant at 0.732 M.

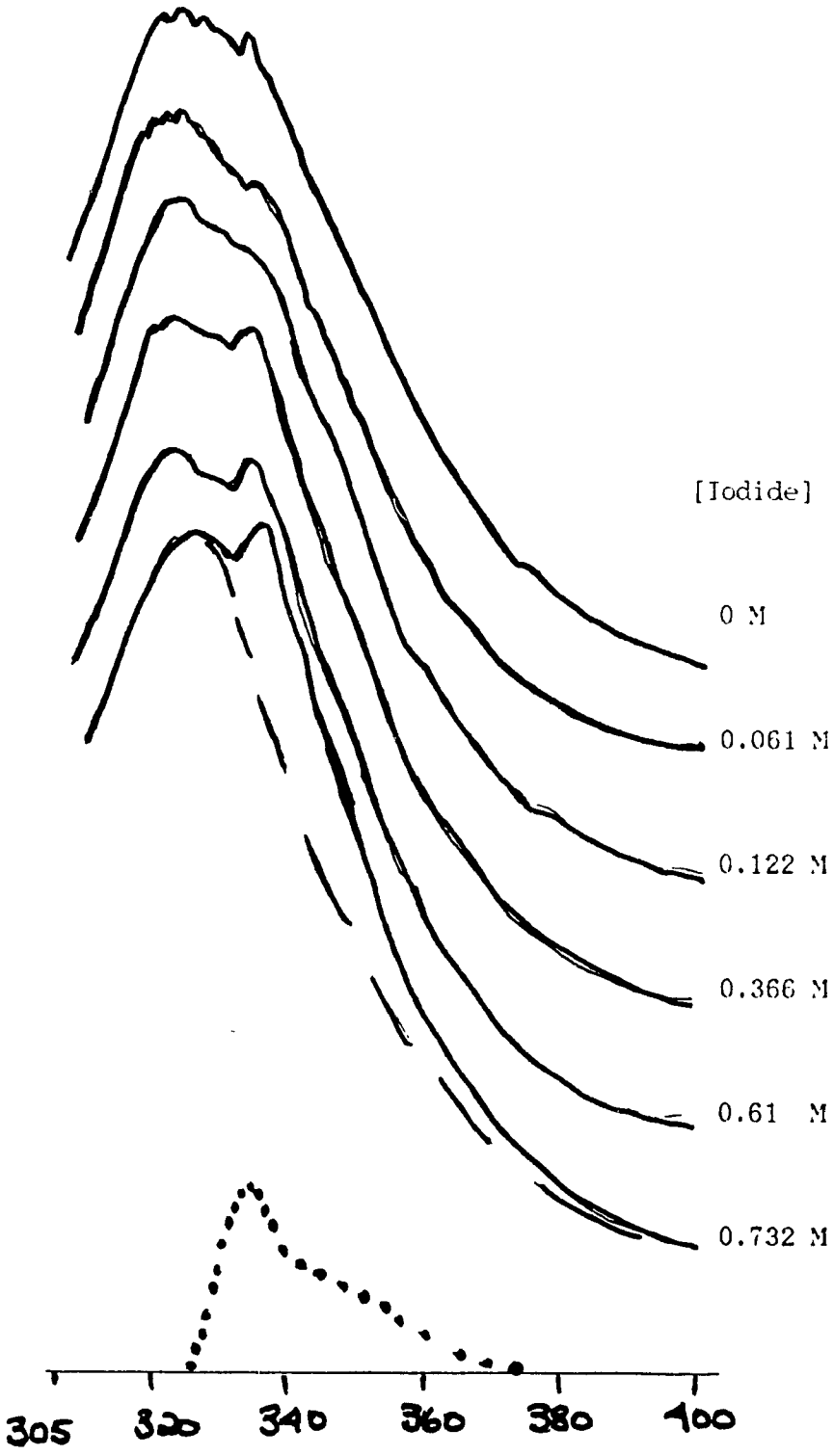
[Iodide]
0 M
0.061 M
0.122 M
0.366 M
0.61 M
0.732 M
305
320
340
360
380
400
WAVELENGTH, nm.

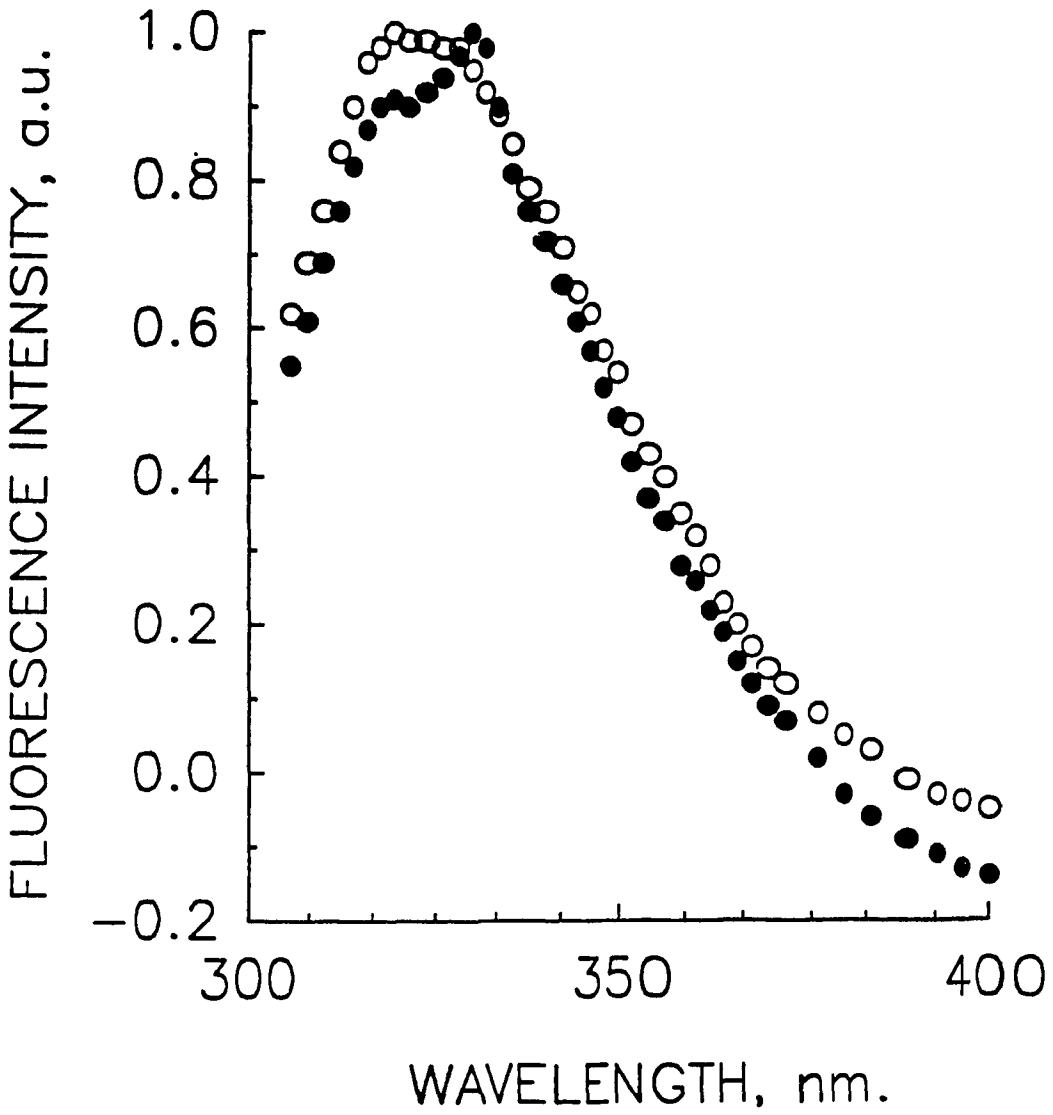

Fig.4.35: NORMALIZED FLUORESCENCE EMISSION SPECTRA OF CoP IN 100 mM Pi pH7, λ_{ex}=295 NM - Spectra were obtained in the presence (closed circles) and absence (open circles) of 0.732 M KI. [CoP] was 1 μM, 1 mM Na-thiosulfate, T=19°C. Emission and excitation slits were 5 nm. Ionic strength constant at 0.732 M.

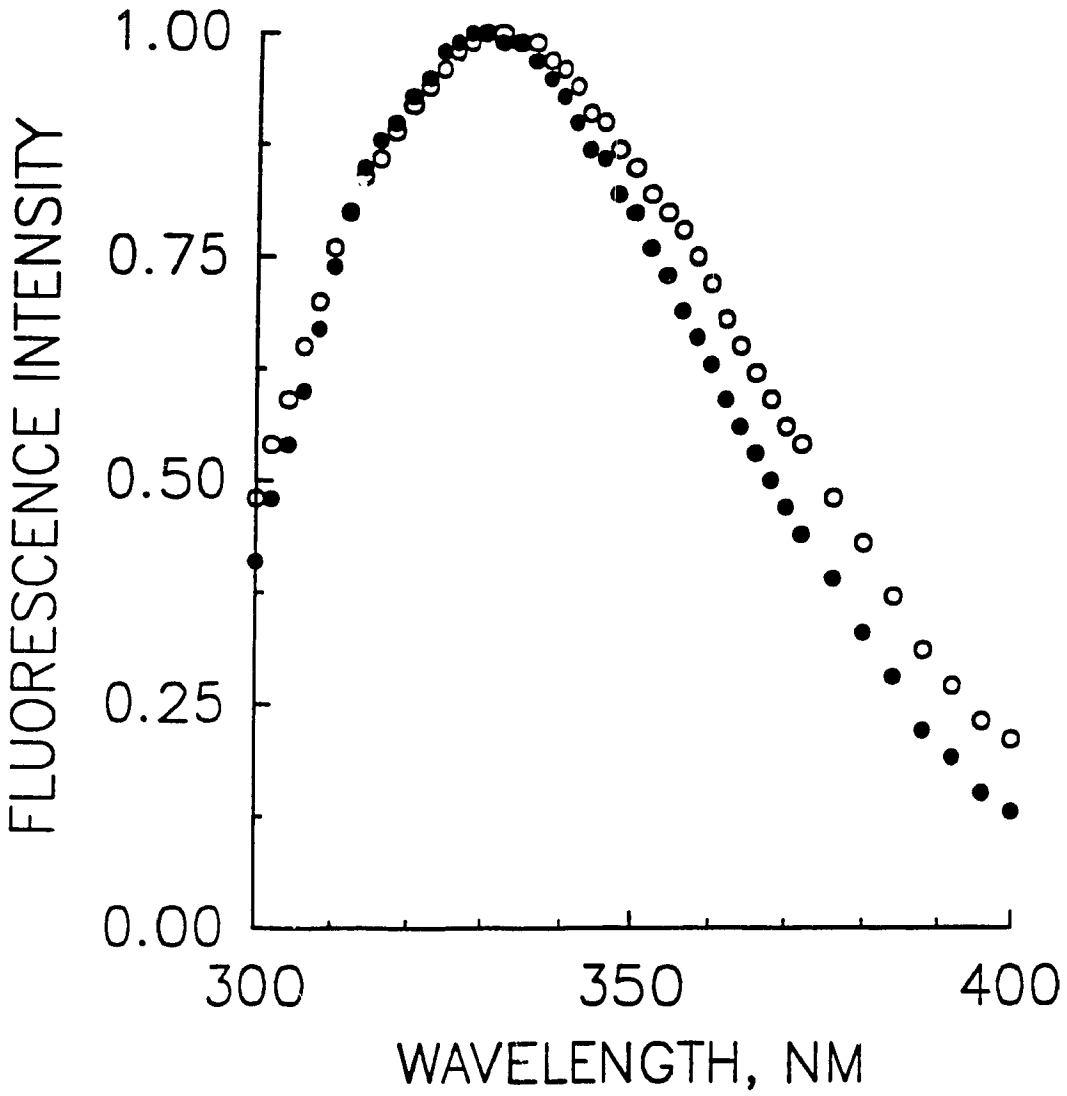

Fig.4.36: NORMALIZED FLUORESCENCE EMISSION SPECTRA OF CcP IN 100 mM Pi pH7, λ_{ex}=280 NM - Spectra were obtained in the presence (closed circles)and absence (open circles) of 0.732 M KI. [CcP] was 1 µM, 1 mM Na- thiosulfate, T=19°C. Emission and excitation slits were 5 nm. Ionic strength constant at 0.732 M.

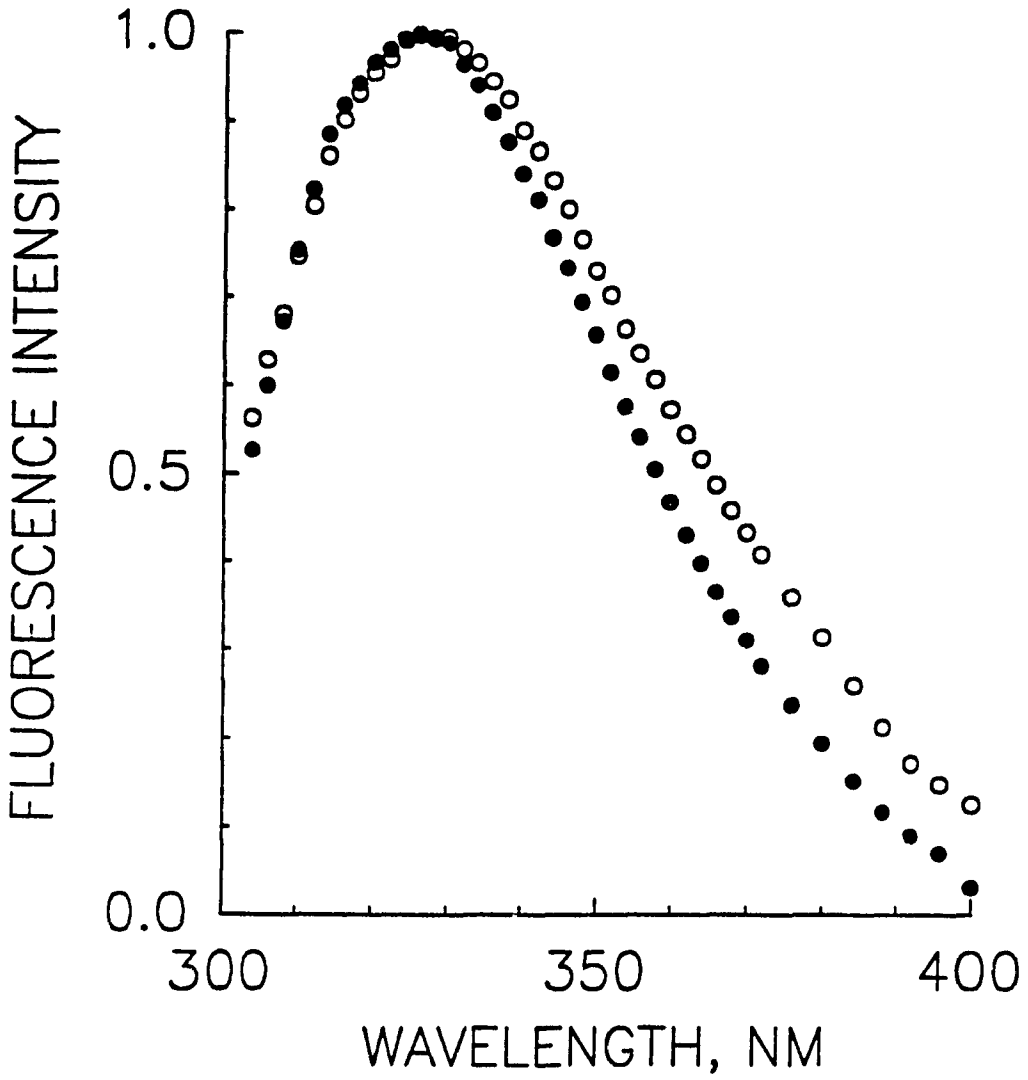

Fig.4.37: NORMALIZED FLUORESCENCE SPECTRA OF CcP IN 100 mM MOPS BUFFER pH7, λ_{ex}=280 NM - Spectra are in the presence (closed circles) and absence (open circles) of 0.732 M KI. [CcP] was 1 μM, 1 mM Na- thiosulfate, T=19°C. Emission and excitation slits were 5 nm. Ionic strength constant at 0.732 M.

(Fig.4.38) it is observed that in the presence of quencher the maximum emission band is centered at ca. 332 nm. The relative decrease in fluorescence is also shown to be towards the blue-edge of the band. Although these results are generally compatible to those observed in phosphate buffer at 295 nm a clear definition of two distinct species with separate emission maxima is not observed.

Similar results are obtained for quenching of the control mixture, CcP/Ru-His, and the ruthenated cytochrome c peroxidase species, Ru-CcP. The results of the latter are shown in figure 4.39. Extrapolation of the lower wavelength peak for both CcP and Ru-CcP fluorescence in the presence of 0.732 M KI resolves the peak at 332 nm. A difference spectrum between the original spectrum and the extrapolated one gives rise to a fluorescence emission band with a maximum at 331 nm. for both CcP and Ru-CcP (dotted line in figures 4.31 and 4.39). These results are comparable to those obtained in the acrylamide quenching experiments. Although the 331 nm band appears to "grow" with increasing quencher concentrations it is most probably a constant contributing factor to the overall fluorescence but as quenching of tryptophans which emit in its spectral region increases, this peak is unmasked and becomes more pronounced relative to the total fluorescence observed.

Iodide quenching of the tryptophan standard, N-ATA, is shown in figure 4.40. The emission maxima of the resultant spectra remains constant at 354 nm. No shifts in the emission spectra or definition of different emitting species is observed. This simple response to iodide quenching is attributable to the existence of a

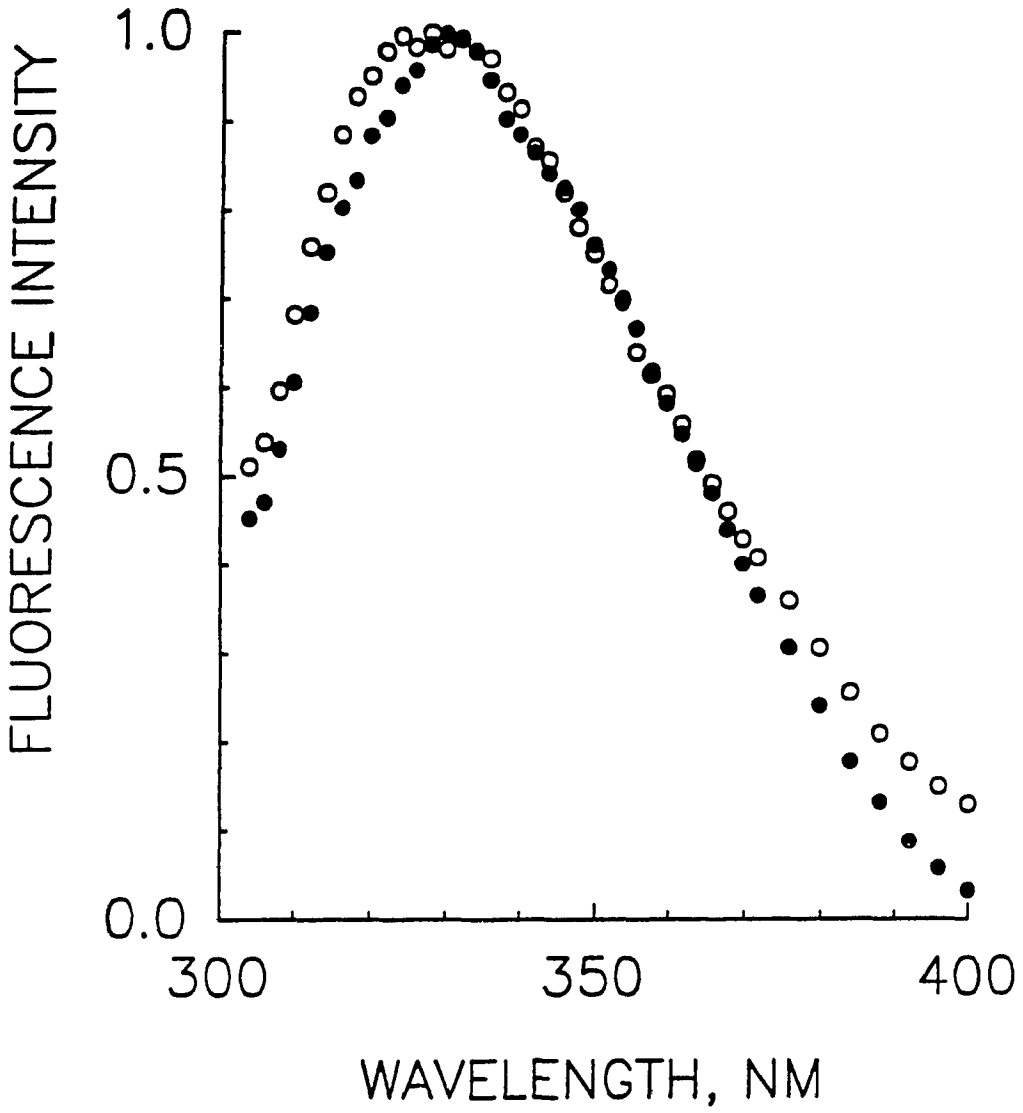

Fig.4.38: NORMALIZED FLUORESCENCE SPECTRA OF CcP IN 100 mM MOPS BUFFER pH7, λ_{ex}=295 NM - Spectra are in the presence (closed circles) and absence (open circles) of 0.732 M KI. [CcP] was 1 µM, 1 mM Na- thiosulfate, T=19°C. Emission and excitation slits were 5 nm. Ionic strength constant at 0.732 M.

Fig.1.39: IODIDE QUENCHING OF Ru-CcP FLUORESCENCE :- Spectra were staggered for visual purposes. The excitation wavelength was 295 nm. Emission and excitation slits were 5 nm. The buffer system was 0.1 M phosphate, 1 mM Na-thiosulfate, pH7. [Ru-CcP] =1 μM. Ionic strength constant at 0.732 M. T=19°C.

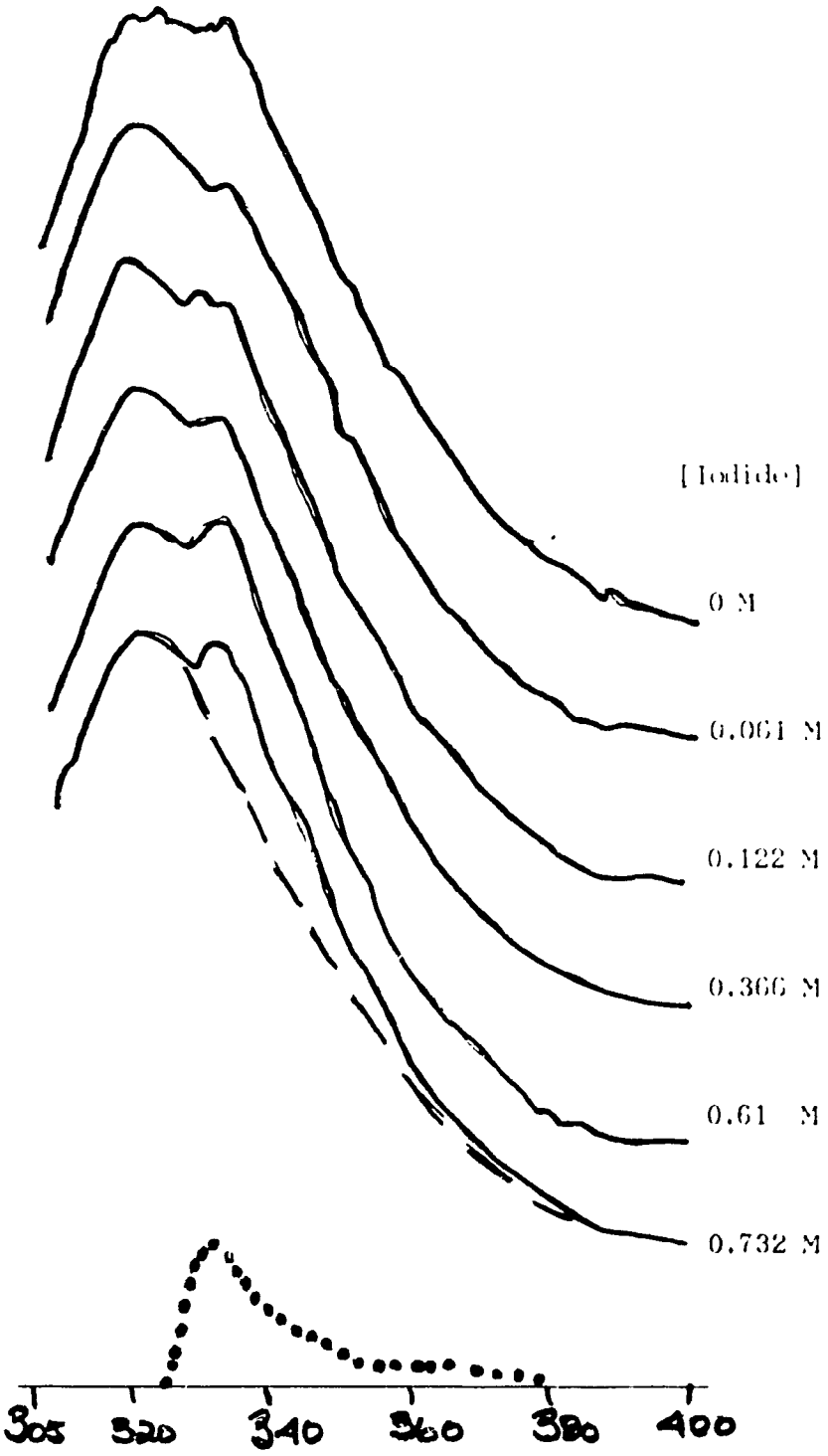
[Iodide]
0 M
0.061 M
0.122 M
0.366 M
0.61 M
0.732 M
305
320
340
360
380
400
WAVELENGTH, nm.

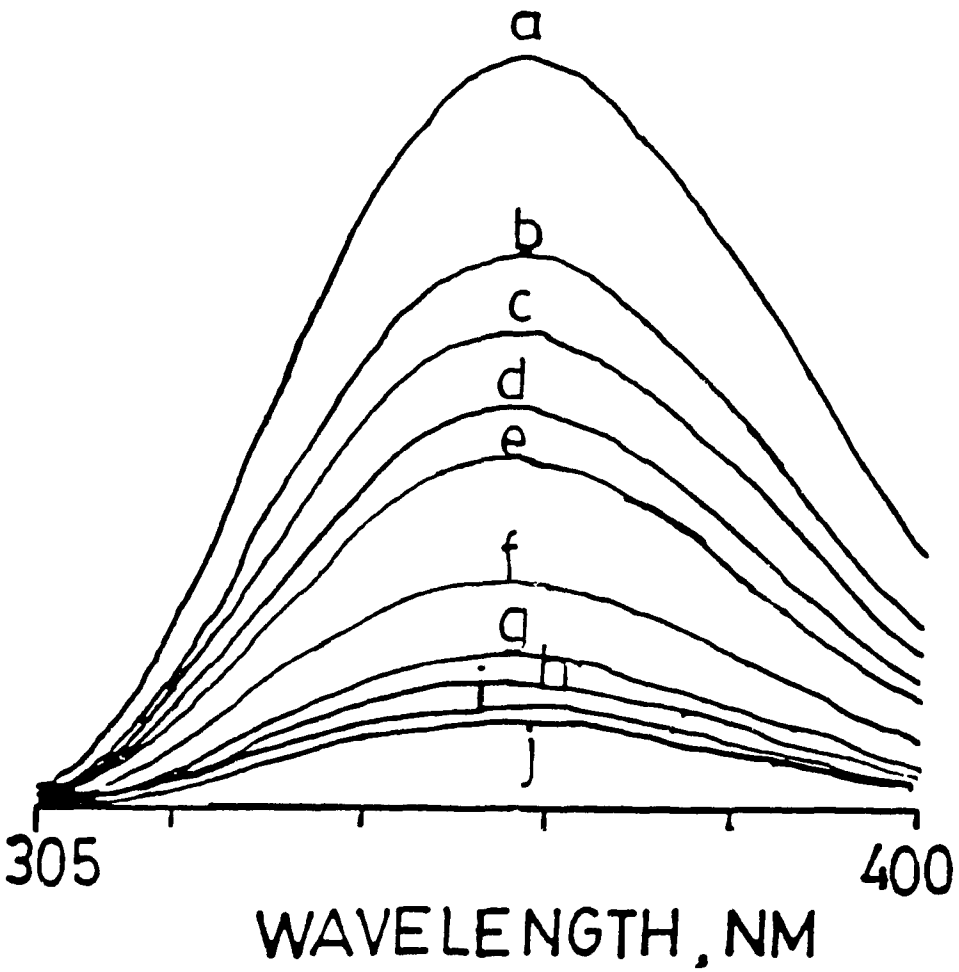

Fig.4.40: IODIDE QUENCHING OF N-ATA FLUORESCENCE :- Spectra are non-staggered. The excitation wavelength was 295 nm. Emission and excitation slits were 5 nm. The buffer system was 0.1 M phosphate, 1 mM Na-thiosulfate, pH7. Ionic strength constant at 0.732 M. T=19°C. The iodide concentrations were (a) 0 M, (b) 0.03 M, (c) 0.061 M, (d) 0.091 M, (e) 0.12 M, (f) 0.24 M, (g) 0.36 M, (h) 0.48 M, (i) 0.61 M and (j) 0.732 M.

single population of emitting species. By contrast the complexity observed in the fluorescence emission spectra of CcP tends to indicate the existence of separate species with distinct fluorescence emission properties.

A Stern-Volmer plot of iodide quenching of CcP fluorescence is depicted in figure 4.41. The quenching of CcP, Ru-CcP and CcP/Ru-His is essentially the same and the Stern-Volmer quenching constant, K_{SV}, is 1.5 M^{-1} as determined from the initial portion of the graph. In contrast, the Stern-Volmer constant for N-ATA quenching is 11.38 M^{-1}. These data suggest the presence of two populations of fluorescent species, as seen in the inset of figure 4.11 which presents the Stern-Volmer plot for CcP and KI on an expanded scale. The initial portion of the plot at low KI concentrations defines a population of quencher-accessible fluorophores, whereas at higher concentrations there appears a second less sensitive population of fluororphores.

4.2.4 CESIUM CHLORIDE QUENCHING OF CcP FLUORESCENCE

Acrylamide and iodide are often the preferred quenchers of tryptophan fluorescence due to their quenching efficiencies. The quenching efficiency of both iodide and acrylamide is unity (Lakowicz, 1983). An alternive ionic quencher of tryptophan fluorescence to iodide is cesium. The negative nature of the iodide ion lends itself to be associated primarily with a positive surface environment on the protein. In contrast, the cesium ion, being positive, prefers a surface of negative charge. For this reason cesium quenching of fluorescence is often used in conjunction with iodide quenching

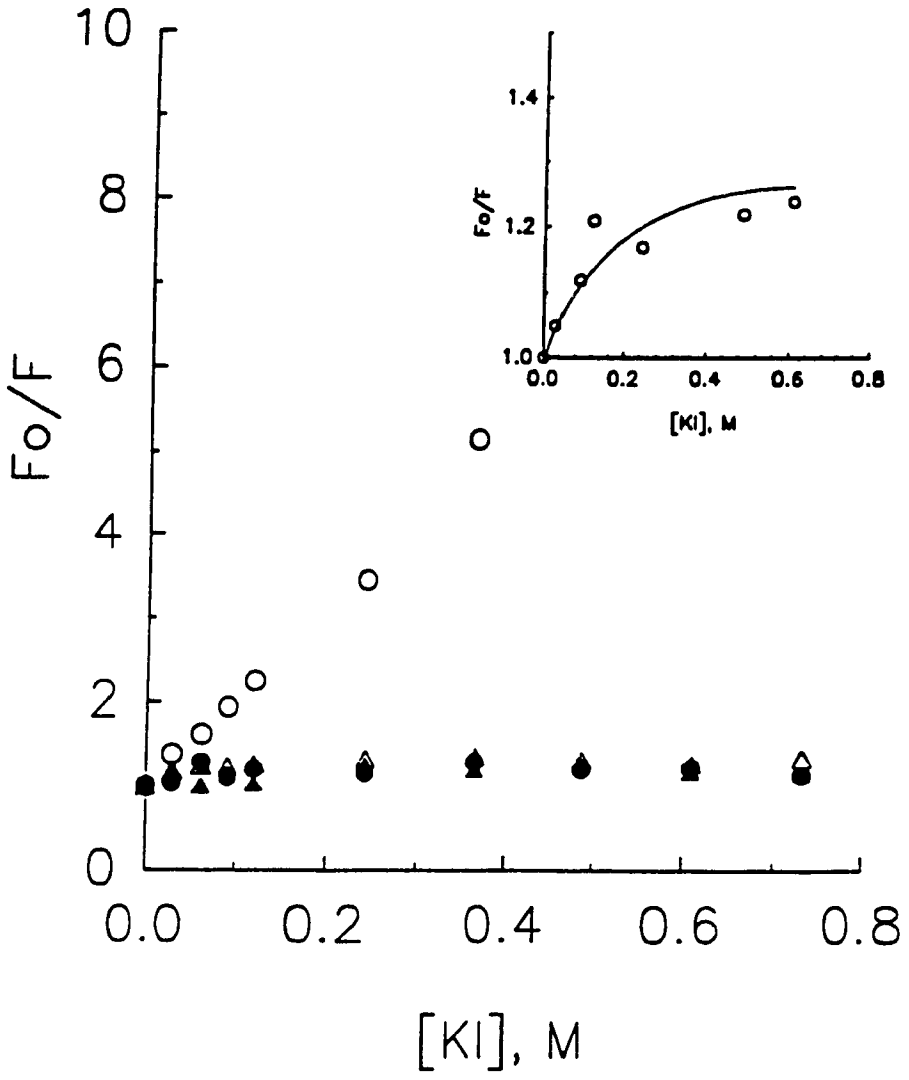

Fig.4.41: STERN-VOLMER PLOT OF IODIDE QUENCHING OF CcP FLUORESCENCE :- The excitation wavelength was 295 nm. 5 nm emission and excitation slits. Samples are N-ATA (open circles), CcP (closed circle), Ru-CcP (open triangle) and Ru-His/CcP (closed triangle). Inset plot is an expanded view of the Stern-Volmer plot for fluoresence quenching by iodide of native CcP. Enzyme concentrations were 1 μM. All samples were in 100 mM NaPi, 1 mM Na-thiosulfate, pH7, T=19°C. Ionic strength constant at 0.732 M.

experiments in order to provide a more complete picture of fluorescence due to surface tryptophans. Although cesium is a capable quencher of tryptophan fluorescence it has a lower quenching ability than iodide.

Figure 4.42 demonstrates the fluorescence emission spectrum of native CcP, upon excitation at 280 nm, in the presence and absence of 0.732 M cesium chloride. In the presence of cesium chloride a sharpening of the spectral band is observed with a marked decrease in fluorescence intensity at longer wavelengths. By contrast, the fluorescence emission spectrum of Ru-CcP in the presence and absence of cesium chloride (Fig.4.43) does not display a significant decrease of fluorescence at longer wavelengths. A decrease of ca. 22% in the fluorescence intensity at 350 nm is observed for CcP, whereas only a 5% decrease in seen in the ruthenated species.

Progressive quenching of tryptophan fluorescence in CcP and Ru-CcP with increasing cesium chloride concentrations is shown in figures 4.44 and 4.45, respectively. Spectral band shapes are not altered except for some sharpening of the band in the red-edge. The emission maximum is slightly blue-shifted upon quenching of native CcP. Emission maxima of 326 nm and 321 nm were observed for native CcP in the absence and presence of cesium, respectively. Emission maxima of ca. 323 nm were observed for Ru-CcP in both instances. The fluorescence emission spectrum of CcP in the presence of 0.732 M CsCl is resolved into two peaks when excitation is at 295 nm (Fig.4.46). These two peaks appear at 322 nm and 331 nm. One peak

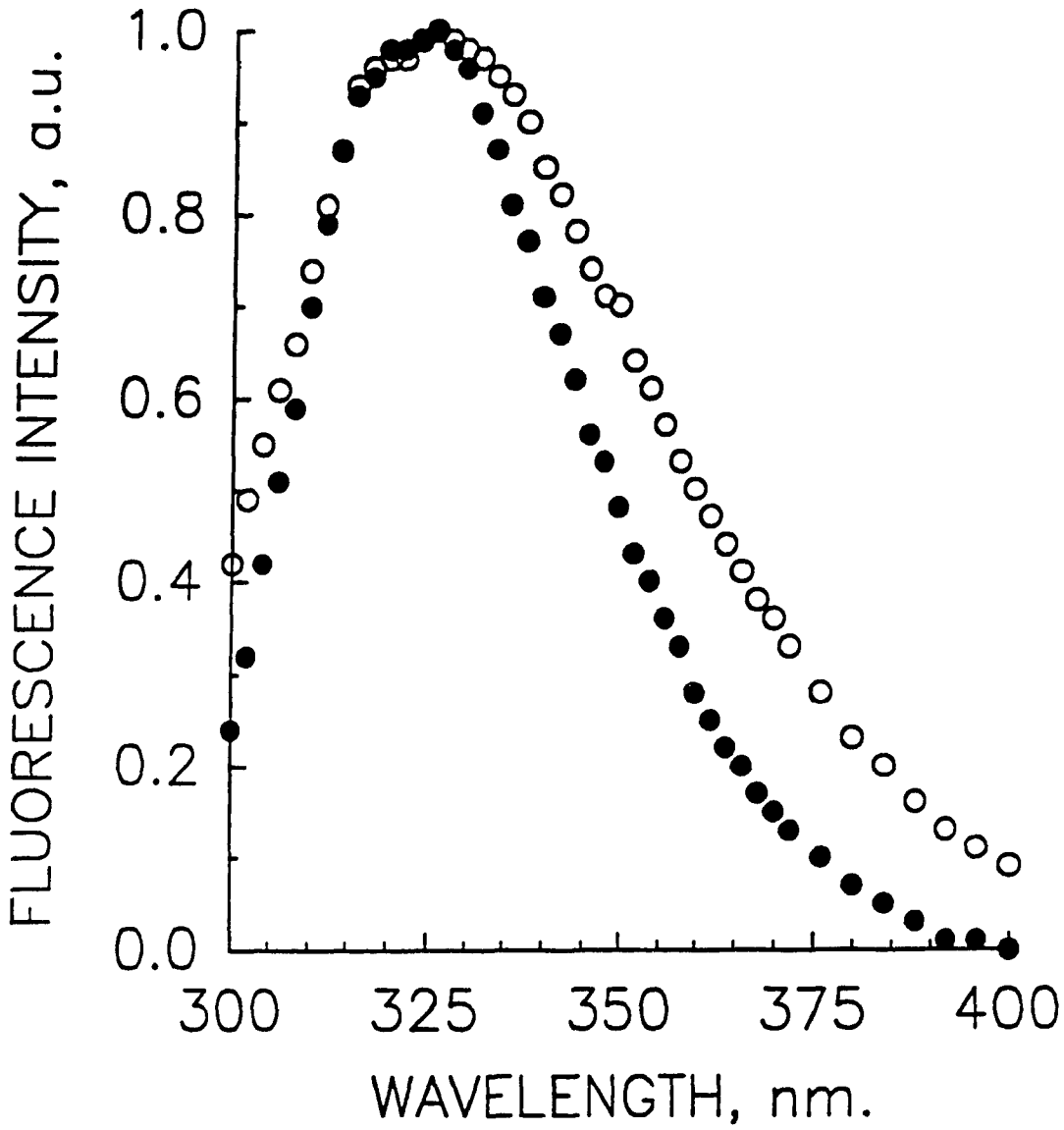

Fig.4.42: FLUORESCENCE EMISSION SPECTRA OF CcP IN THE ABSENCE AND PRESENCE OF 0.732 M CsCl- The excitation wavelength was 280 nm. Emission and excitation slits were 5 nm. 0 M CsCl (open circle), 0.732 M CsCl (closed circle). [CcP] was 1 μM, 0.1 M NaPi, pH7, T=19°C. Ionic strength constant at 0.732 M.

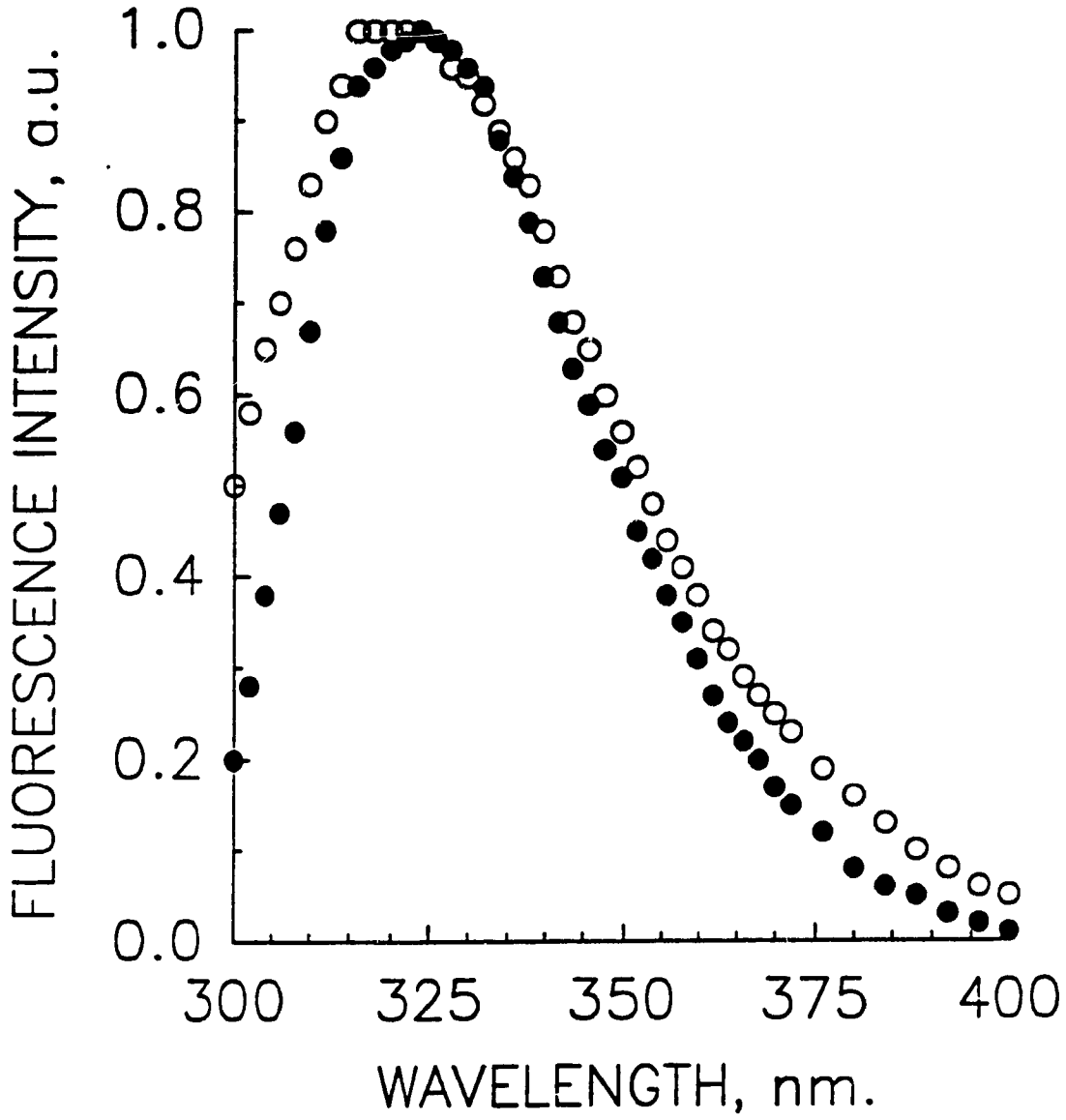

Fig.4.43: FLUORESCENCE EMISSION SPECTRA OF Ru-CcP IN ABSENCE AND PRESENCE OF 0.732 M CsCl - The excitation wavelength was 280 nm. Emission and excitation slits were 5 nm. 0 M CsCl (open circle), 0.732 M CsCl (closed circle). [Ru-CcP] was 1 μM, 0.1 M NaPi, pH7, T=19°C. Ionic strength constant at 0.732 M.

Fig.4.44: FLUORESCENCE EMISSION SPECTRA OF CcP AS A FUNCTION OF CESIUM CHLORIDE CONCENTRATION - The excitation wavelength was 280 nm. Emission and excitation slits were 5 nm. Spectra were staggered for visual purposes. [CcP] was 1 μM, 0.1 M NaPi, pH7, T=19°C. Ionic strength constant at 0.732 M.

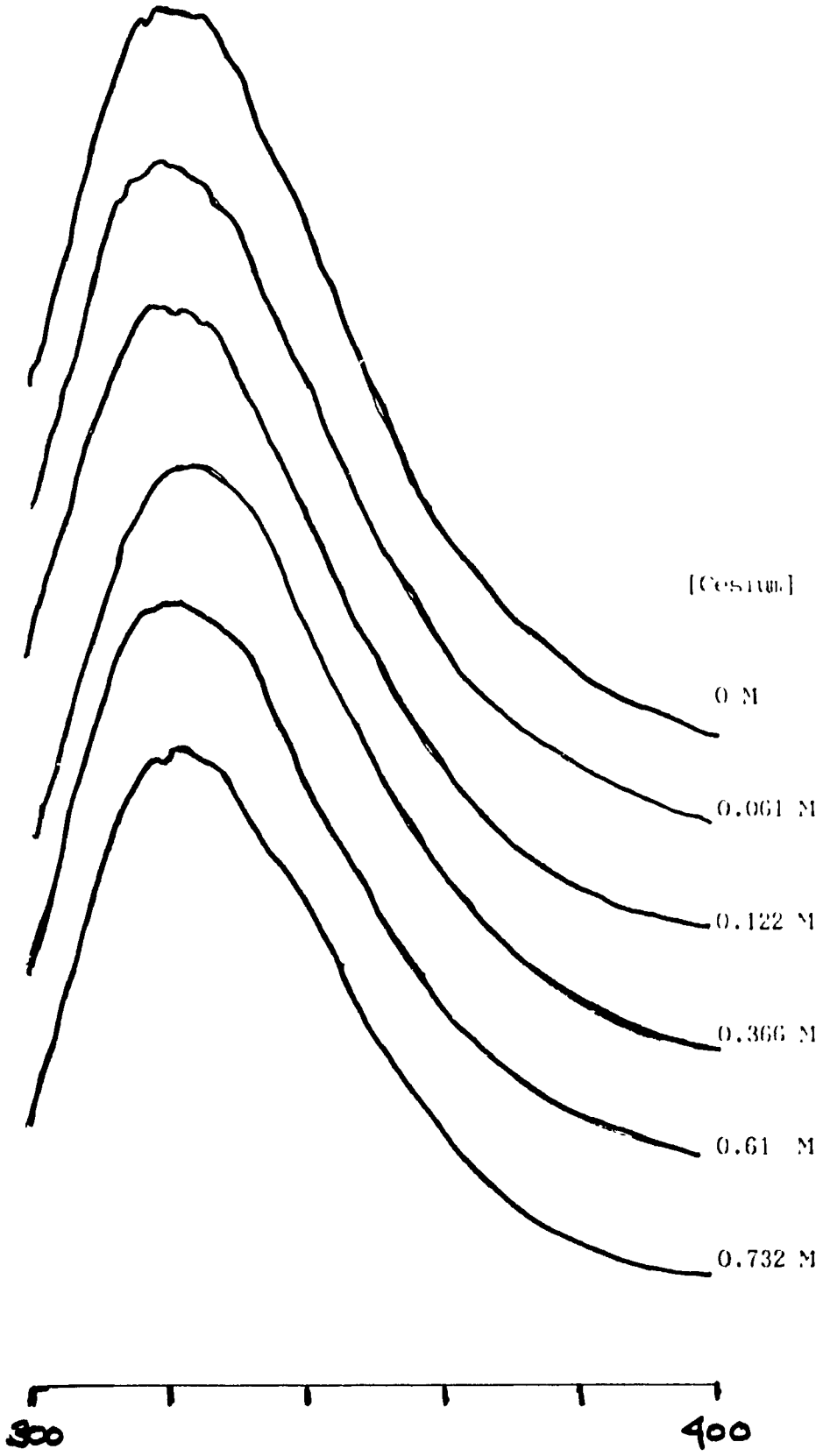
[Cesium]
0 M
0.061 M
0.122 M
0.366 M
0.61 M
0.732 M
300
400
WAVELENGTH, nm.

Fig.4.45: FLUORESCENCE EMISSION SPECTRA OF Ru-CcP AS A FUNCTION OF CESIUM CHLORIDE CONCENTRATION - The excitation wavelength was 280 nm. Emission and excitation slits were 5 nm. Spectra were staggered for visual purposes. [Ru-CcP] was 1 μM, 0.1 M NaPi, pH7, T=19°C. Ionic strength constant at 0.732 M.

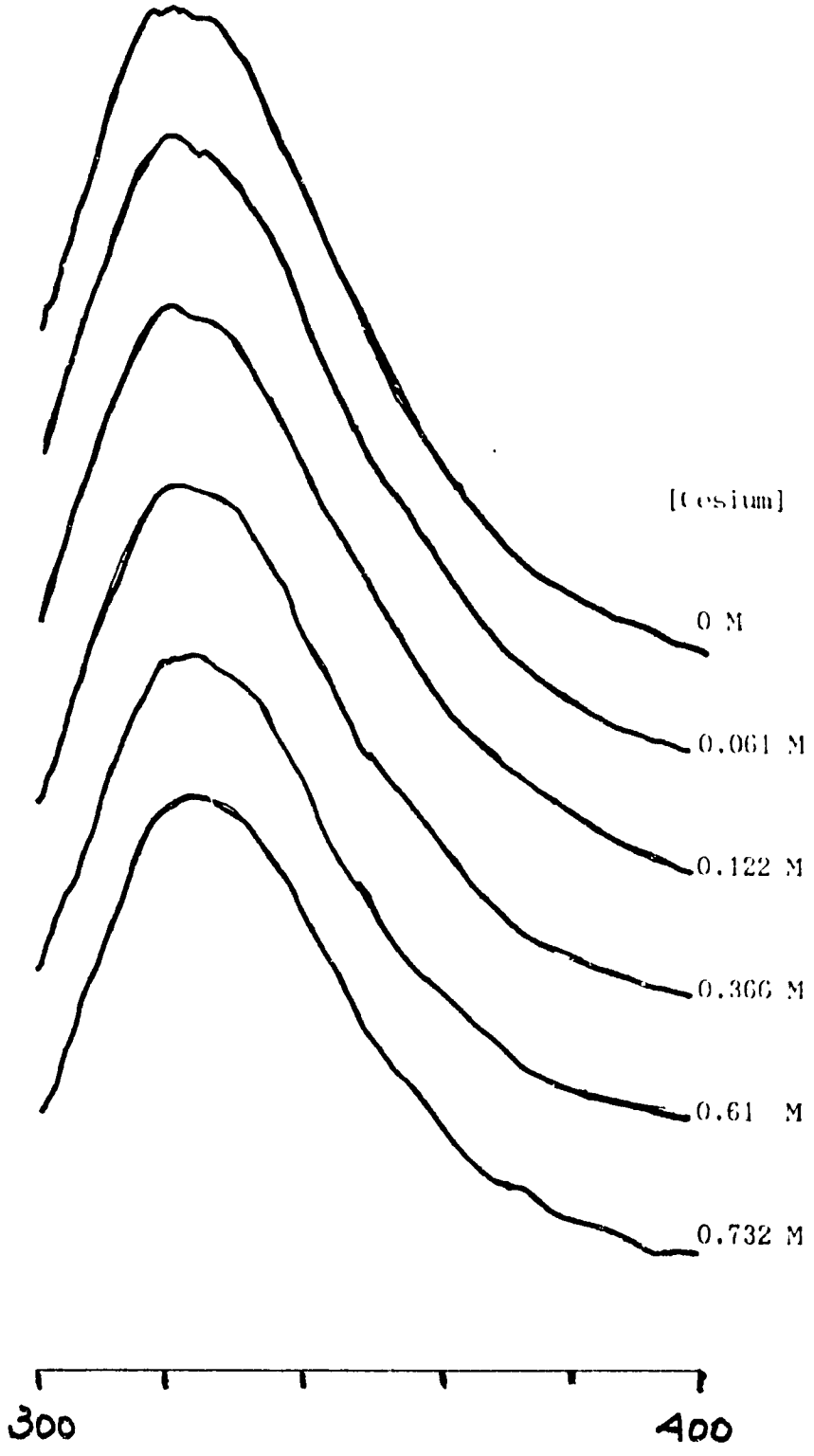
[Cesium]
0 M
0.061 M
0.122 M
0.366 M
0.61 M
0.732 M
300
400
WAVELENGTH, nm.

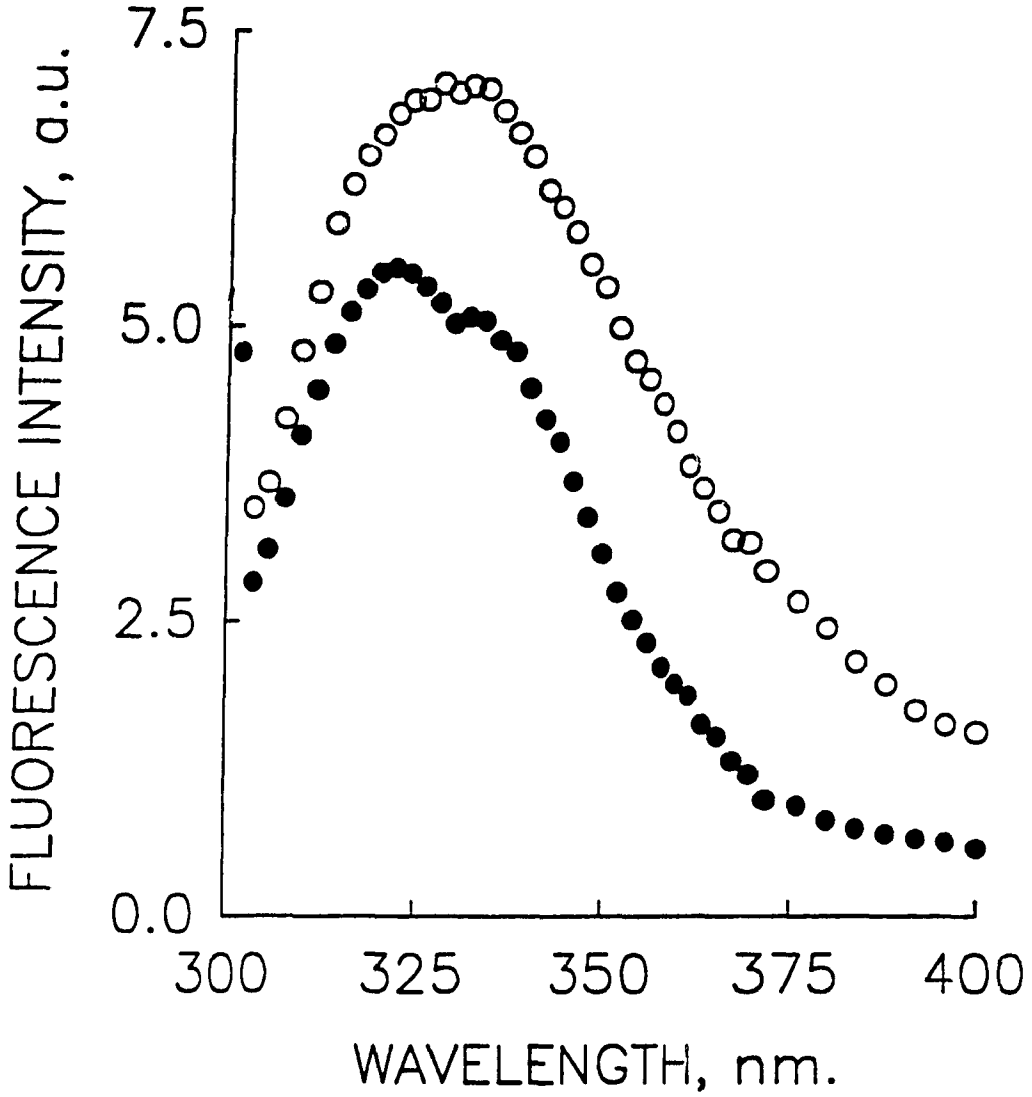

Fig.4.46: FLUORESCENCE EMISSION SPECTRA OF CcP IN THE ABSENCE AND PRESENCE OF 0.732 M CsCl- The excitation wavelength was 295 nm. 5 nm emission and excitation slits. 0 M CsCl (open circle), 0.732 M CsCl (closed circle). [CcP] was 1 μM, 0.1 M NaPi, pH7, T=19°C. Ionic strength constant at 0.732 M.

is observed at 332 nm in the absence of cesium chloride.

Quenching of tryptophan fluorescence by a quencher which is unable to permeate the protein matrix can be used to measure the fraction of fluorescence which is solely due to tryptophans localized on the surface of the protein. The fraction of the total initial fluorescence, denoted as f_a, can be determined from a modified Stern-Volmer plot based on the following equation (Lakowicz, 1983):

$$\frac{F_0}{\Delta F} = \frac{1}{f_a k [Q]} + \frac{1}{f_a}$$

where F_0 is the total fluorescence observed in the absence of quencher, Q, ΔF is the incremental difference of the fluorescence in the absence of Q and in the presence of Q, k is the Stern-Volmer quenching constant for the quencher-accessible fluorophores and [Q] is the concentration of quencher. A Stern-Volmer plot of cesium chloride quenching is portrayed in figure 4.47. Stern-Volmer constants, k_{sv}, were determined from the slopes and are stated in table 4.3 along with the percentage of quencher-accessible fluorophores, f_a, as determined from the modified Stern-Volmer plot shown in figure 4.48. Due to the poor quenching effiency of Cs^+ and the extent of overlap in experimental data from the three different CcP samples, k_{sv} can be estimated to be essentially the same for all ca. 0.66 M^{-1}.

4.2.5 FLUORESCENCE MONITORING OF CYTOCHROME c PEROXIDASE DENATURATION BY UREA

Since CcP seems to possess a complex intrinsic fluorescence spectrum relative to a simple tryptophan model it was

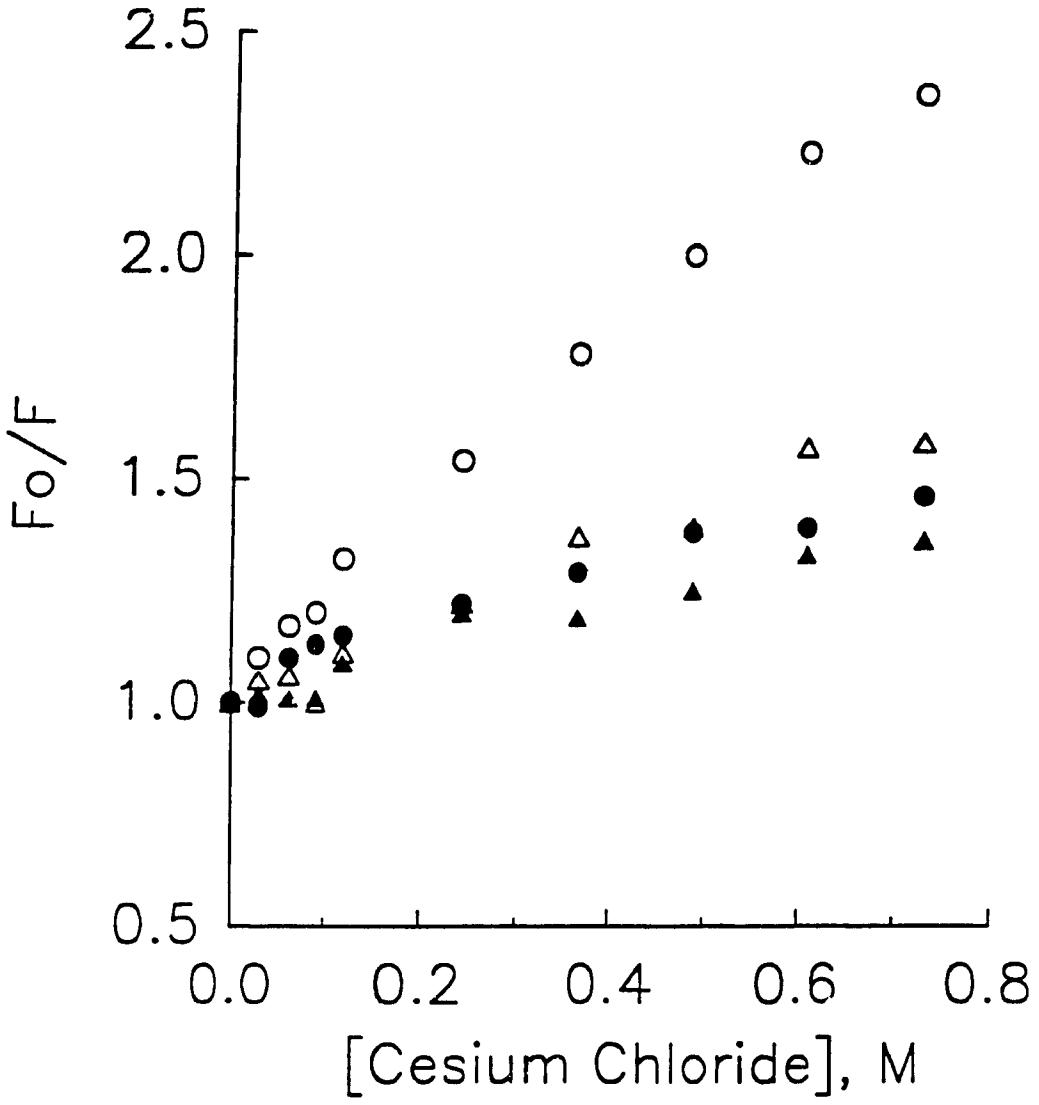

Fig.4.47: STERN-VOLMER PLOT OF CESIUM CHLORIDE QUENCHING OF CcP :- Samples are N-ATA (open circle), CcP (closed circle), Ru-CcP (open triangle) and Ru-His/CcP (closed triangle). Enzyme concentration was 1 μM. All samples were in 0.1 M NaPi, pH7, T=19°C. Ionic strength is constant at 0.732 M. Excitation at 280 nm. Emission and excitation slits at 5 nm.

Table 4.3: Stern-Volmer constants and fluorophore accessibility data for CcP, Ru-CcP and CcP/Ru-His using CsCl as the quencher.

Protein Sample	K_{SV} M^{-1}	f_a %
CcP	0.615	31.01
Ru-CcP	0.852	36.71
CcP/Ru-His	0.516	42.21
N-ATA	1.88	76.0 (100)

K_{SV} = the Stern-Volmer constant

f_a = the percentage of fluorophores which are accessible to the quencher used

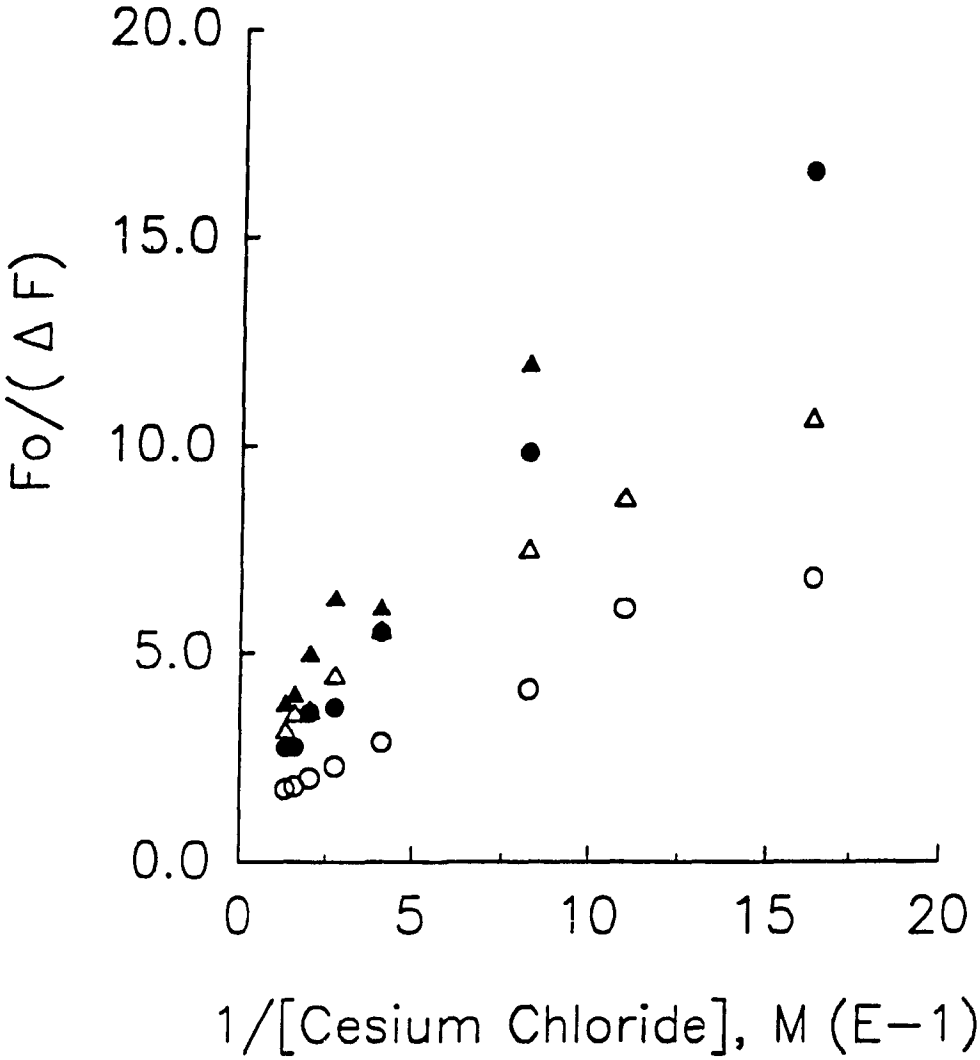

Fig.4.48: MODIFIED STERN-VOLMER PLOT OF CESIUM CHLORIDE QUENCHING OF CcP - for the determination of the percentage of accessible fluorophores to cesium chloride. N-ATA (open circle), Ru-CcP (closed circle), CcP (open triangle) and Ru-His/CcP (closed triangle). Enzyme concentrations were 1 μM in 0.1 M NaPi, pH7, T=19°C. Excitation at 280 nm. Emission and excitation slits at 5 nm. Ionic strength constant at 0.732 M.

deemed of interest to look at the denatured unfolded protein in which case any conformation dependent effects might be minimized. Figure 4.49 illustrates the Soret band spectrum of CcP at different concentrations of urea. The native protein has a Soret maximum at 408 nm, which remains relatively unchanged at lower urea concentrations (<2 M). At 4 M urea, the Soret is red-shifted to 415 nm. The 415 nm band may be due to a CcP-urea complex but its exact nature is not clear. At concentrations greater than 4 M the heme band is broadened and is centered at about 400 nm. The blue-shift of the heme band to 400 nm is indicative of heme which is displaced from the protein. The displacement of heme as monitored by the shift to 400 nm is used as the criterion to determine if the protein is in a denatured state. Since the heme of CcP is relatively buried, unfolding of the protein matrix is likely associated with the displacement of the porphyrin. The effect of urea on the tryptophan fluorescence of CcP is shown using excitation wavelengths of 280 nm and 295 nm, figures 4.50 and 4.51, respectively. Drastic changes in the fluorescence occur at concentrations < 4 M urea. These changes are revealed in the form of increased fluorescence intensity and a red-shift of the fluorescence emission maximum. These changes also coincide with the changes observed in the absorption spectrum. The denatured protein in 8 M urea exhibits a 10-fold increase in the fluorescence intensity as compared to the native protein (0 M urea) indicating that more tryptophans are contributing to the fluorescence of CcP. The emission maximum is at 352 nm in the denatured protein indicative that the tryptophans are in an hydrophilic environment, possibly, completely

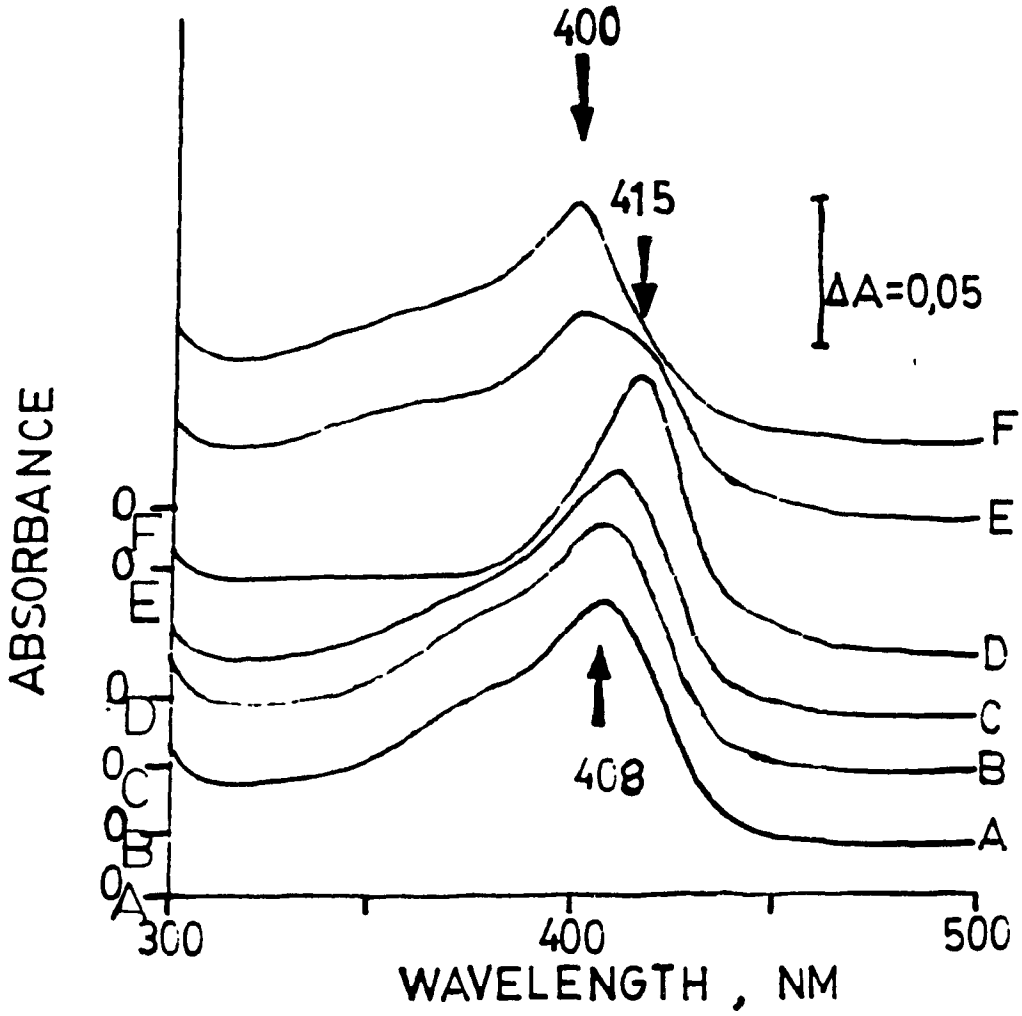

Fig.4.49: ABSORPTION SPECTRA OF THE SORET REGION OF CcP- the peroxidase concentration was 1 μM in 0.1 M NaPi, pH7, T=19°C. The urea concentrations are (A)= 0 M, (B)= 1 M, (C)= 2 M, (D)= 4 M, (E)= 6 M and (F)= 8 M. Spectra are staggered and the appropriate baseline is denoted by the "0" with the corresponding subscript on the y-axis.

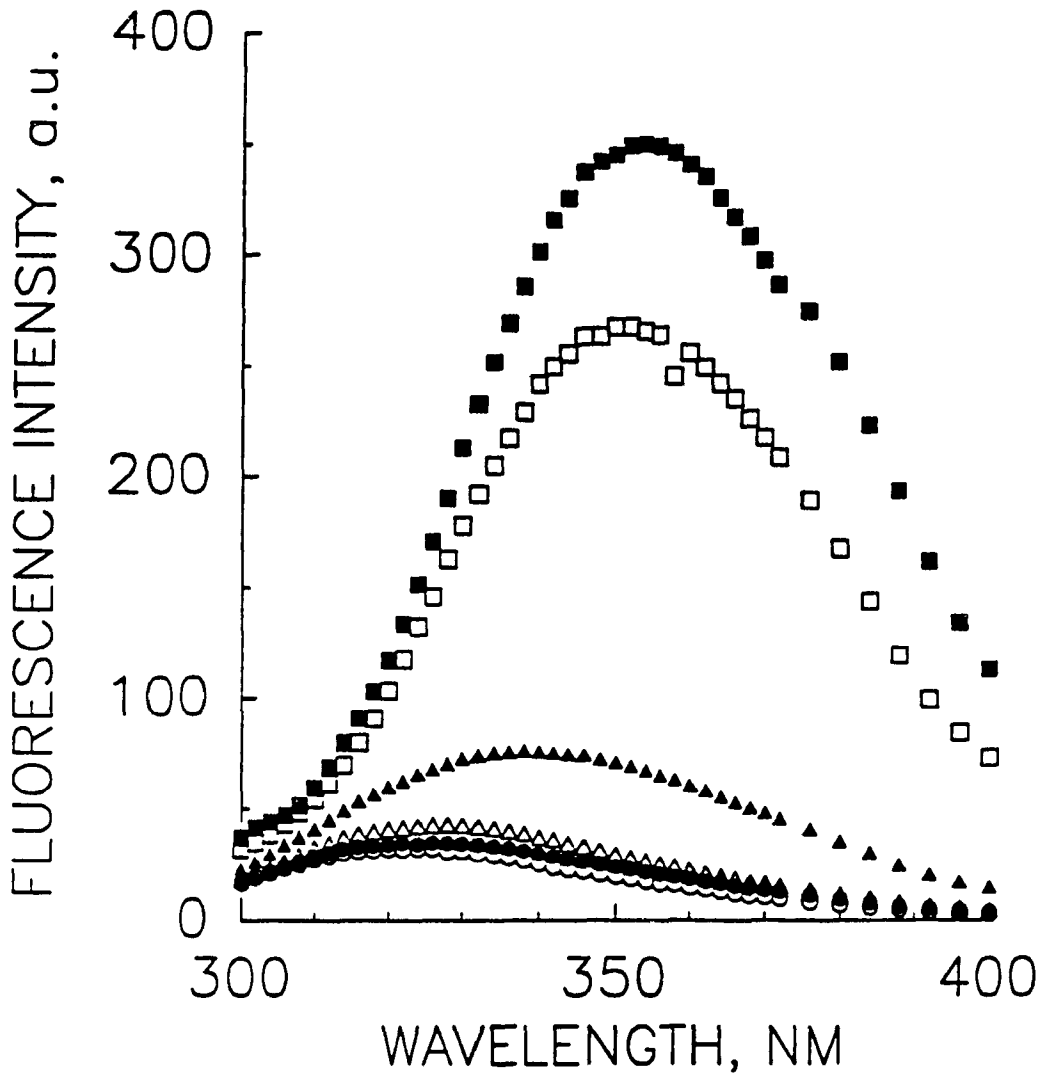

Fig.4.50: FLUORESCENCE EMISSION SPECTRA OF CcP AS A FUNCTION OF UREA CONCENTRATION, EX=280 NM - the peroxidase concentration was 1 μM in 0.1 M NaPi, pH7, T=19°C and the urea concentrations were as follows :- 0 M (open circles), 1 M (closed circles), 2 M (open triangles), 4 M (closed triangles), 6 M (open squares), 8 M (closed squares). Emission and excitation slits were 5 nm.

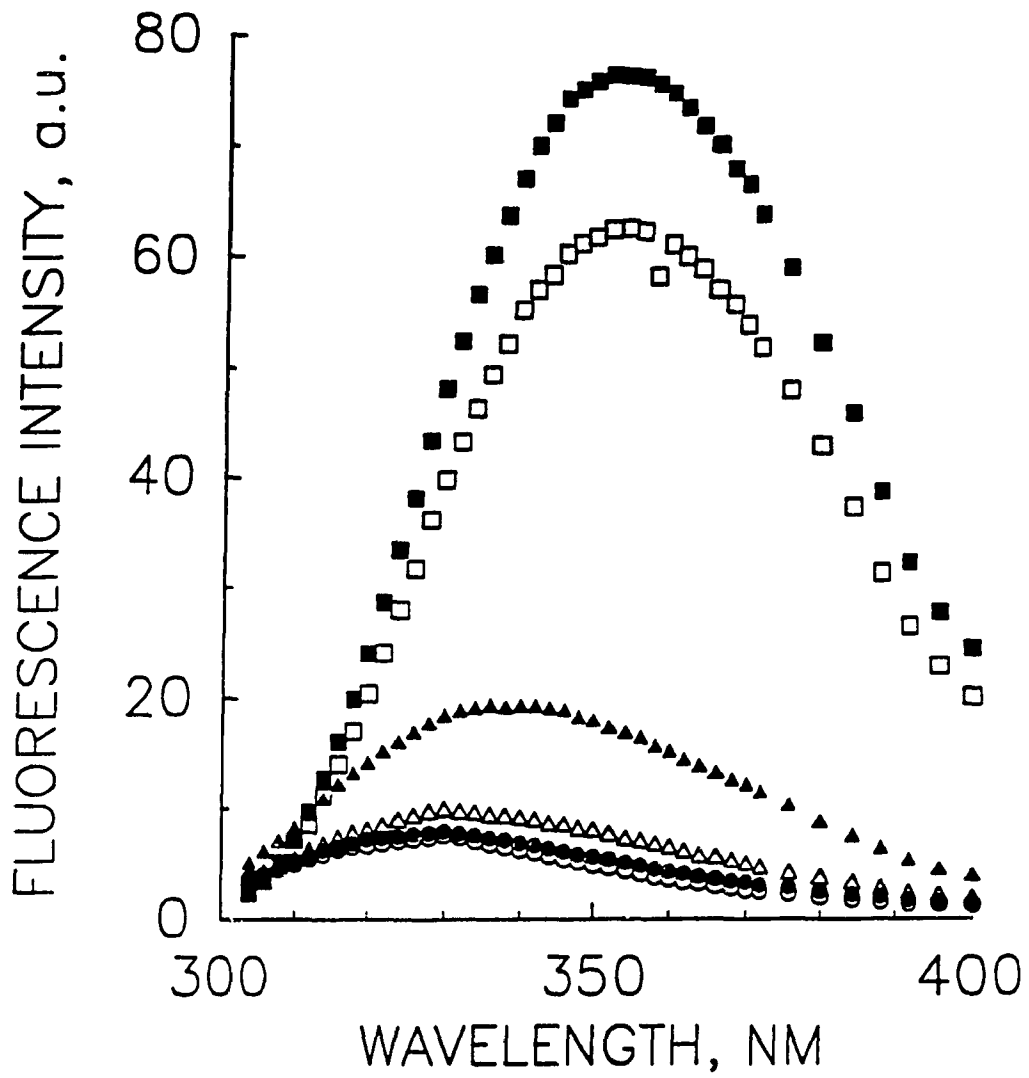

Fig.4.51: FLUORESCENCE EMISSION SPECTRA OF CcP AS A FUNCTION OF UREA CONCENTRATION, EX=295 NM - the peroxidase concentration was 1 μM in 0.1 M NaPi, pH7, T=19°C and the urea concentrations were as follows :- 0 M (open circles), 1 M (closed circles), 2 M (open triangles), 4 M (closed triangles), 6 M (open squares), 8 M (closed squares). Emission and excitation slits were 5 nm.

exposed to solvent. The dependence of the fluorescence intensity of CcP fluorescence on urea concentration is shown in figure 4.52. The intensity values were normalized in order to best compare the results obtained at the two different excitation wavelengths. For both, a single sigmoidal curve is obtained with a transition occurring, from native to denatured state, at ca. 4 M urea. The fluorescence intensity enhancement of the denatured protein as compared to native is 10-fold for both 280 nm and 295 nm results. Similarly the dependence of the fluorescence emission maxima on the urea concentration is shown to follow a sigmoidal curve (Fig.4.53). The inflection point occurs at ca. 4 M urea. The preliminary tryptophan fluorescence emission results for the reversibility of the denaturation process of CcP are shown in figure 4.54. The accompanying absorbance spectra (Fig.4.55) demonstrate that the CcP sample which has had the urea diluted out, i.e. "renatured" CcP, has a Soret maximum at 409 nm. The denatured CcP, with a urea concentration of 8 M, has a Soret maximum at 400 nm. The fluorescence results also show that upon dilution of the urea a partial reversibility of the denaturation process occurs as indicated by the 14 nm blue-shift. The fluorescence intensity is also diminished by 31% compared to that in the denatured sample. The same results are observed upon excitation at 295 nm. By comparison to a sample which was originally incubated in 2 M urea the emission maximum of the "renatured" sample is red-shifted by ca. 8 nm and its relative fluorescence intensity is 2.5 times greater. Although it may seem that the "renatured" sample consists of a mixed population of native

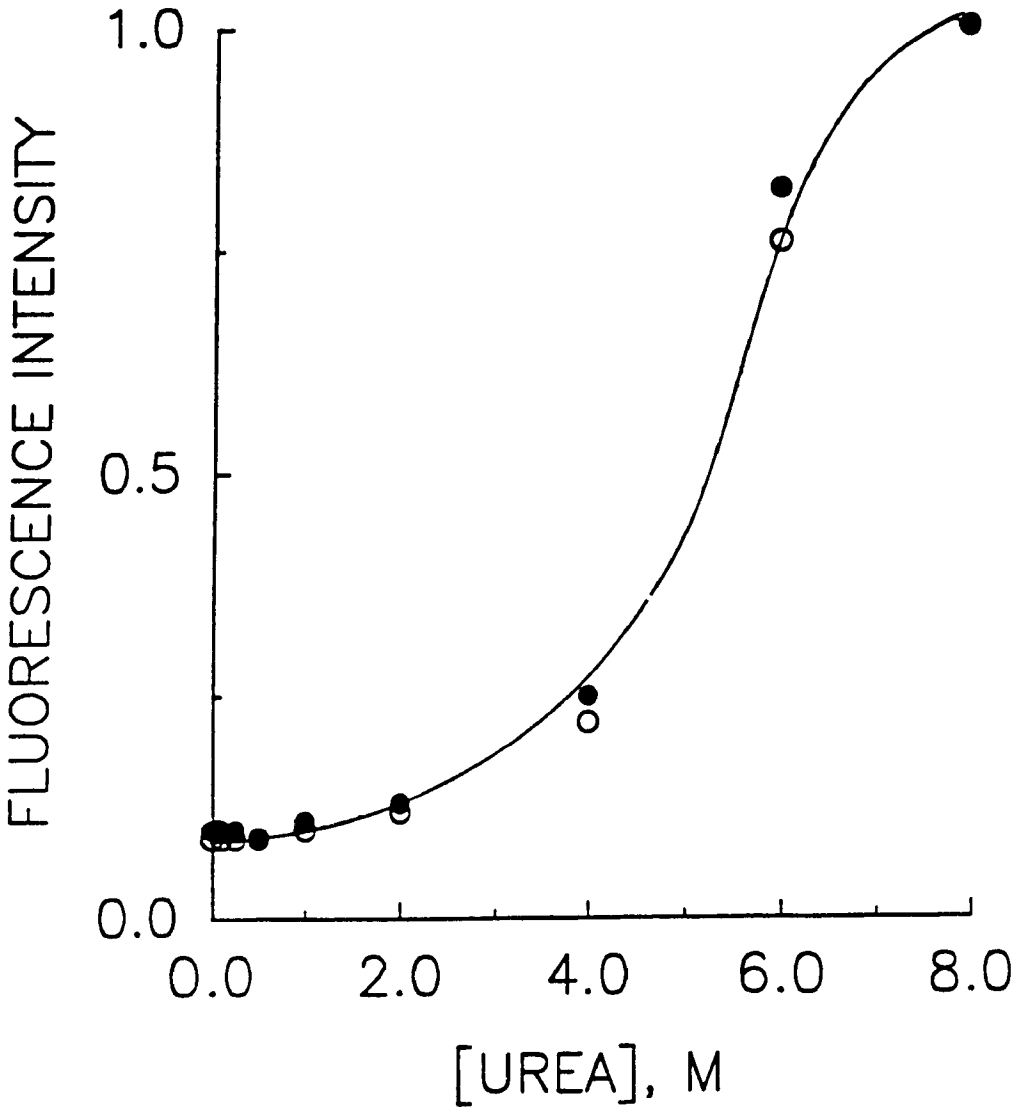

Fig.4.52: CcP FLUORESCENCE INTENSITY DEPENDENCE ON UREA CONCENTRATION - peroxidase concentration is 1 μM in 0.1 M NaPi, pH7, T=19°C. Fluorescence intensity values were normalized for comparative reasons. The excitation wavelengths were 280 nm (open circles) and 295 nm (closed circles). Emission and excitation slits were 5 nm.

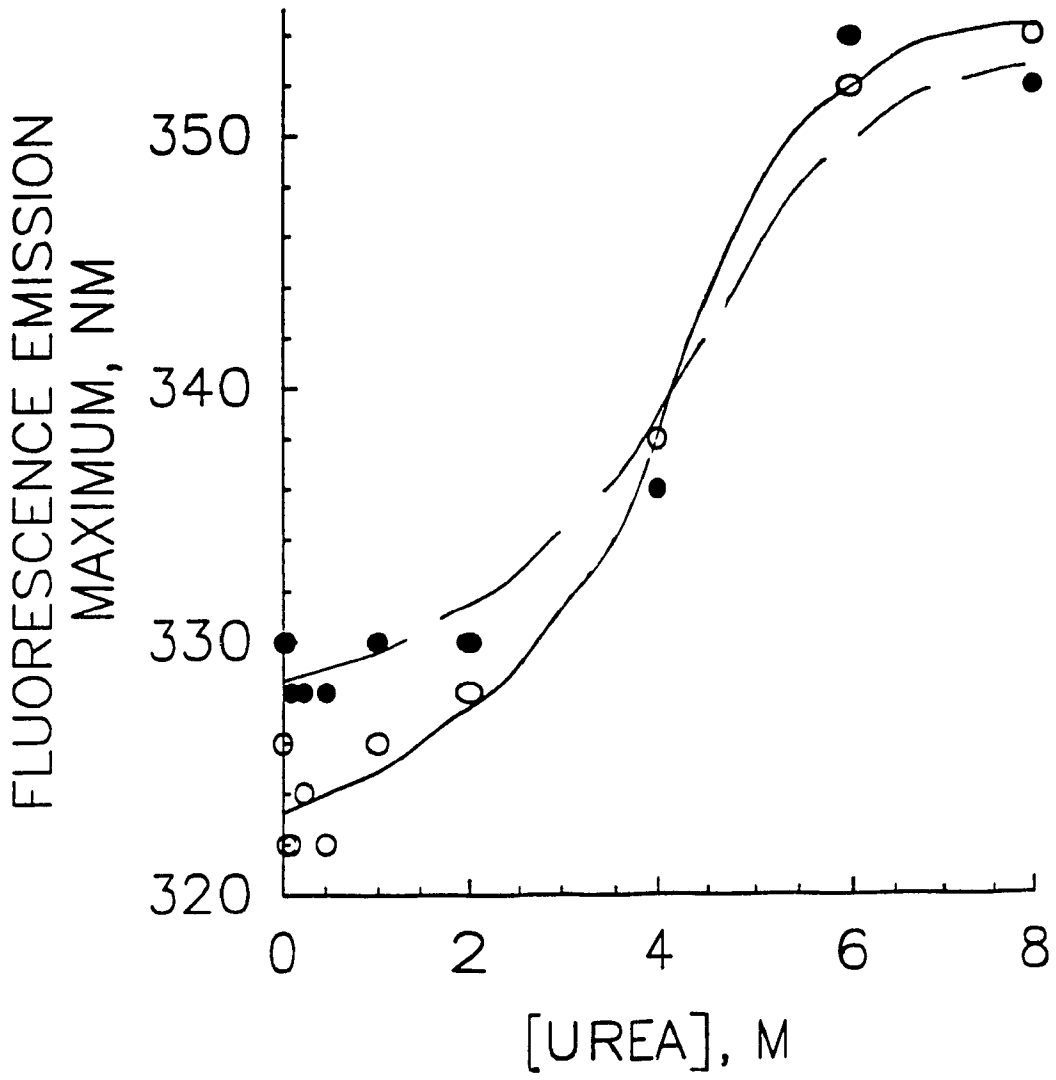

Fig.4.53: FLUORESCENCE EMISSION WAVELENGTH MAXIMUM DEPENDENCE ON UREA CONCENTRATION - peroxidase concentration was 1 μM in 0.1 M NaPi, pH7, T=19°C. The excitation wavelengths were 280 nm (open circles) and 295 nm (closed circles). Emission and excitation slits were 5 nm.

Fig.4.54: FLUORESCENCE EMISSION SPECTRA OF DENATURED AND "RENATURED" (cP - the peroxidase concentration was 0.5μM in 0.1 M NaPi, pH7, T=19°C. The [urea] was 8 M and 1.6 M in the denatured and renatured samples, respectively. The denatured protein is represented by the circles and the "renatured" protein by the triangles. The excitation wavelengths were 280 nm (open symbols) and 295 nm (closed symbols). Emission and excitation slits were 5 nm.

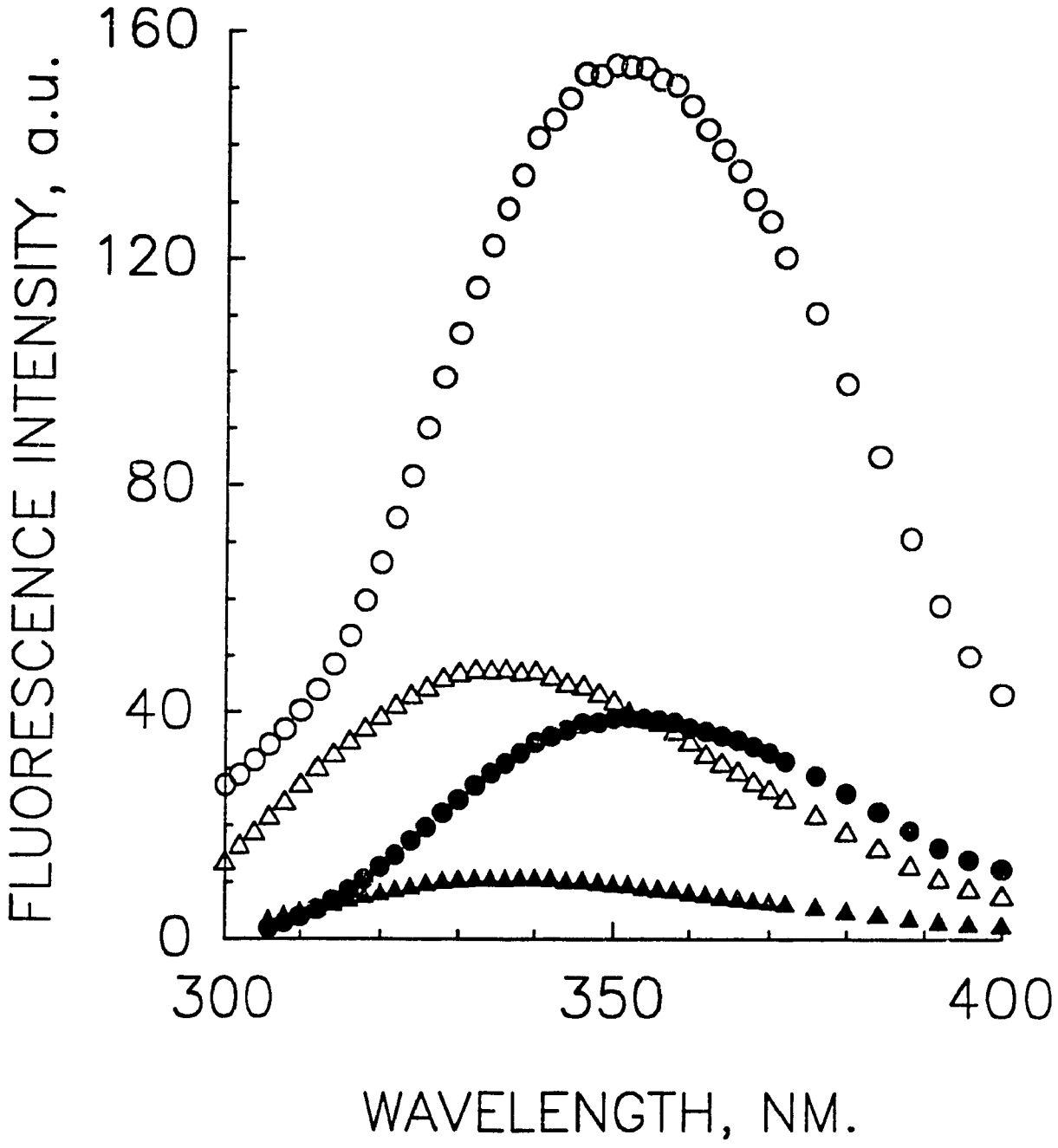
160
120
80
40
0
FLUORESCENCE INTENSITY, a.u.
300
350
400
WAVELENGTH, NM.

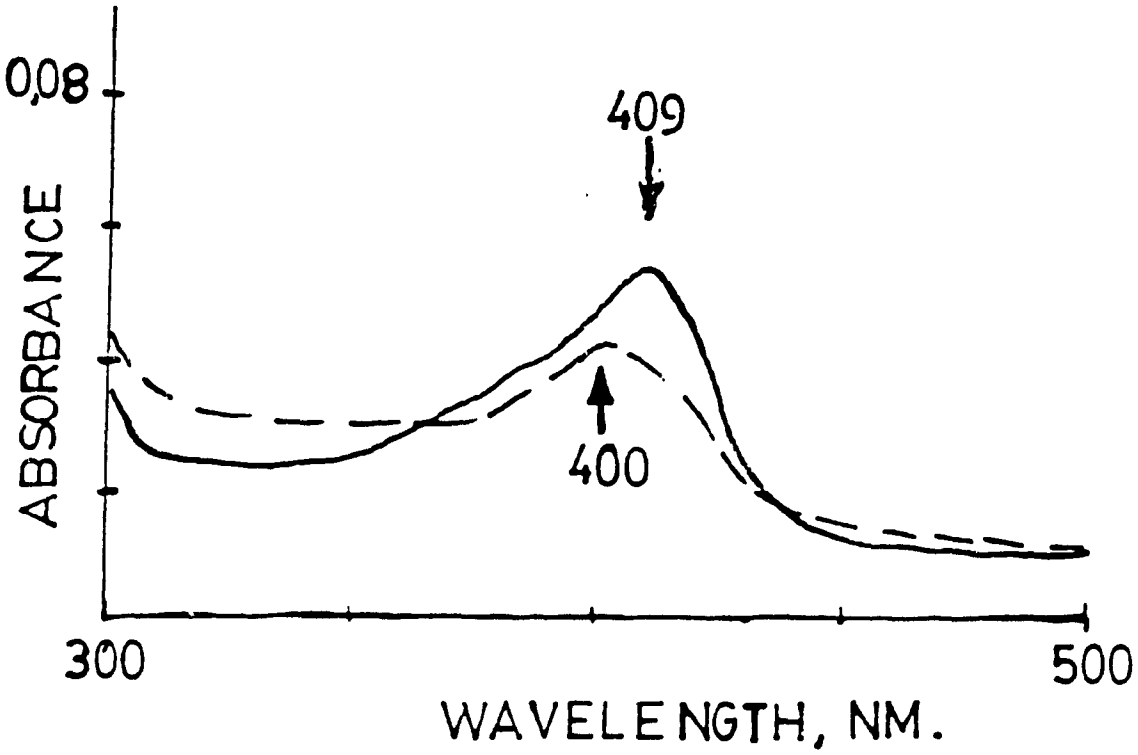

Fig.1.55: ABSORPTION SPECTRA OF THE SORET REGION OF DENATURED AND "RENATURED" CcP - the peroxidase concentration was 0.5 μM in 0.1 M NaPi, pH7, T=19°C. The [urea] was 8 M and 1.6 M in the denatured and renatured samples, respectively. The denatured species is symbolized by a solid line. The dashed line symbolizes the "renatured" CcP.

CcP and irreversibly denatured CcP, the Soret maximum of the "renatured" species is typical of native CcP. From the absorption and fluorescence results of the "renatured" CcP, it is assumed that the "renatured" CcP is in a partially refolded state where the heme entourage is probably native but the protein matrix farther from the heme pocket is not as tightly packed or completely refolded to a native-type state.

5. DISCUSSION

5.1 CYTOCHROME OXIDASE FLUORESCENCE

The search for the existence of conformational changes in cytochrome oxidase has in the past been centered on differences in the kinetics of its different redox forms (Jensen et al., 1984; Scholes & Malmström, 1986; Fabian et al., 1987). Direct evidence of conformational changes in cytochrome oxidase has been found by studying the motion of the protein using fluorescent probes (Kawato et al., 1980; kawato et al., 1981) or by monitoring the effect of cytochrome oxidase binding on the fluorescence of zinc porphyrin cytochrome c (Alleyne & Wilson, 1987). Alleyne and Wilson (1987) propose that conformational changes occur upon reduction of heme a and/or Cu_A. In all these cases the existence of conformational changes in cytochrome oxidase are derived from observed changes in the fluorescent properties of an independent fluorophore. Cytochrome oxidase has been shown to have substantial steady-state fluorescence from its numerous tryptophan residues (Hill et al., 1986). It is the aim of this thesis to use the natural occurring fluorophores of the oxidase to investigate redox-linked conformational changes. For example, such an approach has been successfully used to demonstrate the effect of liposome addition to cytochrome b_5 (Dufourcq et al., 1975).

It has been shown that the steady-state tryptophan fluorescence from cytochrome oxidase can be observed in samples which include the reductant sodium dithionite (Copeland et al., 1987). Although dithionite absorbs strongly at 315 nm and

qualitatively influences emission from tryptophan there is sufficient light transmission to allow for efficient excitation of the tryptophan chromophore. The uncorrected dithionite-reduced $\underline{aa}_3$ tryptophan fluorescence spectrum has a maximum at 346 nm (Copeland et al., 1987; and see results figure 4.2). The emission maximum for fully oxidized resting cytochrome $\underline{aa}_3$ is 328 nm consistent with previous reports (Hill et al., 1986; Copeland et al., 1987). However, the corrected emission spectrum of dithionite-reduced cytochrome $\underline{aa}_3$ is at 326 nm, indicating that the absorbance of the reductant contributes a large inner filter effect and is responsible for the 18 nm red-shift observed in the raw spectrum. The magnitude of the 315 nm absorbance band of dithionite and therefore the concentration of this species determines the emission maximum.

Copeland et al. (1987) suggested that the red-shift observed in the reduced cytochrome $\underline{aa}_3$ is due to reduction of Cu_A specifically. However, the time course of Cu_A reduction is observed to follow that of the hemes which is in sharp contrast to the time course of the fluorescence emission maximum. Therefore, the red-shift observed in the uncorrected fluorescence emission maximum cannot be attributed to reduction of Cu_A and is not an indication of a conformational change dependent on the redox state of Cu_A as was originally postulated by Copeland et al. (1987, 1988). In addition, the same effect is observed in the fluorescence emission spectrum of carboxypeptidase A in the presence of dithionite. Since this enzyme is incapable of redox activity, then a change in redox

state can be ruled out as the cause of the observed fluorescence changes. It is shown in fig.4.8 that fully oxidized resting $\underline{aa}_3$ can be made to have a fluorescence emission spectrum characteristic of that observed in the fully dithionite-reduced oxidase, when its fluorescence emission is monitored in the presence of a dithionite filter. It has been established that although a fluorescence emission spectrum can be obtained in the presence of dithionite, this spectrum will be drastically altered due to the inner filter effects caused by the absorbance of the reductant. The dramatic 20 nm red-shift observed in the fluorescence emission maximum of the oxidase is solely due to the presence of the chemical reductant, dithionite, and is not related to either the redox state of Cu_A or a conformational change arising upon reduction of the center.

The close relationship observed between the levels of dithionite and the red-shift in the fluorescence emission maximum suggested that studies of dithionite-reduced oxidase must be performed under conditions such that the optical properties of the sample were not excessively altered. The fact that the fluorescence emission maximum of the mixed-valence CO-bound $\underline{aa}_3$ is identical to that of the fully oxidized, resting enzyme suggests that there are no gross conformational changes in the enzyme upon reduction or ligation of cytochrome $\underline{a}_3$.

Redox-state dependent conformational changes have also been linked to the reduction of cytochrome $\underline{a}$ (Scholes & Malmström, 1986; Ellis et al., 1986; Brudvig et al., 1984). In the event that such a change would be visible in the steady-state fluorescence of

the protein, then this change would be expected between the spectrum of the mixed-valence CO-bound $\underline{aa}_3$ and fully reduced CO-bound $\underline{aa}_3$. The 2 nm blue-shift in the emission maximum observed upon reduction of cytochrome $\underline{a}$, although reproducible, is too small to be firmly attributed to a change in the physical state of the enzyme. Conformational change studies show that upon reduction the oxidase expands (Cabral & Love, 1972; Kornblatt et al., 1975) and becomes more susceptible to cleavage by proteases (Yamamoto & Okunuki, 1970) Without knowing the crystal structure of the enzyme, the direct consequence of such a change in the physical state of the enzyme to the environment of 51 tryptophans is impossible to predict. Based on the volume and proteolysis susceptibility data, it is most likely that the average environment of the fluorescing species would become more solvent accessible. This solvent accessibility could translate into either a red-shift in the tryptophan fluorescence if the contribution of each fluorophore is unchanged or a blue-shift in the fluorescence spectrum if the solvent-accessible tryptophans are quenched such that the effective fluorescence is derived from those fluorophores present in a hydrophobic environment. With such a large number of fluorophores it is unlikely that discrete changes may be visualized in the tryptophan fluorescence.

The idea that cytochrome oxidase links electron transfer from cytochrome $\underline{c}$ to O_2 to translocation of protons across the membrane is generally accepted. Studies now focus on determining the molecular mechanism of this function which is

common to both respiratory and photosynthetic electron transfer systems. Most work is focused on determining which redox center is responsible for the linkage between electron transfer and proton translocation. Two basic schemes for proton pumping predominate the literature. The first scheme involves proton pumping directly linked to the redox state of either cytochrome a or Cu_A. The other is indirectly linked to the redox state of cytochrome a or Cu_A and directly involved with subunit III, postulated to be an inherent proton channel. Proton wells or conduction pathways are required for the operation of a redox-driven proton pump (Mitchell, 1968). Hypothetically, these wells function primarily by the conversion of the electrical potential component of the electrochemical proton gradient into a pH or protonic activity differential (Krab & Wikström, 1987). Konstantinov et al. (1986) have shown the existence of such a phenomenon between the mitochondrial matrix and the binuclear center of cytochrome oxidase. The binuclear center of a_3 has been demonstrated to be an unlikely candidate for proton pumping (Wikström & Casey, 1985), therefore the redox center intimately involved in proton translocation is either cytochrome a or Cu_A or both. In determining which of these centers is the most likely to be the redox link between electron transport and proton translocation, it must be considered that a pH-dependent midpoint potential, E_m, is a most probable requirement for the redox center which couples these two processes. Erecinska et al. (1971) have shown that the apparent E_m of Cu_A is pH-independent and independent of the energy state of the mitochondria. Callahan & Babcock (1983)

have proposed that the hydrogen bond existing between the formyl group of cytochrome a and a residue on the protein, most likely tyrosine, could be directly or indirectly involved in proton pumping. The strength of this bond has been shown (Babcock & Callahan, 1983) to be dependent on the redox state of cytochrome a, where it is stronger in the ferrous as opposed to the ferric state. The free energy difference between these two states was calculated to be ca. 100 mV as concerns the hydrogen bond strength. This would translate into a difference in E_m between donor and acceptor forms of the enzyme of ca. 200 mV, which is comparable t the maximal protonmotive force in mitochondria (Krab & Wikstrom, 1987). Such a mechanism provides a direct method for protonation-deprotonation centered at or close to the redox center.

Indirect proton translocation can be regarded as a protonation-deprotonation step linked to the redox state of cytochrome a and/or Cu_A but occurring at a site away from the redox centers. Indirect proton translocation therefore involves the existence of a proton channel. Such a role has been assigned to subunit III. Evidence for the translocation of protons through subunit III has been gathered by several groups. Saraste et al. (1981) have shown that beef heart aa_3 depleted of subunit III can catalyze electron transfer but does not pump protons. Likewise, DCCD, a compound shown to bind specifically to the proton-translocating proteolipid of various ATPases, has been shown to inhibit proton translocation in reconstituted cytochrome oxidase vesicles (Casey et al., 1979) where it binds specifically to

subunit III (Casey et al., 1980). Furthermore, there exists a good deal of homology between the amino acid sequence of subunit III and that of the proton-translocating proteolipid of ATPases (Hoppe et al., 1980).

From the arrangement of the cytochrome oxidase molecule (scheme 5.1) one can predict what the influence of either of these proton translocating mechanisms will be on the environment of tryptophan residues. In the case of the protonation-deprotonation mechanism occurring at or relatively close to the redox center, either cytochrome a or Cu_A, it is reasonable to expect that influence on the tryptophan environment will be limited to that region of the protein. By contrast, if the redox-linked protonation-deprotonation occurs at subunit III then this would entail most probably rearrangement of several tryptophan residues lying in the region of protein between subunit III and the redox centers. Although the results obtained do not assign a direct role for either of the redox centers in the coupling mechanism, the lack of any visible differences between reduced and oxidized cytochrome oxidase in its steady-state fluorescence tends to support the occurrence of a local conformational change in the vicinity of the coupling redox center rather than a long range conformational change as is required to link the change in redox state at cytochrome a or Cu_A with proton translocation at subunit III.

As has been previously shown (Nicholls & Chanady, 1981) 3,10-dimethyl-5-deazaisoalloxazine proved to be an effective reductant of cytochrome oxidase with the added advantage that it

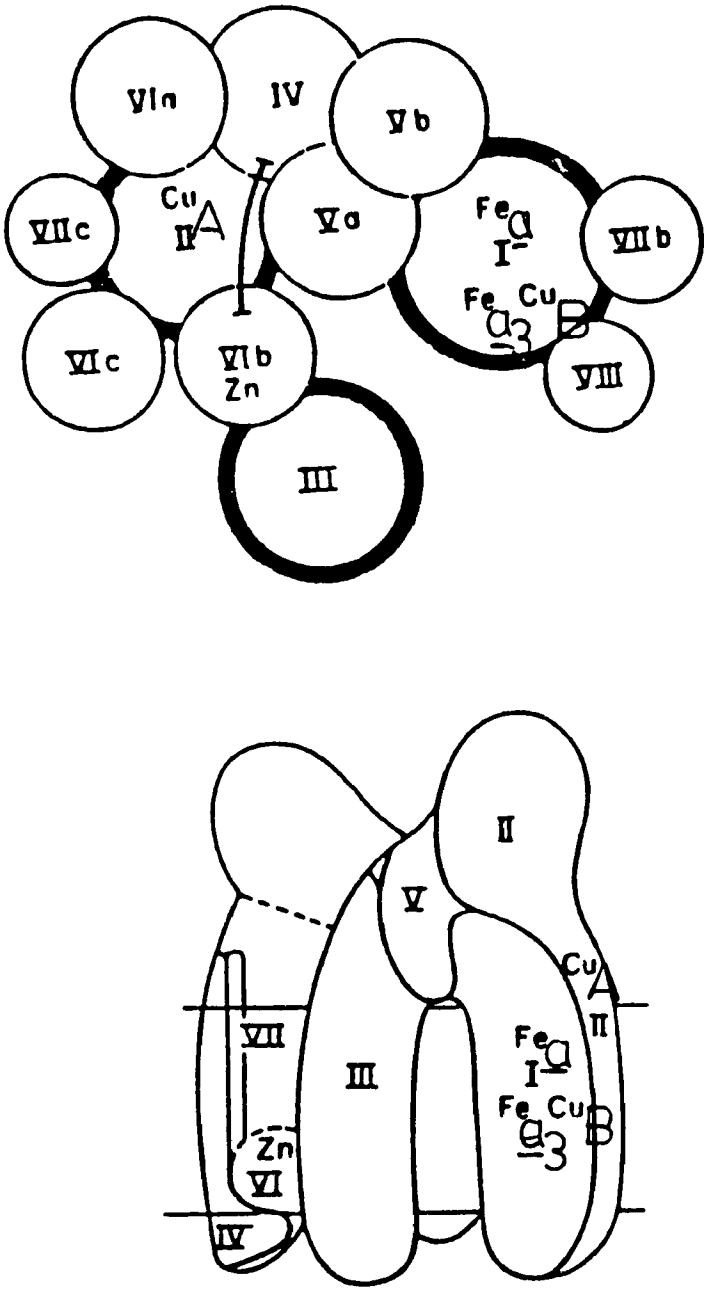

Scheme 5.1: SUBUNIT ARRANGEMENT IN CYTOCHROME OXIDASE- adapted from Chance et al. (1988).

contributes minimally to the optical spectrum of the sample. Similarly to the fully dithionite-reduced CO-bound oxidase, the fully photo-reduced CO-bound enzyme has a fluorescence emission maximum at 326 nm. Deazaflavin itself contributes to the fluorescence emission spectrum. The two bands observed in the fluorescence spectrum of the photocatalyst are derived from different fluorophores, since they do not exhibit similar properties upon irradiation. The fluorophore contributing to the 157 nm band is either quenched or its population diminished upon irradiation. The fluorescence of the 330 nm fluorophore appears to be independent of irradiation. The differences in the fluorescence spectra of deazaflavin in the presence and absence of oxidase in conjunction with the postulated scheme for the photocatalytic mechanism of deazaflavin can possibly be used to identify the fluorophore contributing to the 457 nm fluorescence band.

From Scheme 2.5 the photochemical process occurring upon irradiation can be followed. In the presence of enzyme deazaflavin radicals will reduce the enzyme and regenerate the oxidized deazaflavin molecules. In the absence of enzyme deazaflavin radicals will decay via a dismutation reaction. The cycle favoured in the presence of oxidase does not include the generation of the reduced photocatalyst but involves its consumption. If the non-irradiated deazaflavin sample consists of both oxidized and reduced deazaflavin molecules then in the presence of enzyme these reduced deazaflavin molecules would be consumed in the generation of the dimer but would not be

regenerated since there is only regeneration of the oxidized molecules in the event of a redox reaction with a suitable partner such as the oxidase. In the absence of oxidase the reduced deazaflavin molecules are recycled. The decrease in the fluorescence observed for the 457 nm band of the irradiated photocatalyst in the absence of oxidase can be accounted for by a decrease in the reduced catalyst population. This decrease in population could arise from some of the molecules being present in the form of the dimer.

Cytochrome oxidase tryptophan fluorescence was detectable at concentrations as low as 190 nM. The vesicles used in these experiments have relatively low RCR values. Respiratory control is a concept used to assess the integrity of a mitochondrial preparation. Low values of RCR indicate that the membrane is permeable to protons. The dependence of respiration on the thermodynamic disequilibrium of the system relies on the low permeability membranes have for protons and other ionic species. Scheme 5.2 represents membrane-incorporated cytochrome oxidase. Reconstituted vesicles provide an appropriate experimental system to study the consumption and generation of transmembranous proton gradients. Intravesicular pH changes can be adequately determined with the use of such optical probes as phenol red (Wrigglesworth, 1977). Redox-linked proton translocation in a vesicular system occurs only in the presence of the potassium ionophore, valinomycin and K^+ (i.e. in the absence of a transmembrane electrical gradient). For this reason the controlling factor of enzyme

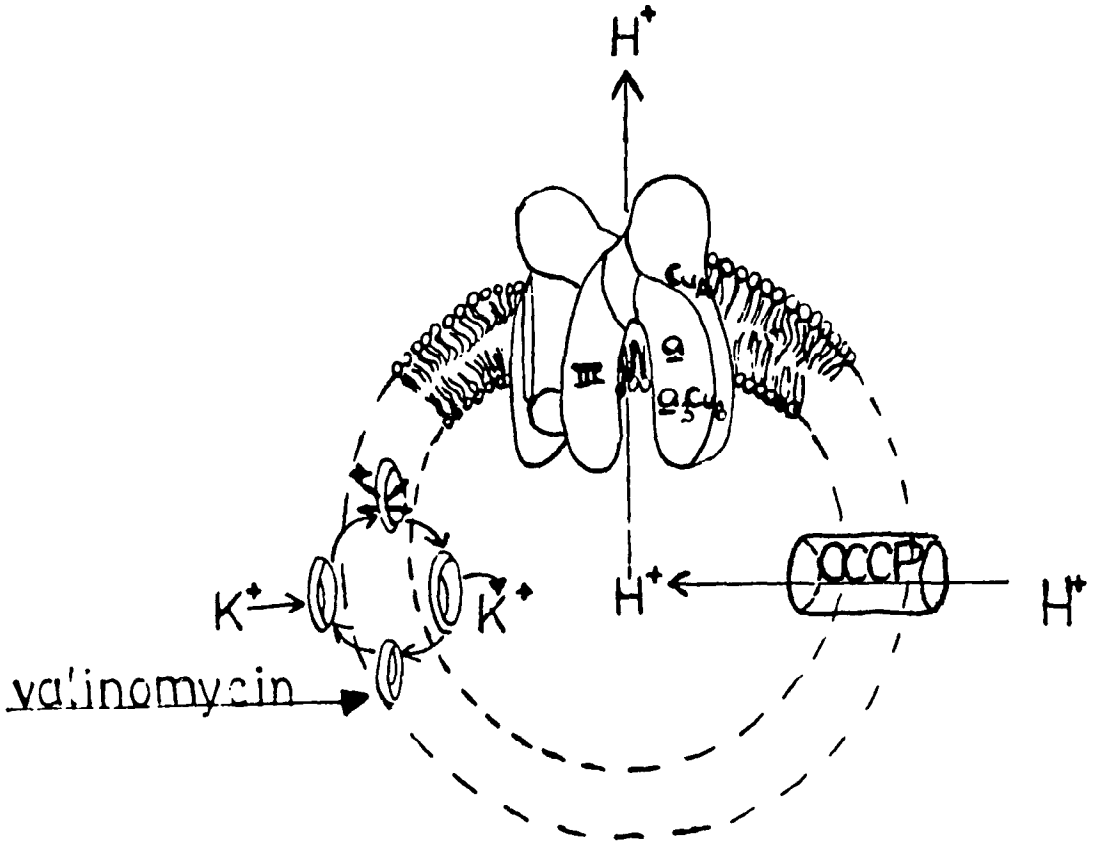

Scheme 5.2: SCHEMATIC REPRESENTATION OF MEMBRANE-INCORPORATED CYTOCHROME OXIDASE.

turnover will be the pH gradient across the inner mitochondrial membrane and not the build up of charge separation. In the event that ATP is being generated by the mitochondrion, re-entry of protons through the ATPase cause the the oxidase to continuously turnover thereby supplying the required protons the ATPase. Build up of sufficient ATP wil cause the ATPase to shut down which in turn induces a rapid build of a proton gradient across the mitochondrial membrane thereby "turning off" the oxidase. In the presence of a protonophore such as CCCP the oxidase will continuously turnover in order to maintain the balance between proton re-entry and proton extrusion.

The vesicles used in this study have a high permeability to protons which allows membrane-incorporated cytochrome oxidase to turnover in an uncontrolled manner. At high RCR values respiration would be controlled and the enzyme could only be forced to turnover until a State 4 rate is achieved. State 4 respiration is the respiratory state of mitochondria in the presence of substrates but in the absence of ATP synthesis. Theoretically in this state the enzyme should not turnover since no ATP is being synthesized. Practically, the rate of turnover in State 4 is measureable although low. The perceived rate is due to the incomplete impermeability of the inner membrane to protons. This impermeability allows a slow leak of protons into the matrix even in the absence of ATP synthesis. For this reason enzymatic turnover continues in order to maintain the rate of proton re-entry counterbalanced by the rate of proton extrusion. In mitochondrial

preparations this leak in protons is often due to the slow cycling of Ca^{2+} across the membrane (Nicholls, 1982). In preparations where cytochrome oxidase has been reconstituted into phospholipid vesicles the occurrence of the proton leak is often more pronounced. In this case, several factors may contribute to the increased proton permeability such as the retention of detergent molecules and non-incorporation of the protein into the phospholipid micelle. In the case of the former, the presence of detergent molecules in the micelle provide the necessary 'proton-channel', thereby reducing the impermeability of the membrane. In the latter case, protein molecules may not be incorporated in the phospholipid micelles but surrounded by them such that it is essentially "free" in solution. The low RCR values obtained could arise from either of these cases. Extended dialysis time did not improve the ratios observed as expected since cholate has a high micellar concentration (13-15 mM) (Casey, 1981) and therefore should be easily dialyzed. This suggests that the oxidase-vesicle preparation may be a mixture of membrane-incorporated oxidase and micelle solubilized oxidase. This is further supported by the relatively high (85%) cytochrome c accessibility of the preparation.

The fluorescence spectra of both free oxidase and membrane-incorporated oxidase had similar spectral shape although the membrane-incorporated oxidase emission was blue-shifted by 1-2 nm. Likewise, oxidase vesicles with a ΔpH of 3 units between their matrix and cytosolic sides appeared to be further blue-shifted by

1-2 nm and exhibit a 20% decrease in the fluorescence intensity. Under the conditions stated, these slight differences in the two vesicle preparations are difficult to attribute to any specific changes occurring in the protein being reflected by the fluorescence of its tryptophan residues. To assign these differences to a conformational change in the membrane-incorporated oxidase would require vesicular preparations having RCR values greater than 4. A positive correlation between the extent of the observed differences and the RCR value could indicate a basis for the assignment of these spectral differences in tryptophan fluorescence to a conformational state of the oxidase found in the presence of a ΔpH across the membrane. Further investigations are required to clarify this proposal. From the limited observations in this study few conclusions may be derived. The thorough investigation of the tryptophan fluorescence of membrane-incorporated oxidase may provide a method of detecting gross conformational differences in the enzyme under conditions of active ATP synthesis or absence of ATP synthesis. The detection of such conformational differences would provide a link for electron transfer-driven proton translocation. Furthermore, the tryptophan fluorescence of membrane-incorporated cytochrome oxidase is physiologically more relevant than that of free oxidase.

5.2 CYTOCHROME c PEROXIDASE FLUORESCENCE

The tryptophan fluorescence of CcP has a maximum at 326 nm suggesting that the fluorophore is located in a hydrophobic environment. This is supported by the low quenching values obtained

with quenchers of solvent-accessible tryptophans such as I^- and Cs^+. The tryptophan fluorescence of the histidine-60 ruthenium derivative of CcP is observed to be quenched compared to the native protein and its maximum slightly blue-shifted upon excitation at 280 nm. Quenching at the red-edge of the fluorescence spectrum of CcP is observed with cesium chloride at an excitation of 280 nm. No such quenching is observed in the case of the ruthenium-His-60 derivative. These results suggest that a relatively solvent-accessible tryptophan residue in the vicinity of histidine-60 is quenched by the presence of ruthenium at this site. Tryptophan-57 is the only tryptophan residue in the vicinity of histidine-60 (from crystal structure data obtained from Mr. Ted Fox, see figure 5.1). The stable transition metal complex formed between $Ru(III)(NH_3)_5$ and the imidazole side chain of histidine has been shown (Recchia et al., 1982) to be an ideal acceptor of energy transferred from intrinsic protein fluorophores such as tryptophan. The quenching of intrinsic tryptophan fluorescence by this complex has been observed in the ruthenated derivatives of α-lytic protease and lysozyme (Recchia et al., 1982). Although the specific donor-acceptor distance in multifluorescent donor proteins may be impossible to predict from steady-state fluorescence, changes in energy transfer properties to the ruthenium complex upon binding of substrates or ligands or accompanying redox state changes of the enzyme may provide a useful method of monitoring conformational changes in proteins such as cytochrome c peroxidase. These changes can also be monitored through the charge transfer absorption bands

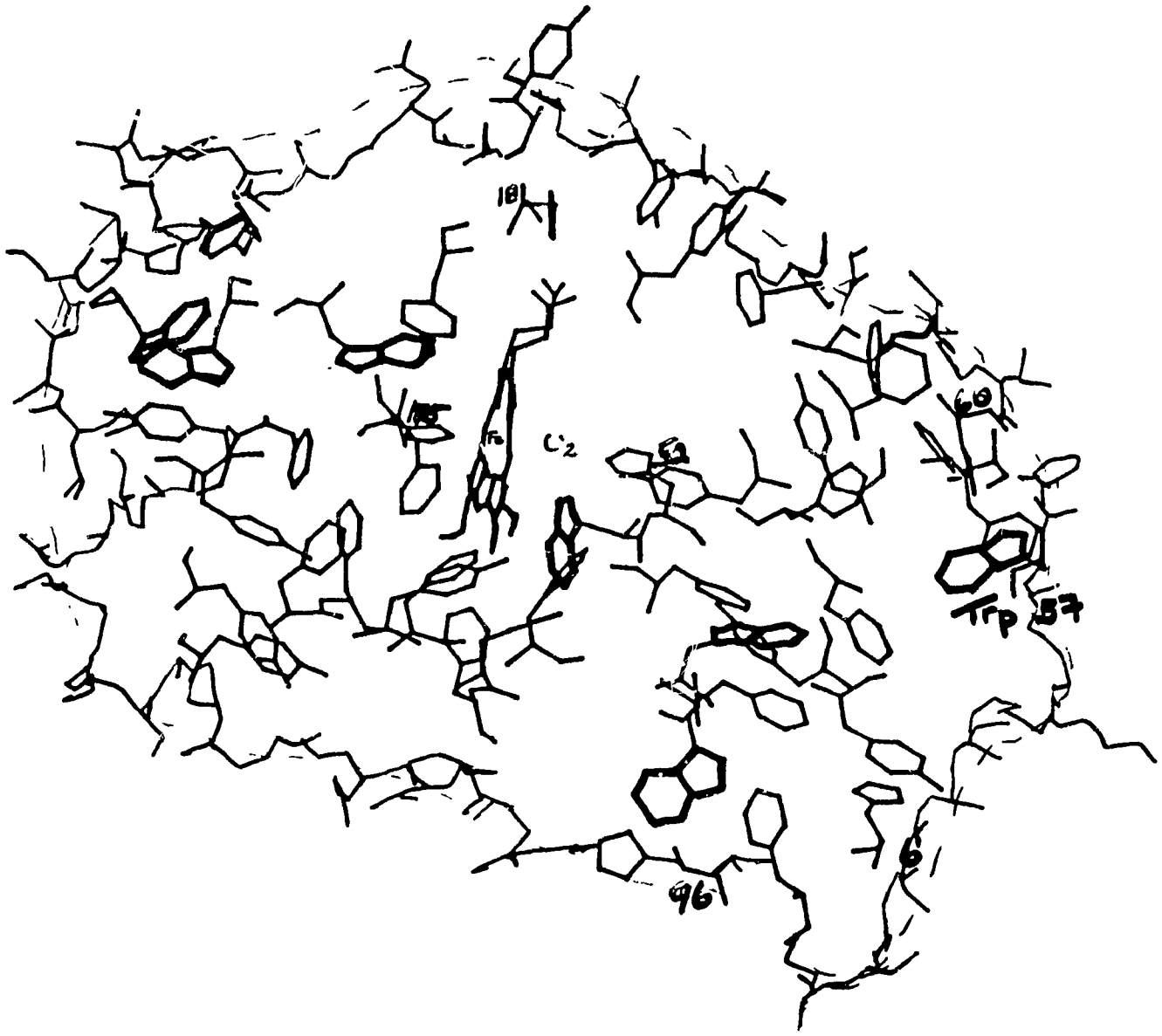

Fig.5.1: CRYSTAL STRUCTURE OF CcP - aromatic amino acids are depicted with tryptophans highlighted. Peripheral amino acids are shown with solid line through them thereby establishing the protein-solvent boundary.

of the complex which have been shown to be environment-sensitive (Matthews et al., 1980).

The tryptophan fluorescence of CcP is shown to be dependent on the excitation wavelength. The emission maximum is red-shifted 4 nm upon excitation at 295 nm compared to 280 nm. The drastic dependence shown in MOPS buffer for 4 different excitation wavelengths is exaggerated. It has been shown recently (Ted Fox, unpublished results) that this drastic dependence can be attributed to the length of illumination time and is reversible. This view is supported herein by the observation that fig.4.29 consisted of fluorescence spectra obtained from a single sample irradiated for a total of 30-40 minutes between the 265 nm and 295 nm spectra. Spectra obtained over shorter excitation periods (fig.4.37 & 4.38) show only the 4 nm red-shift also reported from spectra obtained in phosphate buffer. Therefore, the results indicate that the tryptophan fluorescence of CcP is slightly dependent on the excitation wavelength but care must be taken to avoid exaggerated dependences as was observed in fig.4.29 which is most probably due to the length of irradiation time. An added contribution to this discrepancy may be the nature of the buffer itself. The wavelength dependence is shown to be more pronounced in MOPS than in phosphate buffer (Table 4.1) as are the bandwidth changes for the different excitation wavelengths. In samples which were irradiated over short periods of time the bandwidths of the emission spectra taken in phosphate buffer are wider. It has been shown that tyrosinate fluorescence is enhanced in the presence of Pi (Lakowicz, 1983).

The fluorescence of CcP appears to be due to more than one fluorescing species as suggested by the resolution of a peak at 310 nm upon excitation at 295nm under high quencher concentrations. Resolution of this spectral contribution is only observed upon excitation at 295 nm. The most probable species contributing to the fluorescence spectrum in this fashion is the tyrosinate ion. This ion has been shown to fluoresce in the 340-350 nm region of the fluorescence spectrum and its excitation maximum is at 295 nm (Lakowicz, 1983). Recently, Lee et al. (1989) demonstrated that bovine pancreatic ribonuclease A exhibits fluorescence at 310 nm. This protein contains no tryptophans and six tyrosines. Like the fluorescence observed in RNase A, the CcP fluorescence contribution at 310 nm is small compared to the fluorescence exhibited by the tryptophans. CcP contains 14 tyrosine residues and 7 tryptophans (Takio et al., 1980) The possible presence of the tyrosinate ion in CcP may be of relevance in stabilizing free radicals in the protein during its catalytic cycle. The unusual stability of free radicals in some redox-active enzymes has been recently attributed to tyrosine. Whittaker et al. (1989) demonstrated using Resonance Raman that the radical site of galactose oxidase has a tyrosinate ion. They propose that the tyrosinate ion might stabilize the radical species through formation of a charge transfer complex.

The denaturation of CcP by urea was monitored both spectrophotometrically and by tryptophan fluorescence. The denaturing process, as followed by tryptophan fluorescence, represents a simple 2 state process consisting of native and

denatured protein. In this two state mechanism no other conformational state contributes significantly to the measured optical properties in the denaturation region. Similar results have been obtained for the denaturation of thermophilic ferricytochrome c-552 (Hon-nami & Oshima, 1979; Nojima et al., 1978), cytochrome b_5 (Visser et al., 1975) and thioredoxin (Kelley & Stellwagen, 1981). Monitoring changes in the Soret band is a sensitive measure of unfolding since these reflect changes in the interaction between the heme group and the protein matrix (Shen & Hermans, 1972). Spectrophotometric analysis of the denaturation process of CcP shows the heme of CcP going from 5-coordinate, high spin (<2 M urea) characterized by the 408 nm Soret and the shoulder at 370 nm (Smulevich et al., 1988), to 6-coordinate, low spin (1 M urea) characterized by the Soret at 415 nm and lack of a 370 nm shoulder, followed by the total disruption of the heme-globin interactions (>6 M urea). The appearance of a 6-coordinate heme in the denaturation profile may be a result of either coordination of urea at the sixth position or coordination of an amino acid residue made accessible to the heme upon unfolding of the protein.

Renaturation of CcP is shown to be partially reversible. The heme spectrum of the renatured protein is identical to native, 5-coordinate, high spin. By contrast the fluorescence spectrum of the renatured CcP is not the same as that of native CcP with the same concentration of urea. The refolding process may therefore consist of more than two states. The refolding of thioredoxin by the dilution method is multiphasic (Kelley &

Stellwagen, 1984), the slowest phase being dependent on the incubation time and denaturant concentration in the denaturing process. It is postulated that the denatured state may consist of 2 or more configurational isomers in slow exchange relative to the rate of protein folding. This configurational equilibrium could involve cis and trans isomers of peptide bonds (Brandts et al., 1975). In this case the rapid folding protein would originate from the fractional population of denatured protein molecules that all have native-like isomers, while the slow folding process would be due to an obligatory isomerization of one or more nonnative-like isomers prior to folding. The peptide bonds most likely to accumulate significant populations of nonnative-like isomers in the denatured state involve peptide bonds in which proline residues contribute the amide nitrogen (Brandts et al., 1975). Proline peptide bonds are predominantly trans in the denatured state and the presence of a cis proline in the native protein would slow the refolding process. Although CgP contains 16 prolines (Takio et al., 1980), no Type IV hairpin turns, which involve cis prolines, as well as no cis peptides have been found in the structure of the enzyme (Finzel et al., 1984). The irreversibility of the protein refolding is thereby attributed to the incubation time of the denaturing process. Ahmad (1985) showed that even with a denaturation time of 2 min the renatured protein is significantly different from native.

6. REFERENCES

Ahmad,F., (1985), J.Biol.Chem., 260:10158

Alleyne,T.A. & Wilson,M.T., (1987), Biochem.J., 247:475

Antonini,E., Brunori,M., Colosimo,A., Greenwood,C. & Wilson,M.T., (1977), P.N.A.S., 74:3128

Babcock,G.T., Vickery,L.E. & Palmer,G., (1976), J.Biol.Chem., 251:7907

Babcock,G.T., Vickery,L.E. & Palmer,G., (1978), J.Biol.Chem., 253:2400

Babcock,G.T. & Callahan,P.M., (1983), Biochemistry, 22:2311

Pchmaarai,T.A., Toulme,J.J. & Helene,C., (1979), Photochem. Photobiol., 30:533

Beinert,H., Griffiths,D.E., Wharton,D.C. & Sands, R.H., (1962), J.Biol.Chem., 237:2337

Bickar,D., Bonaventura,C. and Bonaventura,J., (1981), Journal of Biological Chemistry, 259:10777

Blankenhorn,G., (1976), Eur.J.Biochem., 67:67

Boelens,R. & Wever,R., (1980), FEBS Lett., 116(2):223

Brandts,J.F., Halvorson,H.R. & Brennan,M., (1975), Biochemistry, 14:4953

Brudvig,G.W., Stevens,T.H., Morse,R.H. & Chan,S.I., (1981), Biochemistry, 20(13):3912

Brudvig,G.W., Blair,D.F. & Chan,S.I., (1984), J.Biol.Chem., 259:11001

Brunori,M., Colosimo,A., Rainoni,G., Wilson,M.T. & Antonini,E., (1979), J.Biol.Chem., 254:10769

Buse,G., Meinecke,L. & Bruch,B., (1985), **J.Inorg.Biochem.**, 23:149

Brzezinski,P. & Malmström,B.G., (1985), **FEBS Lett.**, 187(1):111

Brzezinski,P. & Malmström,B.G., (1986), **P.N.A.S.**, 83:4282

Brzezinski,P. & Malmström,B.G., (1987), **Biochim.Biophys.Acta.**, 894:29

Cabral,F. & Love,B., (1972), **Biochim.Biophys.Acta**, 283:181

Callahan,P.M. & Babcock,G.T., (1983), **Biochemistry**, 22:452

Campbell,I.D., Dobson,C.M. & Williams,R.J.P., (1985), **Biochem.J.**, 231:1

Casey,R.P., Thelen,M. & Azzi,A., (1979), **Biochem.Biophys.Res. Commun.**, 87:1011

Casey,R.P., Thelen,M. & Azzi,A., (1980), **J.Biol.Chem.**, 255:3994

Casey,R., (1981), **Biochim.Biophys.Acta**, 768:319

Casey,R.P., (1986), **Methods in Enzymology**, Vol.126:13

Caughey,W.S., Wallace,W.J., Volpe,J.A. & Yoshikawa,S., (1976), **The Enzymes**, Vol.XIII, 3rd Ed., Ed. P.D. Boyer, Academic Press, New York, p.299

Chance,B., Waterland,R.A., Tanaka,A. & Poyton,R.O., (1988), **Annals of the New York Academy of Sciences**, Eds. M.Brunori & B.Chance, 550:360

Copeland,R.A., Smith,P.A. and Chan,S.I., (1987), **Biochemistry**, 26:7311

Copeland, R.A., Smith,P.A., Chan,S.I., (1988), **Biochemistry**, 27:3552

Dawson,R.M.C., Elliott,D.C., Elliott,W.H. & Jones,K.M., (1986), **Data for Biochemical Research**, 3rd Ed., Clarendon Press, Oxford

Dufourcq,J., Faucon,J.F., Lussan,C. & Bernon,R., (1975), FEBS Lett., 57:112

Dupont,Y., (1976), B.B.R.C., 71(2):

Eftink,M.R. & Ghiron,C.A., (1976), Biochemistry, 15:672

Ellis Jr.,W.R., Wang,H., Blair,D.F., Gray,H.B. & Chan,S.I., (1986), Biochemistry, 25:161

Erecinska,M., Chance,B. & Wilson,D.F., (1971), FEBS Lett., 16:281

Fabian,M., Thornstrom,P.-E., Brzezinski,P. & Malmström,B.G., (1987), FEBS Lett., 213:396

Faucon,J.F., Dufourcq,J. & Lussan,C., (1979), FEBS Lett., 102:187

Ferreira-Rajabi,L. and Hill,B.C., (1989), Biochemistry, 28:8028

Flamingo,F.C., Altschuld,R.A., Moh,P.P. & Allen,J.C., (1982), J.Biol.Chem., 257(1):639

Finzel,B.C., Poulos,T.L. & Kraut,J., (1981), J.Biol.Chem., 259:13027

Greenwood,C., Wilson,M.T. and Brunori,M., (1974), Biochem.J., 137:205

Greenwood,C., Brittain,T., Wilson, M.T., & Brunori,M., (1976), Biochem.J., 157:591

Greenwood,C., Brittain,T., Brunori,M. & Wilson,M.T., (1977), Biochem.J., 165:413

Halaka,F.G., Babcock,G.T. and Dye,J.L., (1981), J.Biol.Chem., 256:1084

Hill,B.C., Horowitz,P.M. and Robinson,N.C., (1986), Biochemistry, 25:2287

Hon-nami,K. & Oshima,T., (1979), Biochemistry, 18:5693

Hoppe,J., Schairer,H.J. & Sebald,W., (1980), **Eur.J.Biochem.**, 112:17

Jensen,P., Wilson,M.T., Aasa,R. & Malmström,B.G., (1984), **Biochem.J.**, 224:829

Jones,G.D., Jones,M.G., Wilson,M.T., Brunori,M., Colosimo,A. and Sarti,P., (1983), **Biochem.J.**, 209:175

Jones,M.G., Bickar,D., Wilson,M.T., Brunori,M., Colosimo,A. & Sarti,P., (1984), **Biochem.J.**, 220:57

Kawato,S., Ikegami,A., Yoshida,S., & Orii,Y., (1980), **Biochemistry**, 19:1598

Kawato,S., Yoshida,S., Orii,Y., Ikegami,A. & Kinosita Jr.,K., (1981), **Biochim.Biophys.Acta**, 634:85

Keilin,D. & Hartree,E.F., (1939), **Proc.Roy.Soc.Ser.B.**, 125:171

Kelley,R.F. & Stellwagen,E., (1984), **Biochemistry**, 23:5095

Konstantinov,A., Vygodina,T. & Andreev,I.M., (1986), **FEBS Lett.**, 202:229

Kornblatt,J.A., Kells,D.I. & Williams,G.R., (1975), **Can.J.Biochem.**, 53:461

Kornblatt,J.A. & Williams,G.R., (1975), **Can.J.Biochem.**, 53:467

Kornblatt,J.A., (1977), **Can.J.Biochem.**, 55:458

Kornblatt,J.A., (1980), **Can.J.Biochem.**, 58:840

Krab,K. & Wikström,M., (1987), **Biochim.Biophys.Acta**, 895:25

Kuboyama,M., Young,F.C. and King,T.E., (1972), **J.Biol.Chem.**, 247:6375

Lakowicz,J.R. and Weber,G., (1973), **Biochemistry**, 12:4171

Lakowicz,J.R., (1983), **Principles of Fluorescence Spectroscopy**, Plenum Press, New York

Lambeth,D.O. and Palmer,G., (1973), **J.Biol.Chem.**, 248:6095

Lee,F.S., Auld,D.S. & Vallee,B.L., (1989), **Biochemistry**, 28:219

Lemberg,M.R., (1969), **Physiol.Rev.**, 49:48

Malmström,B.G., (1985), **Biochim.Biophys.Acta**, 811:1

Malmström,B.G., (1987), **Cytochrome Systems: Molecular Biology & Energetics**, Eds. S. Papa, B. Chance, L. Ernster, Plenum Publishing Co., New York

Massey,V. & Hemmerich,P., (1977), **J.Biol.Chem.**, 252(16):5612

Massey,V. & Hemmerich,P., (1978), **Biochemistry**, 17:9

Matthews,C.R., Erickson,P.M. & Froebe,C.L., (1980), **Biochim. Biophys.Acta**, 624:499

Michel,B. & Bosshard,H.R., (1989), **Biochemistry**, 28:211

Mitchell,P., (1968), **Chemiosmotic Coupling & Energy Transduction**, Glynn Research Ltd., Bodmin, U.K.

Muijsers,A.O., Tiesjema,R.M. & Van Gelder,B.F., (1971), **Biochim. Biophys.Acta**, 234:481

Muller,M., Thelen,M., O'Shea,P. and Azzi,A., (1986), **Methods in Enzymology**, Vol.126:78

Myer,Y.P., (1972), **Biochem.Biophys.Res.Commun.**, 49:1194

Nicholls,D.G., (1982), **Bioenergetics: An Introduction to the Chemiosmotic Theory**, Academic Press, Montreal,

Nicholls,P., (1972), **Biochem.J.**, 128:98p

Nicholls,P. & Chance,B., (1974), **Molecular Mechanism of Oxygen Activation**, Ed. O. Hayaishi,, Academic Press, New York, p.479

Nicholls,P. and Chanady,G.A., (1981), **Biochim.Biophys.Acta**, 634:256

Nojima,H., Hon-nami,K., Oshima,T. & Noda,H., (1978), **J.Mol.Biol.**, 122:33

Okunuki,K., Hagihara,B., Sekuzu,I. & Horio,T., (1958), **Proc.Int. Symp.Enzyme Chem.**, Tokyo, Kyoto, p.264

Papa,S., (1988), **Progress in Clinical & Biological Research**, Vol.274, Alan R. Liss Inc., New York, Ed. T.E. King, H.S. Mason, M. Morrison, p.707

Petersen,L.C. & Cox,R.P., (1980), **Biochim.Biophys.Acta**, 590:128

Peterson,J.A., White,R.E., Yasukochi,Y., Coombs,M.L., O'Keefe,D.H., Ebel,R.E., Masters,B.S.S., Ballou,D.P. & Coon,M.J., (1977), **J.Biol.Chem.**, 252:4131

Poulos,T.L., Freer,S.T., Alden,R.A., Edwards,S.L., Skogland,U., Takio,K., Eriksson,B., Xuong,N., Yonetani,T. & Kraut,J., (1980), **J.Biol.Chem.**, 255:575

Rocchia,J., Matthews,C.R., Rhee,M.-J. & Horrocks Jr.,W.De W., (1982), **Biochim.Biophys.Acta**, 702:105

Rosen,S., Branden,R., Vannigard,T. & Malmström,B.G., (1977), **FEBS Lett.**, 74:25

Saraste,M., Penttila,T. & Wikström,M., (1981), **Eur.J.Biochem.**, 115:261

Scholes,C.P. & Malmström,B.G., (1986), **FEBS Lett.**, 198(1):125

Scott,R.A. & Gray,H.B., (1980), **J.Am.Chem.Soc.**, 102:3219

Shaw,R.W., Hansen,R.E. & Beinert,H., (1978a), **Biochim.Biophys.Acta**, 504:187

Shaw,R.W., Hansen,R.E. & Beinert,H., (1978b), **J.Biol.Chem.**, 253:6637

Shen,L.L. & Hermans Jr.,J., (1972), **Biochemistry**, 11:1836

Shimizu,O. & Imakuvo,K., (1977), **Photochem.Photobiol.**, 26:541

Smulevich,G., Mauro,J.M., Fishel,L.A., English,A.M., Kraut,J. & Spiro,T.G., (1988), **Biochemistry**, 27:5477

Szabo,A., Lynn,K.R., Krajcarski,D.T. & Rayner,D.M., (1978), **FEBS Lett.**, 94:249

Takio,K. & Yonetani,T., (1980), **Arch.Biochem.Biophys.**, 203(2):605

Takio,K., Titani,K., Ericsson,L.H. & Yonetani,T., (1980), **Arch. Biochem.Biophys.**, 203(2):615

Talbot,J.C., Dufourcq,J., de Borg,J., Faucon,J.R. & Lussan,C., (1979), **FEBS Lett.**, 102:191

Thomson,A.J., Englinton,D.G., Hill,B.C. & Greenwood,C., (1982), **Biochem.J.**, 207:167

Urry,D.W., Wainio,W.W. & Grebner,D., (1972), **Biochem.Biophys.Res. Commun.**, 27:625

Valpuesta,J.M., Goni,F.M. and Macanilla,J.M., (1987), **Arch.Biochem. Biophys.**, 257(2):285

Van Buuren,K., Zuurendonk,P., Van Gelder,B. & Muijsers,A.O., (1972), **Biochim.Biophys.Acta**, 256:243

Visser,L., Robinson,N.C. & Tanfoed,C., (1975), **Biochemistry**, 14:1194

Wang,H., Blair,D.F., Ellis Jr., W.R., Gray,H.B. & Chan,S.I., (1986), **Biochemistry**, 25:167

Wever,R., Van Drooge,J.H., Muisjers,A.O., Bakker,E.P. & Van Gelder,B.F., (1977), **Eur.J.Biochem.**, 73:149

Whittaker,M.M., DeVito,V.L., Asher,S.A., & Whittaker,J.W., (1989), J.Biol.Chem., 264(13):7104

Wilson,D.F. & Miyata,Y., (1977), Biochim.Biophys.Acta, 461:218

Wilson, D.F. & Nelson,D., (1982), Biochim.Biophys.Acta, 680:233

Wikström,M. & Saari,H.T., (1977), Biochim.Biophys.Acta, 462:347

Wikström,M., Krab,K. & Saraste,M., (1981), Cytochrome Oxidase: A Synthesis, Academic Press, Toronto

Wikström,M. & Casey,R., (1985), J.Inorg.Biochem., 23:327

Yamamoto,T. & Okunuki,K., (1970), J.Biochem.Tokyo, 67:505

Yonetani,T., (1966), Biochem.Prep., 11:14

Yonetani,T., (1976), Enzymes, 3rd Ed., 13:345